

POLITECNICO DI TORINO
Department of Engineering
Master Degree in Nanotechnologies for ICTs



**Sustainable energy production in the
context of low carbon economy:
Capacitive Mixing exploiting CO₂
emissions**

Supervisor

Prof. ANDREA LAMBERTI

Candidate

Davide MELE

October 2021

Summary

During last years, the awareness about climate change has been raised. The increase concentration of CO₂ is mainly due to the use of fossil fuels. Thus, the energy production research is focusing its interest on new renewable sources.

In particular, the blue energy is one of the most promising, which is the energy produced by mixing aqueous solutions with different salt concentration. This energy is naturally released at each river estuary and not yet exploited. Among several technologies, one of the most effective is related to Capacitive Mixing (CapMix), which is based on flushing two different salt concentration solutions inside a capacitive system. This causes the alteration of the electrical double layer generating DC power.

In this thesis, such technique is adapted to capture CO₂ through engineered electrolytes, in order to change ions concentration in CO₂ concentration, and exploiting a fluidic electrochemical device based on Electric Double Layer Capacitor (EDLC). The selected electrolyte is an imidazole-based ionic liquid (DABCO-IM) or dilution of it in Propylene Carbonate, giving rise to an electrolyte with an improved mobility and conductivity so that a larger and positive energy gain is obtained at room temperature. In addition, the CO₂ desorption mechanism is investigated through bubbling N₂ with the purpose to characterize this device by a high endurance.

Being able to extract such energy it could be possible to store an amount of power estimated between 1.5 - 2.6 TW covering the global energy demand.

Table of Contents

List of Tables	VII
List of Figures	VIII
1 State of the Art	1
1.1 Pressure-Retarded Osmosis	2
1.2 Reverse Electrodialysis	3
1.3 Energy Harvesting from CO ₂ using pH gradient	5
1.4 Energy Harvesting from CO ₂ using mixing energy	6
2 Electrochemical Devices based on Electrical Double Layer	8
2.1 Electric Double Layer Capacitors	8
2.2 Pseudo-Capacitors	11
2.3 Hybrid-supercapacitors	13
3 CapMix Techniques	15
3.1 Capacitive Double Layer Expansion	15
3.2 Capacitive Donnan Potential	18
4 Performance Evaluation	21
4.1 Key Performance Metrics	21
4.1.1 Total Cell Capacitance	21
4.1.2 Operating Voltage Window	22
4.1.3 Equivalent Series Resistance	23
4.1.4 Time Constant	24
4.1.5 Power and Energy Density	25
4.1.6 Coulombic Efficiency	25
4.1.7 Leakage Current	26

4.2	Test Methods	27
4.2.1	Cyclic Voltammetry	27
4.2.2	Constant Current Charge/Discharge	29
4.2.3	Electrochemical Impedance Spectroscopy	30
4.2.4	Potentiostatic Floating Test or Float Conditioning Test	31
5	Setup	32
5.1	Cells	32
5.1.1	Three-electrodes Cell	32
5.1.2	Two-electrodes Cell	33
5.2	Separator	34
5.3	Gas Diffusion Layer	35
5.3.1	Hard GDL	35
5.3.2	Flexible GDL	35
5.4	Electrolyte	37
5.5	Charge Balancing and associated Upgraded Assembling of the Cell	39
6	Experimental Results	41
6.1	New CapMix Procedure	41
6.2	CapMix Procedure exploited Flexible GDL Electrodes	44
6.3	CapMix Procedure with Float Reduction	47
6.4	CapMix Procedure with Discharge until Float Potential	48
7	Dabco-IM diluted in Propylene Carbonate 1M	52
7.1	Theoretical elements of diluted electrolyte in supercapacitor	52
7.2	Preliminary analysis of Dabco-IM diluted in Propylene Carbonate 1M	56
7.3	CO ₂ Cap Procedure to select the Best Floating Potential	59
7.3.1	Symmetric Cell	59
7.3.2	Asymmetric Cell	68
7.4	Comparison of symmetrical and asymmetrical system	76
8	Conclusions and Future Developments	78
8.1	Conclusions	78
8.1.1	Improved CapMix procedure	78
8.1.2	New electrode material	79
8.1.3	Effect of the Float reduction	79
8.1.4	Effect of the Ionic Liquid dilution exploiting Propylene Carbonate	80
8.2	Future Developments	83
	Bibliography	85
	Acknowledgments	iii

List of Tables

6.1	Comparison of the energies per cycle for 60mV Float at Room Temperature exploiting the previous procedure (Fig. 6.1) [19]. . . .	44
6.2	Comparison of the energies per cycle for 60mV Float at Room Temperature exploiting the new procedure (Fig. 6.3).	44

List of Figures

1.1	Schematic of PRO driven process [3].	3
1.2	Schematic view of RED stack [4].	4
1.3	(a) Schematic of pH-gradient flow cell. (b) Cell voltage and power density profile for the pH-gradient flow cell[6].	5
1.4	(a) Schematic of capacitive electrochemical cell. (b) Measured open circuit voltage[8].	7
2.1	Helmholtz Gouy-Chapman Stern Model[10].	9
2.2	Model of a cylindrical pore and distributed capacitance [9].	10
2.3	Model of an electrochemical double layer supercapacitor [9].	11
2.4	Presentation of kinetic phenomena occurring at the surface of a) electrical double layer capacitance and b) pseudocapacitance [12] . .	12
2.5	Illustration of typical CCCD and CV responses in a) electrical double layer capacitance (green curves) and b) pseudocapacitance (blue curves) [12].	12
2.6	Schematic of Hybrid Supercapacitor [9]	13
3.1	Ideal Charge vs Voltage response for CDLE[13].	16
3.2	Ideal CapMix cycle Voltage vs Charge and exchanged energy[13]. .	17
3.3	Potential profiles across two electrodes in IL bulk direction [10]. . .	17
3.4	(a) Schematic view of a Capacitive Donnan Potential-based Cell. (b) Power production through CDP CapMix [7].	18
3.5	Electro-diffusion of ions through Ion Exchange Membrane at spacer channel-electrode interface [7].	19
3.6	Electrostatic potential profile across the cell playing CapMix [14]. .	19
4.1	(a) Ideal Voltage vs Time response of a CV test for a EDLC system. (b) Voltage vs Time response of a CV for a EDLC system affected by IR drop [11].	22
4.2	Example of Three electrode Cyclic Voltammetry and Coulombic Efficiency	23

4.3	Equivalent Circuit Model of an electrochemical supercapacitor [11].	23
4.4	Approach to determine the ESR in SC using EIS [11].	24
4.5	Dependence of the voltage as function of the time describing the discharge of an EDLC [15].	26
4.6	Determination of the operating voltage window [12].	28
4.7	Equivalent circuit analysis for different cyclic voltammetry profiles.(a) Ideal capacitive system. (b) Blunt profile indicating the ESR presence. [12]	28
4.8	Examples of CCCD curve: (a) non-ideal supercapacitor; (b) faradaic system [12].	29
4.9	Electrochemical Impedance Spectroscopy plot examples [12].	30
5.1	Electrical configuration of three-electrodes cell (on the left) and two-electrodes cell (on the right) [19].	32
5.2	(a) PAT-cell. (b) Overview of the PAT-cell electrical contact area [20]	33
5.3	PAT-Core components:(a) Upper plunger. (b) Sleeve. (a) Bottom plunger. [20]	33
5.4	ECC-Air components overview. [20]	34
5.5	FESEM magnification of the microporous layer of a GDL [19].	35
5.6	Characterization results: (a) Cyclic Voltammetry for positive and negative voltages in order to define the Operating Voltage Window through the Coulombic Efficiency. (b) Capacitance adjustment as a function of potential windows	36
5.7	EIS for a 18mm diameter Flexible GDL performed by three-electrodes measurements.	36
5.8	Cation (a) and anion (b) chemical structure composing DABCO-IM [25].	37
5.9	¹³ C NMR spectra of [DBUH] ⁺ and [IM] ⁻ before (up) and after (down) the CO ₂ exposure [25].	38
5.10	(a) Viscosity vs Shear Rate and (b) cell Specific Capacitance of pure and post absorption DABCO-IM [19].	39
5.11	Fitting of the KAPTON crown on the ECC-Air full-cell bottom [19].	40
5.12	Cyclic Voltammetry with and without KAPTON layer [22].	40
6.1	Previous procedure adopted for the CO ₂ Cap cycle [19].	42
6.2	Energies obtained flushing CO ₂ on hard GDL electrode exploiting the previous procedure (Fig. 6.1) [19].	42
6.3	New procedure adopted for the CO ₂ Cap cycle.	43
6.4	CapMix results obtained flushing CO ₂ on hard GDL electrode [19] (a) and on flexible GDL electrode (b) at Room Temperature.	45

6.5	Float leakage currents related to a cell with hard GDL electrodes (a) and flexible GDL electrodes at room temperature (b).	46
6.6	Example of CapMix with progressive reduction of the Float time.	47
6.7	(a) Comparison of energies and (b) Percentage Energy Gains obtained for several Float lasting adopting the CapMix procedure shown in figure 6.3.	48
6.8	Example of CapMix procedure with constant current discharge until Float Potential.	49
6.9	(a) Comparison of charging energies between the procedure in Fig. 6.3 (1 st Procedure) and one in Fig. 6.8 (2 nd Procedure) obtained for several Float times; (b) Comparison of Float leakage currents related to the procedure in Figure 6.8 for several Float times.	50
6.10	(a) Comparison of energies and (b) Percentage Energy Gains obtained for several Float lasting adopting the CapMix procedure shown in figure 6.8.	50
7.1	(a) 2D chemical structure depiction of Imidazole; (b) 2D chemical structure depiction of Imidazole Carbamate [28].	53
7.2	Comparison of viscosity between pure ionic liquid and post CO ₂ absorption ionic liquid [19]	53
7.3	Solvation shell made up of solvent molecules surrounding solute in a solution [30]	54
7.4	Types of ion pairs in an electrolyte solution: (a) Hydration shell contact type, (b) Shared hydration shell type and (c) Ion contact type [29]	56
7.5	(a) Electrochemical Impedance Spectroscopy (EIS) of the Supercapacitive system characterized by DABCO-IM diluted in Propylene Carbonate 1M as electrolyte; (b) Magnification of the highest frequencies results related to the EIS.	57
7.6	(a) On the left: Specific Capacitance values related to several potential windows, both in cathodic and anodic sides, of the Supercapacitive system characterized by DABCO-IM diluted in Propylene Carbonate 1M as electrolyte; (b) On the Right: Cyclic Voltammetry overlapped with Coulombic Efficiency for several potential windows whose width differ by a gap voltage equal to 10mV, both in cathodic and anodic sides.	58
7.7	Voltage vs Time of the CO ₂ Cap with a null Float Potential using a symmetrical cell.	60
7.8	(a) Energy gain obtained for different duration of the 0 volt Float; (b) Percentage of achieved Energy gain with respect to spent energy for different duration of the Float phase.	61

7.9	Voltage vs Charge graph of the CO ₂ Cap procedure marked out by a value of Float Potential equal to 0 volt and a progressive reduction of the Float time.	61
7.10	Voltage vs Time of the CO ₂ Cap with a 10mV Float Potential using a symmetrical cell.	62
7.11	(a) Energy gain module for different duration of the 10mV Float; (b) Energy gain in percentage referred to spent energy.	63
7.12	Voltage vs Charge graph of the CO ₂ Cap procedure with a Float Potential equal to 10mV and a progressive reduction of the Float time.	63
7.13	(a) Voltage vs Charge curve related to 20mV Float; (b) Voltage vs Charge curve related to 30mV Float; (C) Voltage vs Charge curve related to 40mV Float.	64
7.14	Voltage vs Time of the CO ₂ Cap with a 50mV Float Potential using a symmetrical cell.	65
7.15	Energy gain module for different duration of the 50mV Float.	66
7.16	(a) Energy gain in percentage referred to spent energy for 50mV Float; (b) Energy gain in percentage referred to spent energy for 60mV Float.	67
7.17	(a) Voltage vs Charge curves related to 50mV Float; (b) Voltage vs Charge curve related to 60mV Float.	67
7.18	Voltage vs Time of the CO ₂ Cap with null Float Potential using an asymmetrical cell.	69
7.19	(a) Energy gain obtained for different Float time at zero potential; (b) Percentage of achieved energy gain with respect to spent one.	69
7.20	Voltage vs Charge graph of the CO ₂ Cap procedure related to zero Float Potential using the asymmetrical cell.	70
7.21	Voltage vs Time of the CO ₂ Cap with 10mV Float Potential, using an asymmetrical cell.	71
7.22	(a) Energy gain for different duration of the 10mV Float; (b) Energy gain in percentage referred to spent energy for 10mV Float.	71
7.23	Voltage vs Charge curves related to 10mV Float potential, using an asymmetrical cell.	72
7.24	(a) Voltage vs Charge curve related to 20mV Float; (b) Voltage vs Charge curve related to 30mV Float; (C) Voltage vs Charge curve related to 40mV Float, using an asymmetrical cell.	72
7.25	Voltage vs Time of the CO ₂ Cap with 60mV Float Potential, using an asymmetrical cell.	73
7.26	(a) Energy gain for different duration of the 50mV Float; (b) Energy gain for different duration of the 60mV Float	74
7.27	(a) Percentage Energy gain referred to spent energy for 50mV Float; (b) Percentage Energy gain referred to spent energy for 60mV Float.	75

7.28	(a) Voltage vs Charge curve related to 50mV Float; (b) Voltage vs Charge curve related to 60mV Float.	75
8.1	New procedure adopted for the CO ₂ Cap cycle.	78
8.2	Comparison of energy gains obtained for several Float times adopting the CapMix procedure shown in figure 8.1.	79
8.3	Voltage vs Time of the CO ₂ Cap using a symmetrical cell.	80
8.4	(a) Energy gain module for different duration of the Float; (b) Energy gain in percentage referred to spent energy for several Float time.	81
8.5	Voltage vs Charge.	81
8.6	Voltage vs Time of the CO ₂ Cap using an asymmetrical cell.	82
8.7	(a) Energy gain for different 60mV Float times; (b) Voltage vs Charge.	83

Chapter 1

State of the Art

Carbon dioxide (CO_2) is the main waste product of the current global industry. It is released into the atmosphere causing a series of climatic events which can have effects on human life in the long term as the global climate change. This means the needed for a short-term reaction to reduce CO_2 emissions but at the same time find new renewable energy sources. One solution is to capture emissions with liquid solutions which can be aqueous-based or ionic liquids. In particular, this thesis is focused on an electrochemical device exploiting a system similar to a super-capacitor, based on Electric Double Layer, to capture CO_2 in an ionic liquid and at the same time aims to recover energy. Thus the conversion of chemical energy, due to the absorption of CO_2 in solution, into electrical energy. This is possible by exploiting a very promising technology called Capacitive Mixing. It is the energy produced by mixing aqueous solutions with different salt concentration inside a capacitive system, causing the alteration of the electrical double layer generating DC power. This energy is naturally released at each river estuary and not yet exploited. Indeed if it were extracted and stored, then it is estimated an amount of power ranging between 1.5-2.6 TW, covering the global energy demand. The thesis work is subdivided as follows:

- Chapter One: State of Art of current techniques for the generation and storing of free energy obtained from both salinity and gas gradients. These are the starting points of the technology proposed in this work.
- Chapter Two: Presentation and description of several Electrochemical Capacitors with the aim of giving the fundamental knowledge about the most used existing super-capacitors and providing more details on Electric Double Layer Super-Capacitor which is the one used in this work.
- Chapter Three: Overview of the existing Capacitive Mixing techniques focusing mainly on one used which is the Capacitive Double Layer Expansion.

- Chapter Four: Evaluation of the techniques used to characterized the device and materials composing it. In particular, some metrics are of great importance such as the Equivalent Series Resistance (ESR), the Total Specific Capacitance and the Coulombic and Energy Efficiency.
- Chapter Five: The Setup is explained in detail showing the various components, materials and assembling method.
- Chapter Six: Experimental results on initial and basic setups are exhibited highlighting the problems and how they have been resolved through the use of new materials, substances and their combinations.
- Chapter Seven: The most significant and useful achievements implementing identified solutions are shown.
- Chapter Eight: Conclusions on the obtained results are summarized while future targets are set on the basis of achieved ones.

1.1 Pressure-Retarded Osmosis

Pressure-Retarded Osmosis (PRO) is a membrane-based technology powered by salinity gradient. It exploits natural osmosis of water from a low concentrated salt solution (feed solution) to a high concentrated salt solution (draw solution) divided by a semipermeable membrane made up of an active layer and a support layer [1]. This water transport causes an increase in volume and pressure in draw side producing mechanical potential by depressurization (Fig.1.1). By means of a hydraulic pressure lower than the osmotic one, water flows toward a hydro turbine producing sustainable power, called salinity gradient power (SGP)[2].

For the purpose of continuous operation of the turbine it is necessary that the system is steadily out of equilibrium and this is guaranteed through the sustained supply of fresh and salt water in the respective sides.

However, PRO process has to face several issues. First of all, the absence of specialized PRO membranes, which is the chief factor to make possible commercialized implementation, and optimization of the process involving pre-treatment and the amount of energy consumption related to recovery device [2].

Performances of PRO process are usually evaluated through W per unit of membrane area. In order to be workable the power density has to range between 4-6 W/m², but an initial attempt was able to produce of 1 W/m². This result is mainly due to non-ideality of the semipermeable membrane. Among the adverse, the transport of the solute (salt) from draw solution to feed one can be observed accumulating inside the support layer, thus the rejection rate of the membrane is not ideally.

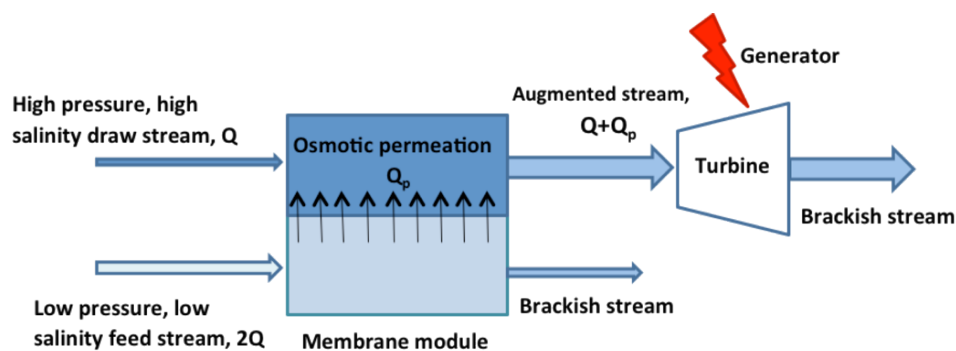


Figure 1.1: Schematic of PRO driven process [3].

Newest achievements in membrane technologies allowed to revalue PRO process. Namely, flat-sheet and hollow-fiber membranes are two semipermeable membranes designed to improve efficiency focusing on high salt rejection rate and high water permeability [1]. Flat-sheet is PA-based TFC combined with ethanol based post-treatment of the support layer. Some numerical simulations show that it can enhance PRO performances up to 18 W/m^2 . Hollow-fiber membrane is charming due to its higher packing than flat-sheet membrane. These new technologies let upgrades such as reduction of membrane price and energy consumption mainly by applying pressure exchanger in PRO process. Despite the last improvements, there are still many challenges to address to make PRO commercial including development of effective performance membrane to gain larger power density, optimization of treatments taking in consideration several features of feed solution often polluted by organic and inorganic elements and economic viable process [1].

1.2 Reverse Electrodialysis

Reverse electrodialysis (RED), similar to previous technology, is a membrane-base process whose driving force is the electrical potential. It is distinguished by the use of cathode and anode located at the ends of an electrochemical cell and in the middle cation exchange membranes (CEMs) and anion exchange membranes (AEMs) separated by spacers which are alternately placed giving rise to a stack (Fig.1.2) [4]. The spacer has a dual aim: the build of separated regions and set a defined intermembrane distance. High concentrated salt solution and low concentrated salt solution are put in contact through a stack of AEMs and CEMs resulting in a motion and accumulation of cations toward cathode and anions toward anode. Such phenomenon prompts a current due to REDOX reaction and electrochemical potential difference, which can be used to supply an external load

connected to the system.

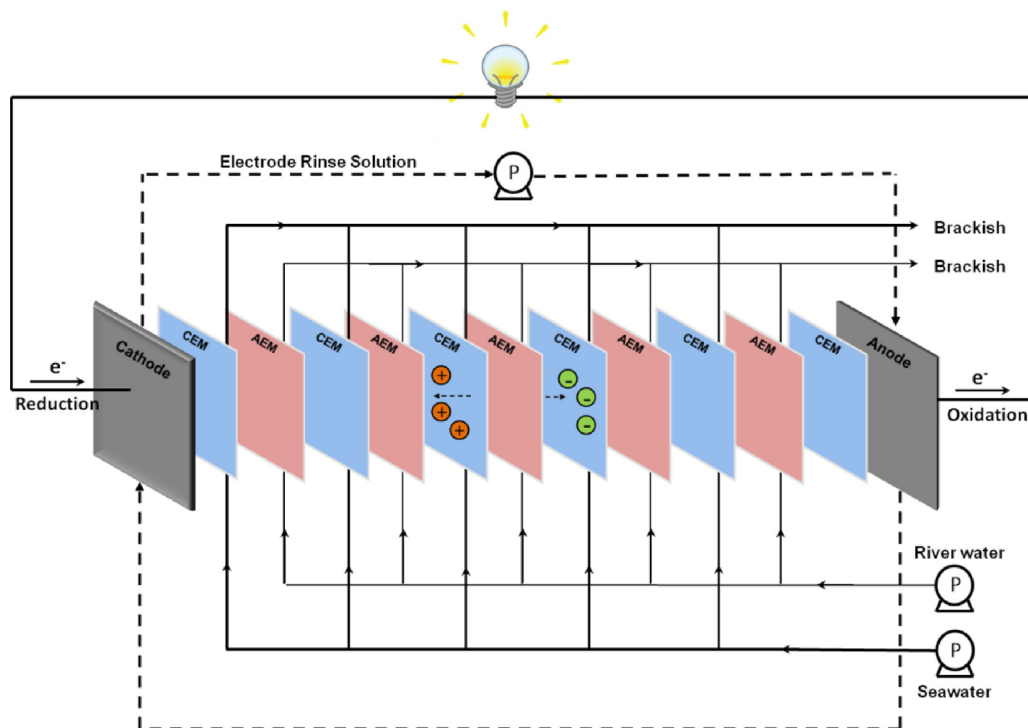


Figure 1.2: Schematic view of RED stack [4].

The maximum power density pulled out in recent development is 2.2 W/m^2 but actually the net power density is 1.2 W/m^2 since the effort due to pumping device has to be considered. An improvement of the power gain can be accomplished using a thinner spacer but on the other hand this solution causes the increasing of power consumption, in terms of pumping losses to bring the feed water through the stack, and of resistance to ion transport which lowers, finally, the power output. Thus, to overcome such issues, the proposal of Vermaas et al. [5] is the designing of a spacer-free RED stack combined with a smaller cell. From a theoretical point of view, this solution induces an advantageous feedback since it allows a shortening of pumping power enabling the reduction of intermembrane distance and residence time which are directly proportional to ion transport resistance leading a smaller cell and so a greater net a power density gain up to 10 %. However nowadays a design that fulfils the necessary requirements is not currently feasible [5]. Indeed, in order to have a practical deployment, RED-specific membrane is needed, since membrane characteristics mainly affect the RED process performance, and go beyond geometrical limits related to the cell length. The most relevant membrane properties impacting on RED power generation are ion-exchange capacity (IEC), swelling degree (SD), membrane resistance and permselectivity. In particular, a

homogeneous ion exchange matrix is essential because in case of heterogeneity of the membrane uncharged regions can be clearly distinguished being resistance higher and so lowering the IEC.[4].

1.3 Energy Harvesting from CO₂ using pH gradient

This technology is based on an approach able to harvest energy through a series of chemical reactions involving CO₂ dissolved in water. More precisely, CO₂ in water proceeds inducing the formation of carbonic acid (H₂CO₃) which in turn dissociates itself in bicarbonate (HCO₃⁻) and protons (H⁺) spontaneously. Such products, thus, are capable to adjust the pH value of the solution entailing a pH-gradient useful to develop pH-dependent potential[6]. In order to accomplish this mechanism a proper setup has been developed (fig.1.3a). It is characterized by two electrodes of MnO₂ (depicted both in black) and two channels separated by an inexpensive non-selective membrane (shown in orange). Thereby, the potential difference, dropping across the membrane in open circuit configuration, can be exploited to generate power. Both channels are fueled simultaneously employing a peristaltic pump. Each one with a different solution therefore either lower pH solution (distinguishable by dark blue) or a higher pH value solution (distinguishable by light blue) which were generated respectively by sprinkling the solutions with CO₂ (pH 7.7) and air (pH 9.4)[6].

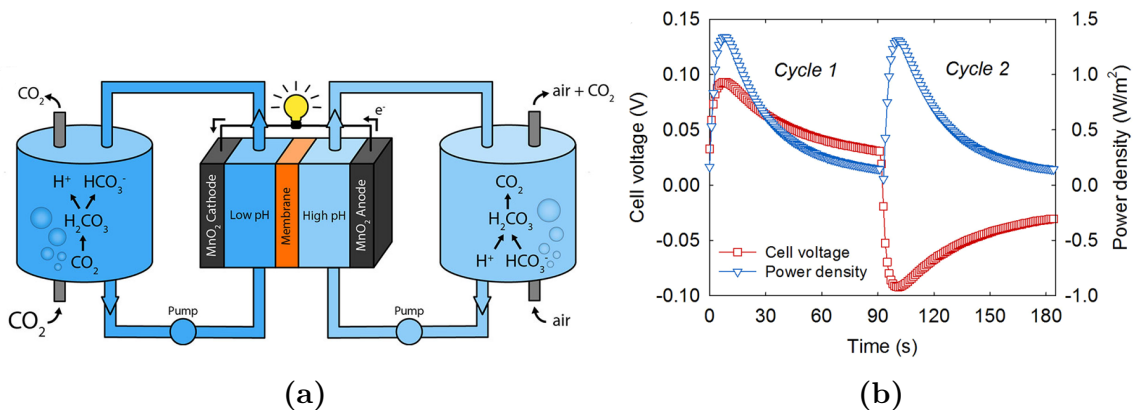


Figure 1.3: (a) Schematic of pH-gradient flow cell. (b) Cell voltage and power density profile for the pH-gradient flow cell[6].

In figure 1.3b the cell voltage and the power density with respect to membrane area are assessed exploiting an external resistance. In the starting cycle (cycle

1), CO₂ and air-sprinkled solutions are flushed in the channels. Then, the fluxes are switched in the next cycle (cycle 2) producing power and reversed cell voltage. The derived average power density is 0.52 W/m² which is not feasible for practical implementation. In order to improve the yielded power density a new cell has to be designed deepening the chemistry study. Moreover, according to *Bruce E. Logan et all* further fuels could be used, such as H₂, besides the exploiting of higher temperature so that having access to a larger amount of energy [6].

1.4 Energy Harvesting from CO₂ using Capacitive Mixing

Among the new renewable sources a promising idea is to harvest free energy coming from the mixing of fresh water (such as river water) with salt water (such as sea water)[7]. The most validated method to gain such kind of energy is the Capacitive Mixing (CapMix), which is a technique developed to extract a huge amount of energy by means of mixing two solutions characterized by a gradient. A device based on CapMix should be able to drain anions and cations through specialized electrodes. Some CapMix techniques are "Capacitive Double Layer Expansion" (CDLE) and "Capacitive Donnan Potential" (CDP).

An example in the field of CDP is an ion-selective membrane assisted method. In this case, instead of using salt-gradient, it is based on the principle of mixing solutions containing different concentrations of CO₂. Thus, mixing exhausted gas and air, the former holds CO₂ concentration higher than the latter[8], it is possible to get mixing energy which is released since the Gibbs energy is lower than those of the two original solutions. In order to harvest this energy, both CO₂ emission and air are kept in touch through aqueous electrolyte[8]. As well known, once CO₂ is sparged in aqueous solution the produced carbonic acid dissociates into protons (H⁺) and bicarbonate ions (HCO₃⁻) leading to an increasing of ions concentration in solution. In order to exploit this result, the setup of this technology is characterized by ion-selective membranes urging the diffusion of the ions into different carbon based electrodes[8]. The resulting difference in ion concentration between the air-flushed solution and the CO₂-flushed solution brings to a membrane potential and so a spontaneous current flow. In details, the setting (Fig.1.4a) is made up of two reservoirs containing different water-based solutions, one is air-flushed and the other is CO₂-flushed. Each one is linked to a capacitive electrochemical cell.

The cell, however, consists of two carbon-based electrodes specified by a cation-exchange membrane (CEM) and the other with an anion-exchange membrane (AEM), which allow the transfer of the respective specific species through the membrane. While a spacer in between is employed to pump through the solutions. Exposing alternately the cell to air-flushed water and CO₂-flushed one (5 min for air

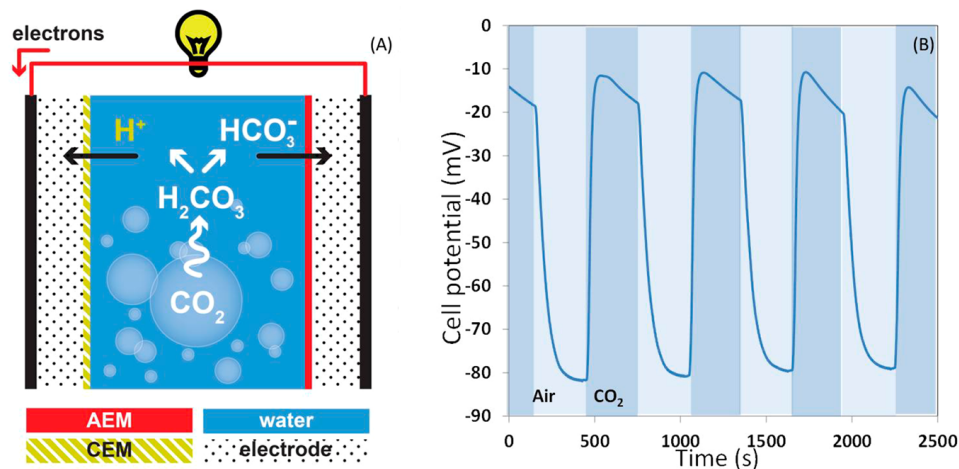


Figure 1.4: (a) Schematic of capacitive electrochemical cell. (b) Measured open circuit voltage[8].

and CO_2), the open circuit voltage (OCV) is assessed measuring the cell potential by connecting the two electrodes via an external load (R_{ext}). In figure 1.4b, the light blue region represents the air-flushed phase whereas the dark blue region is related to the CO_2 -flushed phase. Together these phases build up a cycle [8]. Repeating the OCV measurements over several cycles, what can be observed is that the OCV response is repeatable, showing in particular the differences depending on the alternation of the flushed solutions. Indeed, the maximal OCV values are observed exchanging the air-flushed solution with the CO_2 -flushed solution. However, this approach is not suitable due to the low energy efficiency as the process of sparging gas into the electrolyte gives rise to a higher energy consumption than the energy produced. Thus, the gas transport of the gas into the electrolyte needs to be improved mainly at the membrane-electrode interface. Such enhancement of power density can be obtained by boosting the absorption of CO_2 on the part of the electrolyte [8].

Anyway, Capacitive Mixing is a technique designed especially to be applied with super-capacitors, which are the subject of the next chapter. Moreover, the idea developed in this thesis is to change the aqueous solution with an Ionic Liquid engineered to absorb CO_2 and analysing a behaviour which is similar to one observed in aqueous system.

Chapter 2

Electrochemical Devices based on Electrical Double Layer

Electrochemical Capacitor (EC) named also Super-capacitor is a device with a growing interest because of its properties such as long cycle life, high energy effectiveness, high power during charge and discharge and robustness. It can be classified in Electric Double-Layer Capacitor (EDLC), Pseudocapacitor and Hybrid capacitor, so a combination of previous ones. EC is characterized by electrode-electrolyte interface, huge surface area (SA) and thinner dielectric, giving rise to a very high value of capacitance, and thus of energy, with a factor of 10^4 with respect to a common capacitor. High energy capability and low Equivalent Series Resistance make this device attractive. However, the energy storage mechanism is always determined by the charge migration and accumulation. For the assembling of this component, carbon-based materials are used [9].

2.1 Electric Double Layer Capacitors

Electrical Double-Layer Capacitor (EDLC) is well explained by Helmholtz double-layer model characterized by the opposite charged layers in correspondence of the electrode-electrolyte interface. Then an improving was introduced by Stern highlighting better the ion distribution of the system which is composed by two regions: the inner region called compact layer and a diffuse layer. In the former, ions (counterions) are strongly adsorbed at electrode surface, while in the latter ions are free to move driven by thermal motion. Thus, the capacitance at electrode-electrolyte interface (the double layer capacitance, C_{dl}) is affected by two

components (Fig. 2.1), so the Helmholtz double layer capacitance (C_H) and the diffuse region capacitance (C_{diff}) which can be molded in series. Obviously, C_{dl} is also affected by electrode material, electrode area and electrolyte properties.

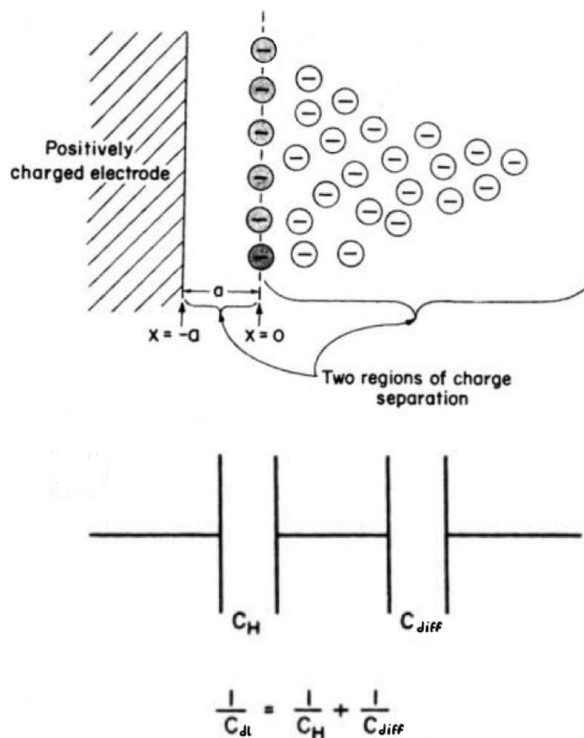


Figure 2.1: Helmholtz Gouy-Chapman Stern Model[10].

The pore is assumed being cylindrical and the distribution of capacitancies can be managed in an equivalent RC circuit as shown in fig.2.2. R_s is the series resistance related to bulk solution and C_{dl} is the double layer capacitance which is distributed on the overall pore wall surface [9]. As it can be observed through the model, the capacitance in proximity of the opening of the pore is less resistive than deeper capacitancies affected by additional resistive contributions. The main characteristics of an EDLC, allowing higher energy storage, are large amount of stored charges on the electrode surface due to high material porosity thus the effective area is much wider than a traditional parallel plate capacitor and very small thickness of the electrical double-layer at the interface electrode-electrolyte. The simplest EDLC is made up of two porous electrodes divided by an ion-permeable separator, in order to prevent short circuit of electrodes, which is soaked with an electrolyte. Applying a voltage across the electrodes cations (positive ions) and anions (negative ions) are attracted towards negative and positive electrodes, respectively. This motions means the realization of two EDL in correspondance

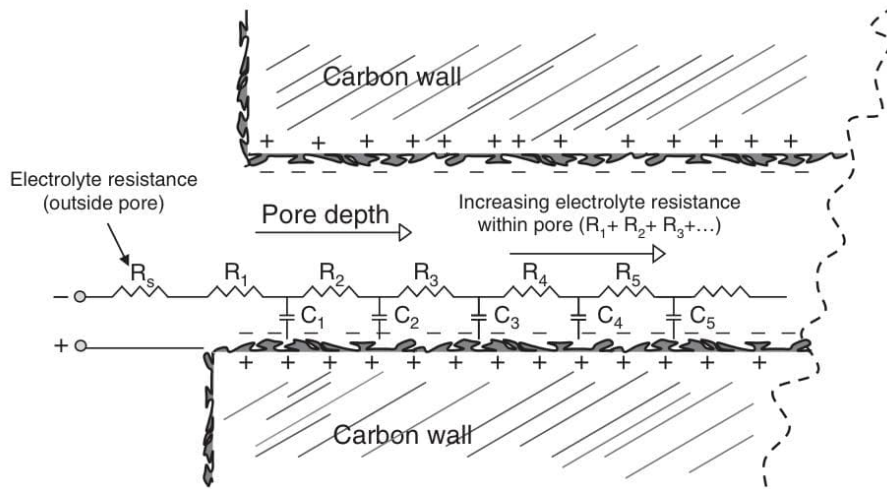


Figure 2.2: Model of a cylindrical pore and distributed capacitance [9].

of the two electrode-electrolyte interfaces, modeled as capacitors in series. In the case of a symmetrical capacitor then the overall capacitance of the cell (C_{dl}) can be computed as $\frac{1}{C_{dl}} = \frac{1}{C_+} + \frac{1}{C_-}$. Because of the symmetry, it can be assumed $C_- = C_+ = C_e$ and thus the cell capacitance is $C_{dl} = C_e/2$.

The measure unit of a capacitance is Farad (F) but usually the provided parameter is the specific gravimetric or volumetric capacitance, for example in the case of electrode capacitance (C_e), the specific capacitance can be C_e ($F g^{-1}$) = $2\frac{C_{dl}}{m_e}$, called gravimetric capacitance, C_e ($F cm^{-3}$) = $2\frac{C_{dl}}{V_e}$, called volumetric capacitance,

C_e ($F cm^{-2}$) = $2\frac{C_{dl}}{S}$, called capacitance per unit area. Where m_e is the mass in gram, V_e is the volume of the active material and S is the single electrode surface area [9].

In fig.2.3, the model of EC is characterized by the so called faradic resistance $R_{f+/-}$ besides the EDLCs ($C_{+/-}$) and the ESR (R_s). In particular, $R_{f+/-}$ are considered being responsible of the discharge of the cell. The performances of EDLC depends on two main factors, so the active material of electrodes, as higher porosity and size of pores determine the charge storage capacity and so the capacitance of the EDLC, and the used electrolyte, in terms of concentration of ions, viscosity and permittivity, affecting the capacitance but mainly the operational voltage and ESR. Other sources of non-ideality are intrinsic electronic resistance of the active material, the resistance at the interface between active material and electrode, the resistance of moving ions in the diffusion layer within the pores [9].

Regarding the material of which the electrodes are made, it is Activated Carbon (AC) which is the most used material for EDLC thanks to its chemical and electrical properties. When characterized by fine pores, AC shows high area-to-volume ratio which is very meaningful for EDLC applications. In general, this means an

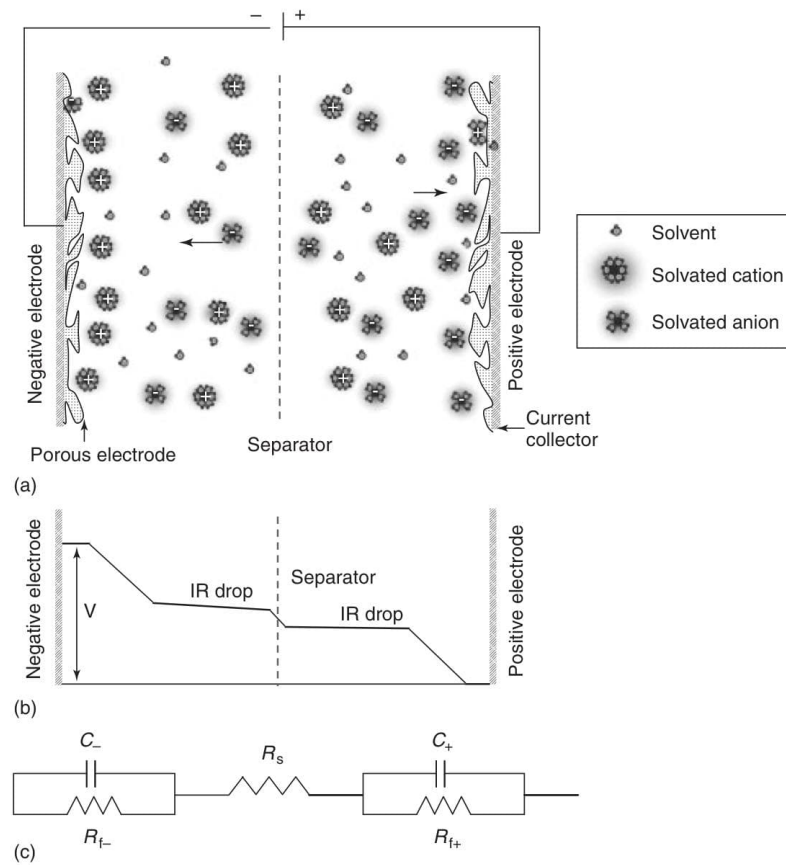


Figure 2.3: Model of an electrochemical double layer supercapacitor [9].

improving of the specific capacitance since it is proportional to surface area, pore size and electrical conductivity.

2.2 Pseudo-Capacitors

Pseudocapacitor is a redox based supercapacitor, meaning that it is owing to a charge transfer phenomena sired by fast reversible redox reactions involving the active material available on the electrode surface. The faradaic charge transfer comes from thermodynamic processes. By Charging, the redox materials on the electrode surface are reduced to lower oxidation state. Then, during discharge the process is reversed [11]. Since charge storage mechanism is mainly faradaic then the behaviour of this supercapacitor is more like a battery instead of EDLC, even if the double layer is not entirely absent at the interface between electrolyte and electrode surface [9]. Indeed, pseudocapacitive materials are marked by both

surface controlled and diffusion controlled processes (Fig. 2.4).

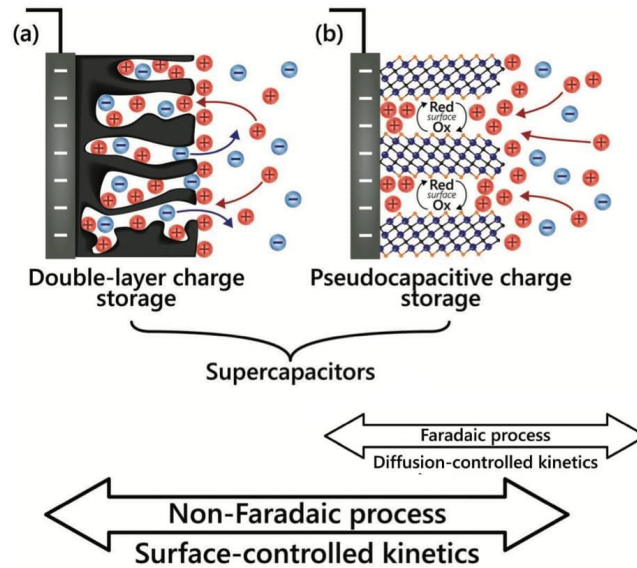


Figure 2.4: Presentation of kinetic phenomena occurring at the surface of a) electrical double layer capacitance and b) pseudocapacitance [12]

Therefore, the electrochemical response of pseudocapacitive systems is similar to capacitive one but with some significant differences that allow us to distinguish from other types of supercapacitors [12]. The key features of a pseudocapacitive

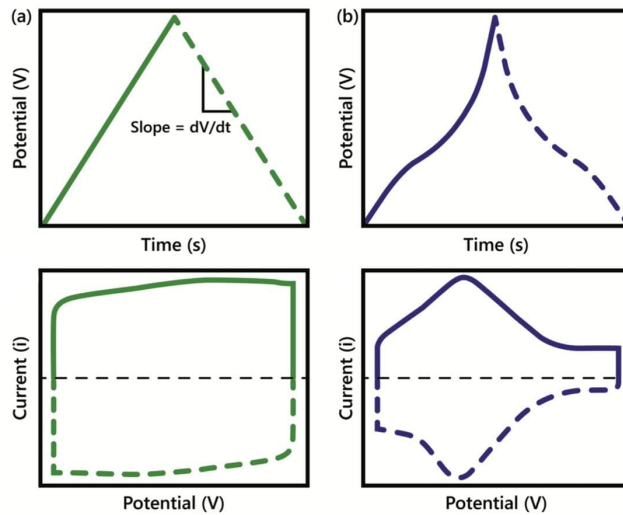


Figure 2.5: Illustration of typical CCD and CV responses in a) electrical double layer capacitance (green curves) and b) pseudocapacitance (blue curves) [12].

material are linear peak of the current vs scan rate curve, symmetric redox peaks in Cyclic Voltammetry (CV), reversible charge transfer and Nyquist plot similar to capacitive material one. In addition, a non-linear CCD response implies the adjustment of the capacitance as the voltage changes in a pseudocapacitive system but generally the capacitance measured by a faradaic material is higher than one associated to a non-faradaic material which however shows a longer cycle life [12].

2.3 Hybrid-supercapacitors

By definition a Hybrid Supercapacitor is a combination of a Double Layer Capacitor and a Pseudocapacitor with the the intent of exploiting the strengths of the two materials. Usually, the system is built using two electrodes made of different materials.

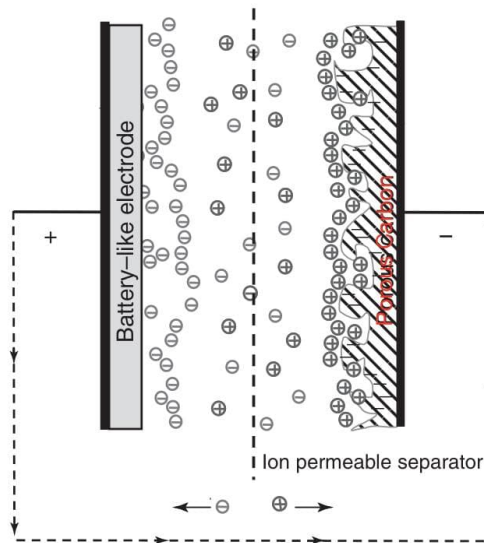


Figure 2.6: Schematic of Hybrid Supercapacitor [9]

One is a battery-type electrode, whose charge storing depends on faradaic processes, while the other one is a carbon based electrode characterized by EDL collecting and releasing charge electrostatically (See Figure 2.6). Therefore, the charge storage mechanism of this device is a combination of two different types of charge storing. Since the capacitance of a faradaic material is much larger than carbon-based one then the total capacitance of the system is approximate only to that of non-faradaic electrode resulting higher than one of the EDL Capacitor, mainly in the case of a symmetric cell. This leads to an increasing of the specific energy density. Anyway, in order to balance the capacitance mismatch often a gravimetric balancing is adopted making the activated carbon electrode thicker [9]. The results, obtained through the combination of these two different capacitive genres, open the doors to

a new promising capacitive system with a very high capacitance, also in the order of kFarad, and therefore a very huge energy density (feature of a Pseudocapacitance) and a longer cycle life (peculiarity of EDL Capacitors) [11].

Chapter 3

CapMix Techniques

Capacitive Mixing (CapMix) is a technique developed to extract a huge amount of energy by means of mixing two solutions characterized by a gradient. This technology often exploits fluidic super-capacitor devices allowing the flow of the solution characterized by different concentrations of ions, gas or pH. These apparatus are based on phenomena which are "Capacitive Double Layer Expansion" (CDLE) and "Capacitive Donnan Potential" (CDP).

3.1 Capacitive Double Layer Expansion

Capacitive Double Layer Expansion (CDLE) is a technique depending on saline concentration applicable with Electric Double Layer (EDL) Supercapacitor. The fundamental relationship of a capacitor is $Q = C \times V$. Thereby, when the system is in open circuit then the charge is constant and consequently potential and capacitance have to change in order to preserve the charge. From this effect it is possible to take advantage through Electric Double Layer Expansion technique since reducing the capacitance then the growing of the potential is induced to keep constant the charge. Subsequently, the increase of the voltage leads to a gain of electrochemical energy ($E = \frac{1}{2}QV$). Brogioli achieved this result building a cell able to develop a four-phase cycle process [7]:

1. The cell is filled with salt water and charged up to a well defined potential V_{charge} by an external power supply allowing the storage of charges on the electrodes surfaces;
2. The device is placed in open circuit condition meaning a constant charge, so the accumulated charge remains the same on the electrodes. Meanwhile, salt water is replaced with fresh one causing the enlargement of the EDL. This magnification produces a decrease of the capacitance. Such assumption

is possible if the system is modeled as a parallel face capacitor. Thus, the capacitance is inversely proportional to the distance between the two planes meaning that a capacitive dropping gives rise to a growing of the voltage, called "Rise Voltage", keeping true the relationship $Q = C \times V$, as well as the amount of stored energy;

3. Subsequently, the cell is discharged to the initial potential (V_{charge}) by extracting the cell energy;
4. The cell, again in open circuit, is flushed with salt water. In this case, the increase in salt concentration causes a narrowing of the EDL due to coulombic forces. Therefore, through the same assumptions made in point 2 it is possible to assume an increase in capacitance and therefore a reduction in voltage in order to keep the charge constant being the system in OCV.

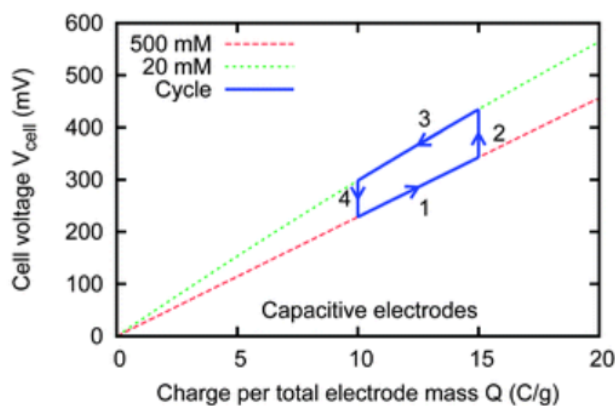


Figure 3.1: Ideal Charge vs Voltage response for CDLE[13].

As shown in Fig.3.1, one of the most significant plot for the understanding of the phenomena. What is of particular interest is the discharging curve, which is characterized by voltage values higher than one related to the charging phase. Among the leading issues of the CDLE technique is the need to exploit an external power supply and leakage current. The latter is the main cause of lack of ideality of the device since the stored energy is not totally recovered thus part of energy is lost. Because of the leakage current a continuous counteracting action by the external power supply is need, meaning an increasing of power loss. One of the origin of the leakage current is due to the presence of a "spontaneous potential" of electrodes, to which the latter drift upon long time [13]. For this reason activated carbon electrodes can not be ideally biased. Anyway, through the Fig.3.2 it is possible to observe the effect of the leakage current on the feasibility of the process. Indeed, the V_{cell} vs Q curves move rightward because of charge loss linked to leakage. So,

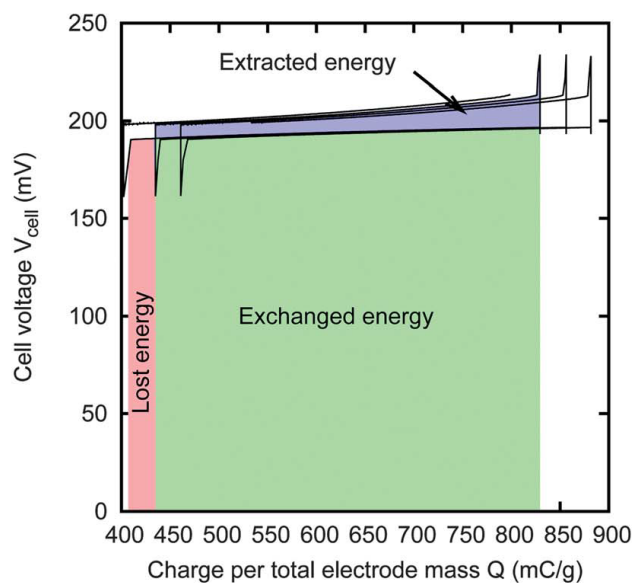


Figure 3.2: Ideal CapMix cycle Voltage vs Charge and exchanged energy [13].

after each cycle the amount of extracted charge is lower than provided one to the cell during the charging phase. According to Brogioli [13] the identified causes are Faradaic reactions taking place on the surface of the carbon electrodes. So, another source of leakage is redox reaction in correspondence of the electric double layer. Thus, the exploitable energy is only one enclosed in the cycle highlighted with blue. While the red area is the lost energy due to the leakage. However, in

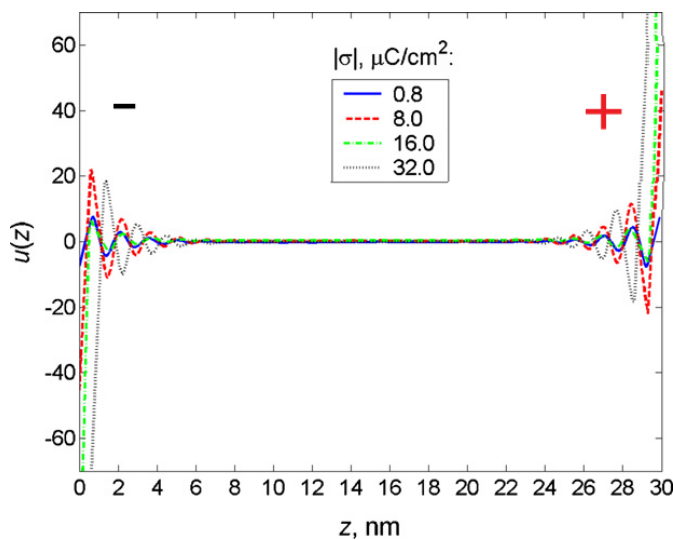


Figure 3.3: Potential profiles across two electrodes in IL bulk direction [10].

this study the used electrolyte is an Ionic Liquid (IL) and the Electric Double Layer (EDL) is obtained by means of ions screening the electrode charges. More precisely, being the IL composed only of ions, thus interactions are not softened by the presence of solvent. This leads to a dual effect: the over-screening, consisting in an excess of screening charges with respect to electrode one, and an alternate distribution of the counter-ions layer with co-ions layer which decay exponentially from interface toward the bulk of the IL as shown in Fig.3.3 [10]. The low cost of the activated carbon materials makes CDLE a very promising method to extract power but issues as leakage current must be solved because applying a greater external voltage also the voltage rise increases same time as the leakage.

3.2 Capacitive Donnan Potential

Capacitive Donnan Potential (CDP) is a technique exploiting electrodes made of activated carbon layer separated by the electrolyte through an Ion Exchange Membrane (IEM). The latter is characterized by an intrinsic potential called Donnan Potential determining the voltage vs time relationship. IEM enables the migration by electro-diffusion of only one kind of ion from the electrolyte to electrode and therefore it is possible to distinguish in Anion Exchange Membrane (AEM) and Cation Exchange Membrane (CEM) [7] (Fig. 3.4a). Thus, thanks to the Donnan Potential this technique works without external supply as it is enough to give rise to an ionic current arranging between two vessels with different salinity separated by an IEM. In CDP ions are stored both in EDLs, at the interface between the

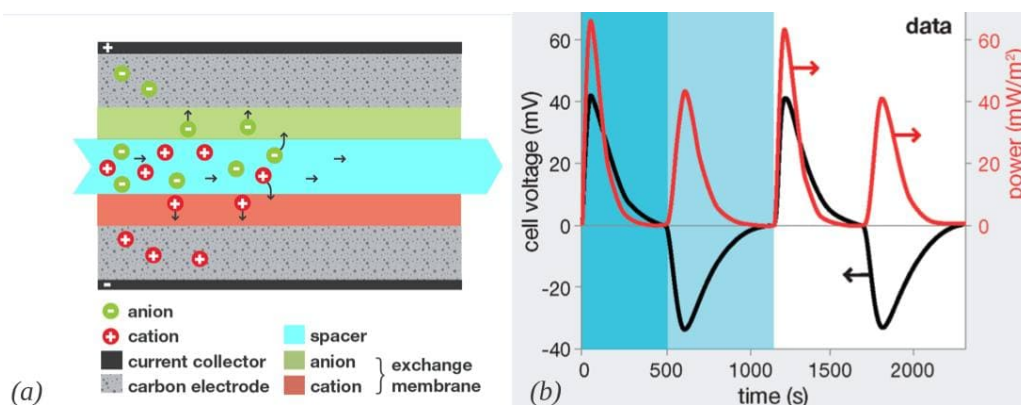


Figure 3.4: (a) Schematic view of a Capacitive Donnan Potential-based Cell. (b) Power production through CDP CapMix [7].

pores of activated carbon electrodes and electrolyte, and in solution between carbon layer and IEM as illustrated in Fig.3.5 [13]. Hence, switching alternately salt and fresh water voltage variations occurs as in the case of CDLE but without any

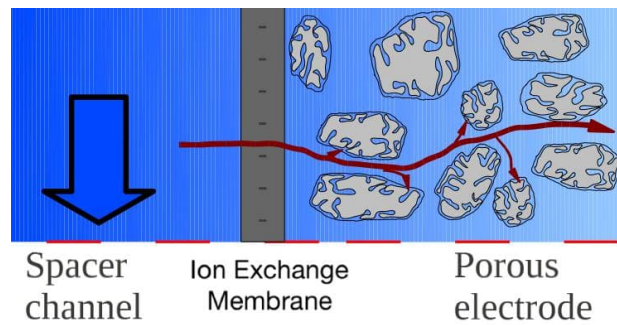


Figure 3.5: Electro-diffusion of ions through Ion Exchange Membrane at spacer channel-electrode interface [7].

external voltage during the charging step since ions spontaneously move under the effect of the IEM (Fig. 3.4b). The working principle of the CapMix can be easily understood by looking at the Figure 3.6. Starting with the cell in equilibrium condition and with fresh water the system shows the potential profile at point 1. AEM has a positive potential with respect to electrode one allowing anions to be attracted, viceversa CEM has a negative potential with respect to electrode one allowing the attraction of cations. Flushing the saline water (point 2) in the

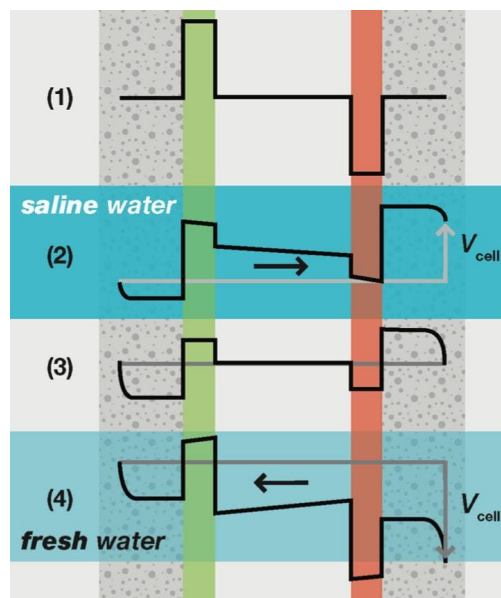


Figure 3.6: Electrostatic potential profile across the cell playing CapMix [14].

reservoir, the potential rises positively across the cell leading to a positive current which forms EDLs in porous of electrodes bringing back the cell at equilibrium

(point 3). Changing again to fresh water (point 4), the cell potential is reversed until the EDLs are again uncharged [14]. Both with positive and negative potential electrical power is produced as shown in Figure 3.4b.

Chapter 4

Performance Evaluation

The evaluation of an EC performances is performed through some fundamental parameters which are the total cell capacitance (C_T), the Operating Voltage Window and the Equivalent Series Resistance (R_{es} or ESR) used to determine Power and Energy Densities. These parameters can be extracted by means of well defined measurement techniques such as Cyclic Voltammetry (CV), Constant Current Charge/Discharge (CCCD) and Electrochemical Impedance Spectroscopy (EIS). Each of the above cited key factors and test methods, which have been performed through the VMP3 potentiostat of BioLogic, are well explained in the following paragraphs as the subject of this chapter.

4.1 Key Performance Metrics

4.1.1 Total Cell Capacitance

The capacitance may be defined as the proportionality constant of a dielectric or electrolyte capacitor according the relationship

$$C = \frac{\delta Q}{\delta V} = I(\frac{\delta V}{\delta t})^{-1}$$

but in the case of Supercapacitor (SC) is more correct speaking of Total Cell Capacitance (C_T) which is suggestive of the storing capability of the device. Usually, instead of showing the C_T it is more useful the Specific Capacitance (C_S) derived by the ratio

$$C_S = \frac{C_T}{\Pi}$$

where Π can be the mass, the volume or the surface of the electrode as stated previously in Paragraph 3.1 "Electric Double Layer Capacitors". The C_T can be computed in many ways. One suggested by Ref[11] is expressed by the equation

$$C_T = \frac{\int_0^{t_o} |i(t)| dt}{2V_o}$$

where t_o is the time needed to charge or discharge the SC with V_o the maximum amplitude of the applied voltage during CV test as depicted in Fig.4.1a.

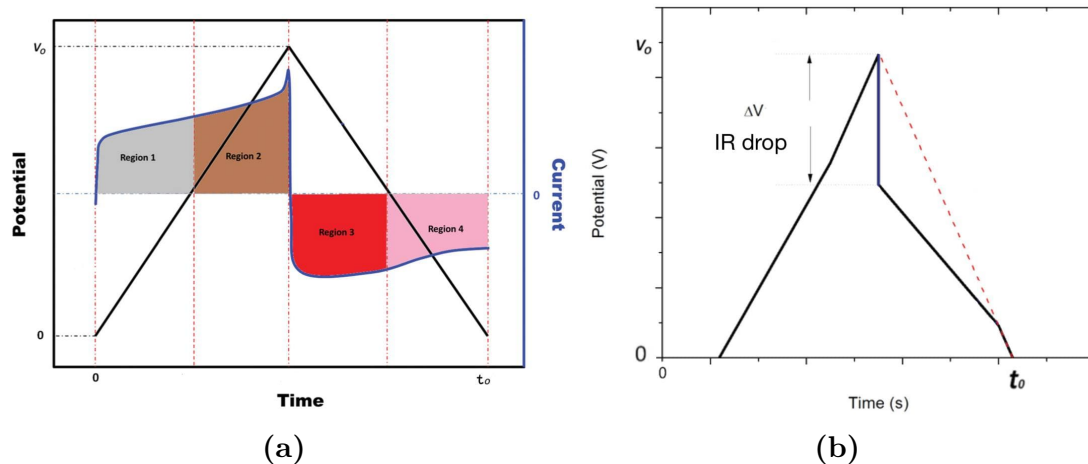


Figure 4.1: (a) Ideal Voltage vs Time response of a CV test for a EDLC system. (b) Voltage vs Time response of a CV for a EDLC system affected by IR drop [11].

Anyway, EDLC based device obtained through the development of molecularly thick Helmholtz double layers should have an answer similar to one of a parallel-faced plane dielectric capacitor [12]. Nevertheless, because of some parasitic the Voltage vs Time curve is not perfectly linear meaning that the slope dV/dt varies, and consequently also the capacitance, as voltage changes. Thus, in order to get as precise as possible capacitance value the adopted method involves the calculation of the exact energy and charge during the discharge phase so that [15][16].

$$\begin{cases} E = \int I v dt \\ Q = \int I dt \end{cases} \rightarrow E = \frac{1}{2} \frac{Q^2}{C} \rightarrow C = \frac{1}{2} \frac{Q^2}{E}$$

4.1.2 Operating Voltage Window

The Operating Voltage Window (OVW) or Operating Potential Window (OPW) is the maximum range of applied potential within the system has to work so that it can operate correctly. It can be estimated through both CCCD and CV tests. Regarding our results only CV is used. Basically, this parameter can be determined using a three electrode system applying a constant gap rising increase of the potential and then evaluating the resulting Coulombic Efficiency (η) and CV imposing a threshold limit of 99% as efficiency. Another possibility proposed by Ref[12] consists

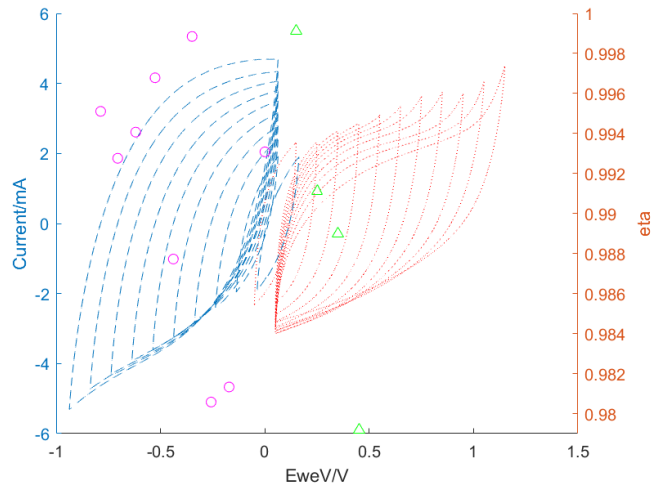


Figure 4.2: Example of Three electrode Cyclic Voltammetry and Coulombic Efficiency

in analysing the stability of the system response of a chronoamperometry test. This metric is mainly influenced by the design of the cell, the material of electrodes and size of the electrodes. For this reason, once the resulting data are extracted these are then used for the charge balancing determining the electrodes size with the aim to control the amount of cations and anions stored by the negative and positive electrode respectively.

4.1.3 Equivalent Series Resistance

The Supercapacitor, actually, does not behave like an ideal capacitor. Essentially, this device can be fashioned with an equivalent circuit characterized by an

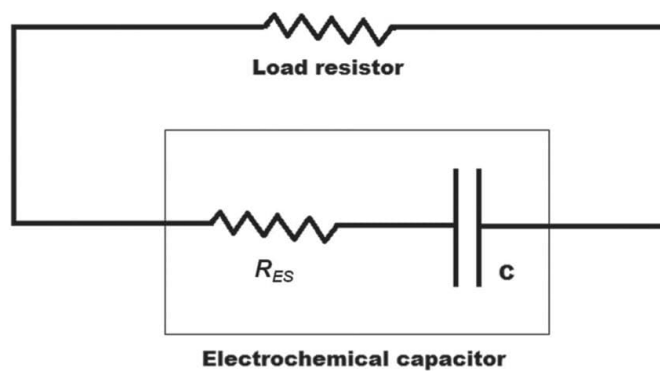


Figure 4.3: Equivalent Circuit Model of an electrochemical supercapacitor [11].

Equivalent Series Resistance (ESR) and an ideal capacitor placed in series [11]. The former is due to the total internal resistance of an electrochemical cell and it is the main responsible for the dissipation of the stored charge lowering the Coulombic Efficiency, and so the performances of the device too, and because of its voltage drop it introduces an upper limit to capacitor voltage during discharge, limiting the maximum power and energy released by the device [12][9]. This undesired effect is observable through CV test since the I vs V curve resembles more to diamond instead of a rectangle (Fig. 4.2). For this reason, the goal is to design the cell and select materials in order to make it as small as possible. A suggested method foresees the use of the EIS investigating the real part ($\text{Re}(Z)$) of the Nyquist Diagram when the Imaginary part ($\text{Im}(Z)$) is null [11] as explained by the Figure 4.4.

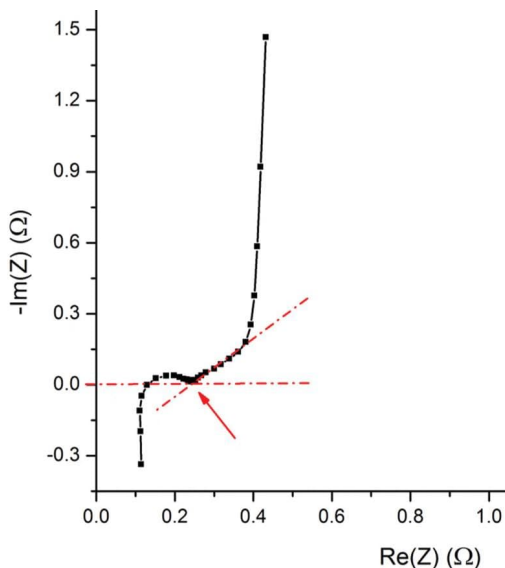


Figure 4.4: Approach to determine the ESR in SC using EIS [11].

4.1.4 Time Constant

The Time Constant τ is defined as $\tau = R_{ES}C_T$ for a supercapacitor and it gives information on how fast is the response of the device. This estimation is made by assuming to model the system as a RC equivalent circuit and therefore the parameter defines the transient of the circuit. Thus, after $t = 4\tau$ it is possible to account the system completely charged or discharged [11].

4.1.5 Power and Energy Density

Power and Energy density are the meaning full parameters to evaluate and compare the efficiency and the performances of a SC device. Referring to Power Density, it is derived as [11]

$$P = \frac{V_o^2}{4\Pi R_{ES}}$$

While the energy is derived by integration of CCCD or CV curve. In case of an EDLC based SC the charging and discharging curve should be linear allowing to compute the stored and realised energy as [11]

$$C_T = \int_0^Q V_o dq = \frac{1}{2} V_o Q$$

since the integral corresponds to the area of a triangle (Fig.4.1b). But being a non-ideal system then the CCCD curve has a slight non-linearity and for the sake of precision the equation used for an accurate computation of the energy density is

$$E = \frac{\int_0^{t_o} v I dt}{\Pi}$$

where t_o is the fully charging or discharging time. Subsequently, the energy so calculated is divided by 3600 seconds to convert the energy in Joule to watt hour

$$E = \frac{\int_0^{t_o} v I dt}{3600\Pi}$$

4.1.6 Coulombic Efficiency and Energy Efficiency

The Coulombic Efficiency is the ratio between delivered and stored charge

$$\eta_C = \frac{Q_{Dis}}{Q_{Ch}}$$

Ideally its value has to be equal to 1 related to an efficiency of 100%, but because of parasitic events the extracted value is always just below 1. Among the widely recognized causes there are a huge ESR and leakage current due to cell assembly issues [11] such as a parasitic resistive path. With the purpose of optimizing η_C , and hence also the Energy Efficiency, it is necessary to look for a proper Operating Voltage Window for the system under study ensuring to obtain as much as possible a rectangular-shaped CV curve and a η equal or grater than 99%.

This can be done by choosing an appropriate combination of electrolyte, electrodes, separator and amount of electrolyte.

$$\eta_E = \frac{E_{\text{Dis}}}{E_{\text{Ch}}}$$

The Energy efficiency η_E , defined as the ratio between the given energy and stored one, is another figure of merit which can be useful to identify the electrochemical window, checking when its value is below a well defined limit value.

4.1.7 Leakage Current and Self-Discharge

A well known problem affecting EDLC-based Electrochemical Cell (EC) is the self-discharge defined as the dropping of the voltage in open-circuit configuration once reached the charged state at a desired potential V_o . Considering the dependence of the voltage as function of the time describing the discharge of a dielectric or electrolytic capacitor, the following equation should illustrate a linear characteristic in time

$$\ln\left(\frac{V(t)}{V_o}\right) = -\frac{t}{RC}$$

where V_o is the initial voltage at which the device has been loaded.

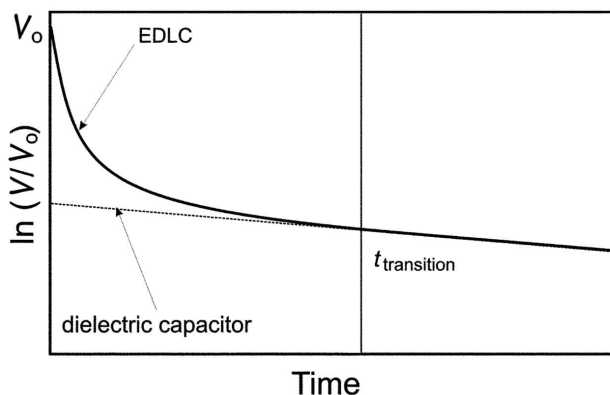


Figure 4.5: Dependence of the voltage as function of the time describing the discharge of an EDLC [15].

Instead, observing a realistic response of EDLC the self-discharge curve is not simply exponential since $\ln(\frac{V(t)}{V_o})$ is not linear but still exponential like mainly in the initial portion while it is linear in the final part which is distinctive of a capacitor (Fig. 4.5) [15]. This implies that besides ohmic leakage current other parasitic events contribute to the self-discharge of a SC such as Faradaic REDOX processes and Charge Redistribution.

- The ohmic leakage current is owing to a parasitic resistive pathway between the electrodes of an electrochemical cell because of faults during its assembling leading to a spontaneous dropping voltage [15].

- Faradaic Reactions are oxidation or reduction reactions occurring on the surface of the electrode giving rise to a self-discharge. Taking into account the positive electrode of a full cell (two-electrode EC), if its potential is higher than oxidation potential of the species in the electrolyte then such species oxidises on the electrode surface letting the migration of the electrons through the double layer up to the surface reducing the positive charge collected on it. Thus, the anions compensating the positive charge are in excess and so released causing Self-discharge. Similarly occurs on the negative electrode with cations but the characteristic phenomenon is the reduction [17].
- Charge redistribution is an effect arising from the non-uniformity charging of the electrode material. Indeed, the outer part of an EDLC is charged to required potential more quickly than bulk side. Thus, when the charge is switched off the system tends to the equilibrium balancing the discrepancy between surface and bulk. Therefore, the charges move toward deeper region of the material carrying out the self-discharge [17]. This effect is strictly dependant on the size and shape of the carbon electrode pores defining its diffusion resistance [17][16][18]. But this phenomenon is not always referred to a discharge. In fact, when a discharge up to null voltage follows the charging, then in the next open circuit it is possible to observe a spontaneous recovery of the voltage which means therefore an increasing voltage. This has been identified as a typical response of a RC system composed of distributed capacitors and resistors connected in "LADDER-LIKE" configuration [15]. This is a further confirmation of the model shown in the figure 2.2 in section "3.1 - Electric Double Layer Capacitors".

4.2 Test Methods

4.2.1 Cyclic Voltammetry

The Cyclic Voltammetry (CV) is a test characterized by the application of a linear potential in time with constant slope called scan rate (mV s^{-1}). Such potential is applied between positive and negative electrode for two electrode measurements while between working and reference electrode in case of three electrodes measurements and ranging for several successive Potential Windows [11]. The plot is current (A) vs voltage (V) as shown in fig.4.6. Starting from this plot it is possible to extract multiple information such as the Operating Potential Window (OPW), defined as the maximum applicable voltage before observing the redox peaks, which are the sign of electrode degradation in an EDLC. In particular, the OPW is identified exploiting three electrode measurement and imposing η_C equal to 99% as lower reference value. Other useful parameters derivable through the CV

are the Specific Capacitance and Coulombic Efficiency by integration of the CV curves [11] adopting two electrode configuration too. More in detail, examining

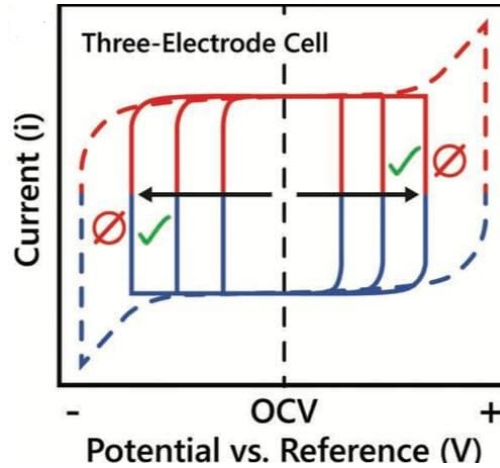


Figure 4.6: Determination of the operating voltage window [12].

the shape of the CV response curve it is possible to perform a first qualitatively check about the resistive and capacitive behaviour of the electrochemical cell. For an EDLC, an ideal result linked to a pure capacitive behaviour is featured by a rectangular shape of CV curve (Fig. 4.7a)

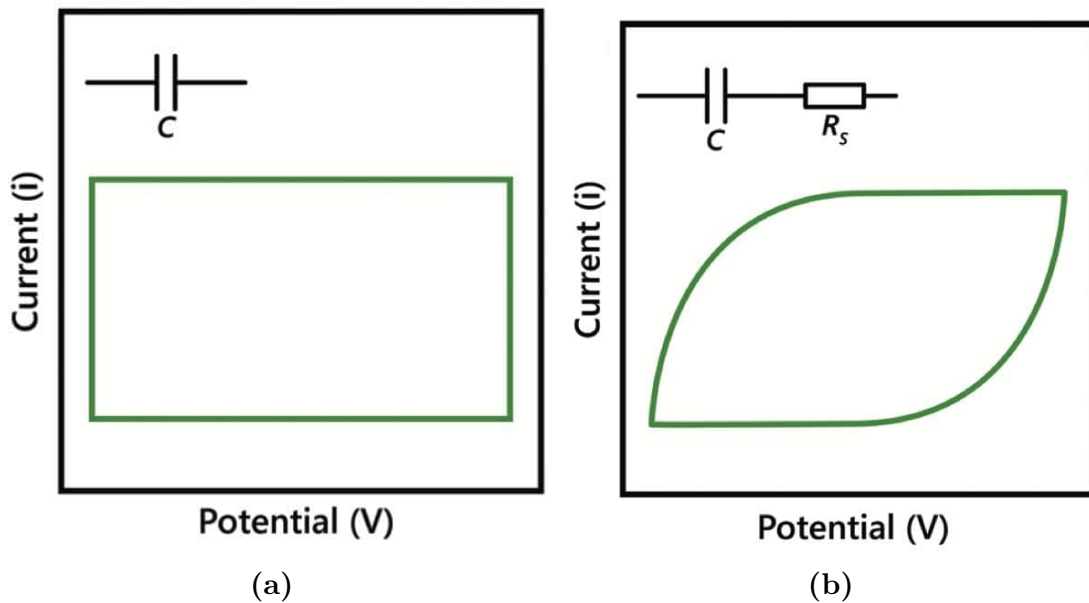


Figure 4.7: Equivalent circuit analysis for different cyclic voltammetry profiles. (a) Ideal capacitive system. (b) Blunt profile indicating the ESR presence. [12]

but, actually, it can be observed that the shape is more similar to rhombus one proving the presence of a resistive parasitic component as displayed in fig.4.7b .

4.2.2 Constant Current Charge/Discharge

Constant Current Charge/Discharge (CCCD) is a test consisting in repetitive charging and discharging of the SC device at constant current. Uncommonly, it is possible to find in literature the application of a constant voltage at the peak voltage value. Often, it is used to distinguish different charge storing mechanisms of a material and also the type of system which is analysed. In the specific case of the double layer SC, the CCCD response is characterized by a linear voltage vs time behaviour (Fig.4.1a) meaning that a single value of capacitance may be computed. While for non-ideal SC or pseudo capacitive materials, the CCCD curve is not linear with slope (dV/dt) varying as the voltage changes during charge and discharge and so the capacitance too. Indeed, CCCD curve shows plateaus for faradaic materials due to redox reactions (Fig.4.8b). Moreover, CCCD could be exploited to identify Operating Voltage Window since when the SC is overcharged it gives rise to a trend similar to Figure 4.8a in EDLC and so also a low value of η .

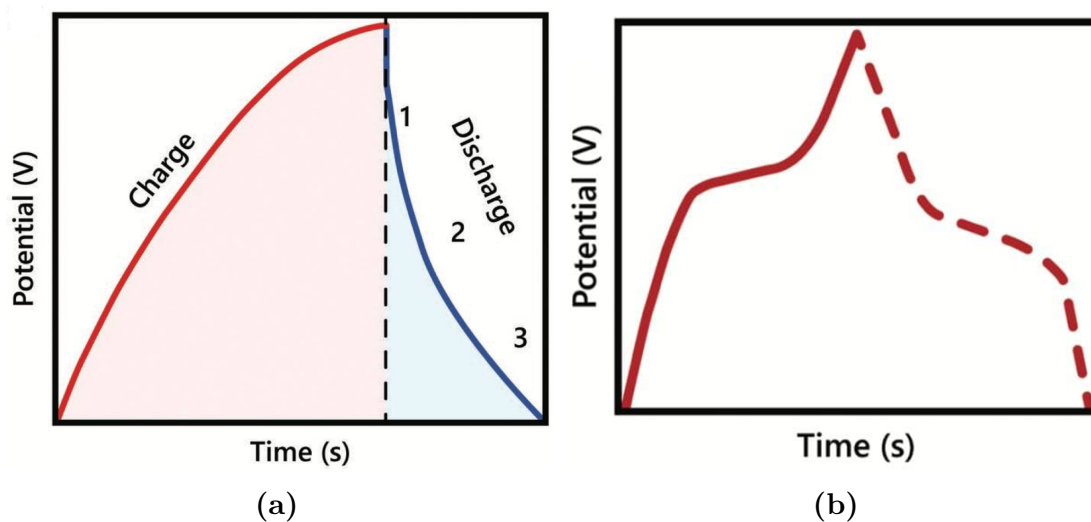


Figure 4.8: Examples of CCCD curve: (a) non-ideal supercapacitor; (b) faradaic system [12].

Other parameters which can be evaluated through this method are C_T and ESR, affecting the IR drop (Fig.4.1b). Such phenomenon is almost unavoidable when CCCD test is performed. This voltage drop depends heavily on the applied constant current and ESR. It occurs at the beginning of the discharge phase immediately after the peak of potential is reached. In addition, the test is widely used to

measure the Cycle Life and Capacitance Retention Rate of the SC device which can be easily evaluated by means of thousands of cycles which then are compared observing the adjustment of the capacitance [11].

4.2.3 Electrochemical Impedance Spectroscopy

Electrochemical Impedance Spectroscopy (EIS) is a method used to measure the impedance linked to the cell. Such impedance is evaluated as function of the frequency exploiting a small sinusoidal voltage overlapping a DC voltage equal to zero as input signal [11]. The aim is to determine the impedance of the device in a frequency range between 1 MHz and 10 mHz, with reference to our study. Further, the parameter of interest is represented by way of Nyquist Plot characterized by being a polar graph having the Imaginary part ($-\text{Im}(z)$) on the Y-axis and the Real part ($\text{Re}(z)$) on the X-axis both at different frequencies. As explained in previous section (4.1.3), one of the most important results deriving from EIS analysis is the ESR assuming to model the system as an ideal capacitor with a resistance in series.

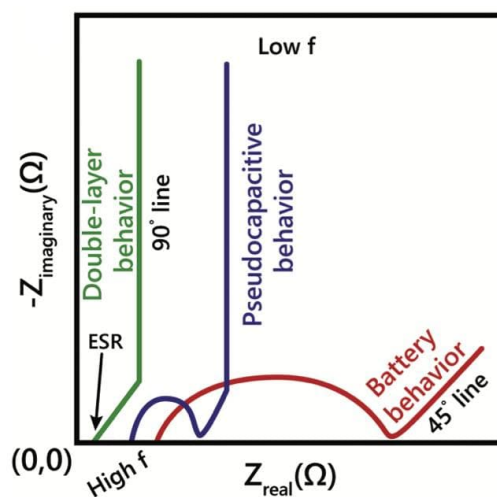


Figure 4.9: Electrochemical Impedance Spectroscopy plot examples [12].

As can be seen in Fig.4.9, an EDLC Super Capacitor should show a curve behaving like one depicted in green. Therefore any semicircle at high frequencies but solely a 45° line. So the ESR depends mainly on the diffusion of ions in the pores of the material used to develop the electrodes [16]. This EIS response distinguishes a system with a good accessibility of the electrolyte molecules to the reactive sites in short time giving rise to the expected interfacial phenomena [12]. When semicircle occurs in Nyquist plot in presence of a EDLC based system then it is due to interfacial contact resistance as a consequence of assembly issues. In addition,

the pressure deriving from assembling is another affecting parameter to take into account since it can influence the high frequency impedance [12].

4.2.4 Potentiostatic Floating Test or Float Conditioning Test

This technique is adopted to afford the charge redistribution among the activated carbon pores. This entails an enhancement because the subsequent open-circuit self-discharge is much lower. Thereby, the Potentiostatic Floating Test allow a smoothing of the charge redistribution phenomenon and in turn of the self-discharge. This result is as effective as the HOLDING TIME is longer until an optimal value is reached [15]. It is noted that the Float Leakage Current is huge at the beginning but then decays soon up to steady-state current. In the first part it is due to the interaction with immediately outer part of the electrode, so the surface, being the most affordable, and the macro pores characterized by a low diffusion resistance [17][16][18]. Overtime, the charges are able to move also in pores with smaller size ensuring the fully charge of AC material and as consequence the reduction of the leakage current due to charge redistribution. This leakage current decay occurs in milliseconds. Based on that, this procedure may be useful in order to evaluate the charge redistribution of the studied system [17]. Regardless, it is necessary to pay attention to the voltage applied amplitude of the Floating Test as a too high potential can cause the degradation of one or both electrodes in case of using of three or two-electrode measurements respectively. Such residues can diffuse easily in mesopores increasing the leakage current manly when it is metallic particulate matter [18].

Chapter 5

Setup

The electrochemical cells used to perform the measurements described in the previous chapter are manufactured by EL-cell GmbH. The characterization of the material used to realize the electrodes is carried out through a three-electrode cell, while a full cell or two-electrode cell is exploited for the study of the CapMix procedure on the EDLCs base device and its characterization. Both devices are tailored to target circular electrodes with a diameter 18mm. Therefore the working electrode of a half cell has a 18mm diameter while the full cell is assembled with 18mm and 12mm electrodes as consequence of the following charge balance analysis but both in Gas Diffusion Layer (GDL). Then, in the middle a separator is placed as well produced by EL-cell and soaked with an Ionic Liquid (IL).

5.1 Cells

5.1.1 Three-electrodes Cell

The three-electrode cell is the PAT-cell composed of a working electrode, consisting in the material under study, a counter electrode and a reference electrode with respect to which the working electrode potential is recorded as shown in the figure 5.1 on the left.

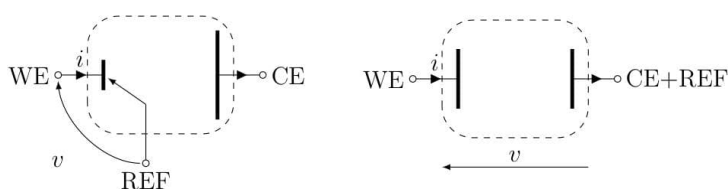


Figure 5.1: Electrical configuration of three-electrodes cell (on the left) and two-electrodes cell (on the right) [19].

One of the most significant component of the PAT-cell is the PAT-Core which is designed in order to be available by means of dedicated contact areas at the cell bottom. The intent of the PAT-Core is to contain and keep aligned the electrodes, the separator and the electrolyte. The use of the PAT-cell is made only through PAT-Stand which is a socket to link the cell with the external equipment.

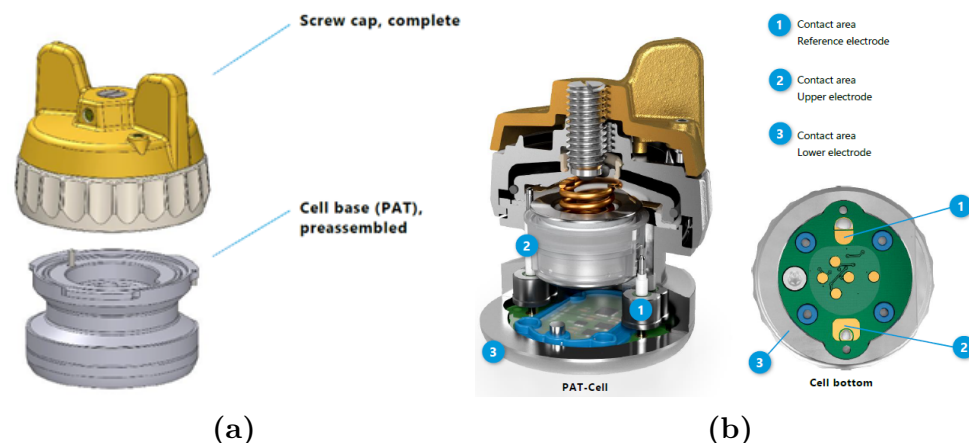


Figure 5.2: (a) PAT-cell. (b) Overview of the PAT-cell electrical contact area [20]

The Core itself is made up of other components which are the plungers, whose purpose is to contact the electrodes with the external probes, and the sleeve yielding the reference contact and keeping the separator.



Figure 5.3: PAT-Core components:(a) Upper plunger. (b) Sleeve. (a) Bottom plunger. [20]

5.1.2 Two-electrodes Cell

The exploited two-electrode cell is the ECC-Air. The cell stores the negative electrode, the positive one and a separator in between. Its electrical scheme is shown in the figure 5.1 on the right. The upper part of the cell, called lid, is featured by four holes two in order to contact electrically the cell and the remaining to flux gases inside through the gas inlet and a gas outlet to drain out it, so that

the compressed gas can diffuse from the backside of the gas diffusion electrode and leave the cell going out by the siphon as shown in figure 5.4a.

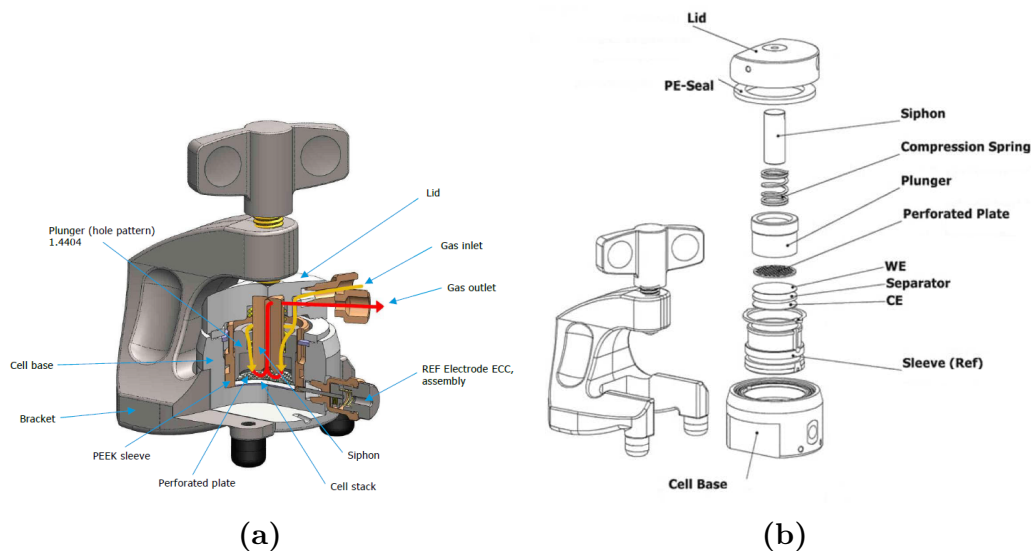


Figure 5.4: ECC-Air components overview. [20]

5.2 Separator

The separator used to assemble the SuperCapacitive Cell is FS-5P which is a double-layered material made up of a layer of FS2226 E being a nonwoven polypropylene (PP) with porosity of 67% and thickness of $180\mu\text{m}$, while the second one is UHMW-PE (Lydall Solupor 5P09B) which is a microporous membrane of polyethylene whose porosity is 86% and thickness $38\mu\text{m}$ [21]. Thus the overall thickness of the separator is about $220\mu\text{m}$. It has been chosen with the aim of ensuring a low contribution to ESR which may be inferred observing the provided table [21] pointing out such material as ideal to perform EIS analysis both in full-cell and half-cell. Moreover, its duty is to hold the electrolyte and avoid any short circuit between the electrodes. Among the additional properties making this material suitable for fuel cell applications there is an excellent wettability due to high porosity and specific treatment of the PP fiber [21]. Further, this separator has been extensively tested in a previous study underlining how it enables a wide potential window, including the application range of the device under study, characterized by a coulombic efficiency higher than 95% [22].

5.3 Gas Diffusion Layer

The device under study is a Fuel cell used to perform the Capacitive Mixing procedure fluxing gases. Thus this system has to allow the flowing through the upper electrode up to the electrolyte as depicted in Fig.5.4a. For this purpose Gas Diffusion Layer (GDL) as electrodes' material is exploited. Two kinds of GDL has been tested, SIGRACET GDL 24BC and EQ-bcgdl-1400S-LD which will be subsequently labelled as Hard GDL and Flexible GDL for simplicity.

5.3.1 Hard GDL

The SIGRACET GDL 24BC is developed by FUEL-CELL. It is a microporous carbon based material with porosity of 76%, air permeability of $0.6 \text{ cm}^3/(\text{cm}^2\text{s})$ and a thickness of $235 \mu\text{m}$. From the electrical properties point of view the sheet resistance is lower than $12 \text{ m}\Omega \text{ cm}^2$. Moreover, another helpful property is the hydrophobicity obtained through hydrophobic treatment of the substrate by PTFE coating since it is directly in contact with IL [23]. In previously works [22][19] this material has been studied assembling a half-cell featured by a 18mm diameter circular electrode made of Hard GDL, FS2226 as separator and the Ionic Liquid DABCO-IM as electrolyte (see section 5.4). These highlight a coulombic efficiency higher than 95% for an Operating Voltage Window ranging between -1 V and +0.3 V extracted by means of three-electrodes measurements. But, for a coulombic efficiency threshold equal to 98% it is possible to select an Operating Voltage Window ranging between -0.5 V and +0.3 V.

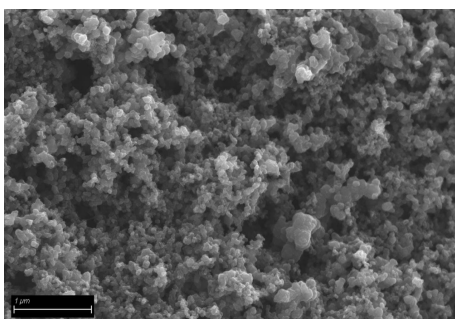


Figure 5.5: FESEM magnification of the microporous layer of a GDL [19].

5.3.2 Flexible GDL

The EQ-bcgdl-1400S-LD is supplied by MTI KOREA. It is a carbon cloth gas diffusion layer (GDL) coated with a microporous layer made of Nafion and Teflon ($50 \mu\text{m}$ thick) with pore diameter of $31 \mu\text{m}$, air permeability of $10 \text{ mL}/(\text{cm}^2\text{s})$ and a

thickness of $454\mu\text{m}$. From the electrical properties point of view the sheet resistance is $2\text{m}\Omega\text{ cm}^2$. Also this material is featured by hydrophobicity [24].

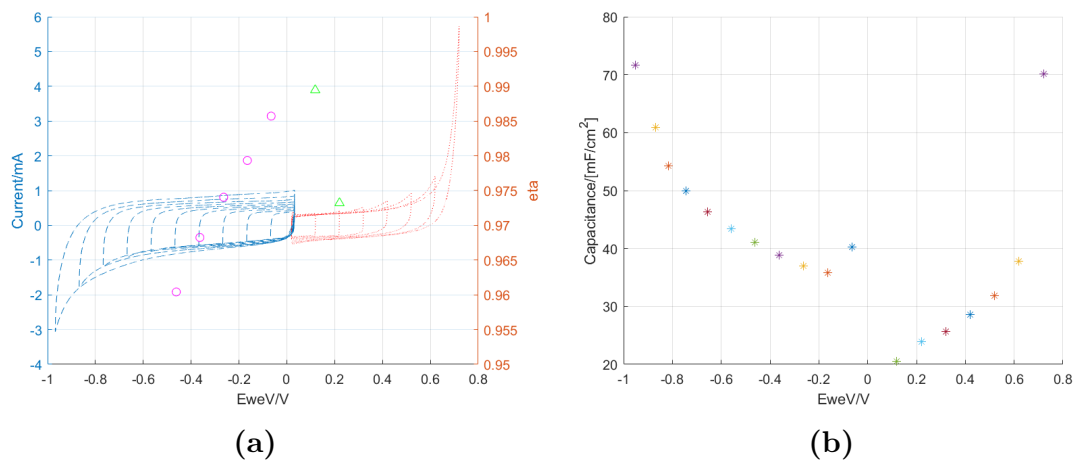


Figure 5.6: Characterization results: (a) Cyclic Voltammetry for positive and negative voltages in order to define the Operating Voltage Window through the Coulombic Efficiency. (b) Capacitance adjustment as a function of potential windows

Assembling a half-cell featured by a 18mm diameter circular electrode made of Flexible GDL, FS2226 as separator and the Ionic Liquid DABCO-IM as electrolyte (see section 5.4), such GDL has been characterized through three-electrodes measurements. Such analysis reveals a coulombic efficiency higher than 95% for an

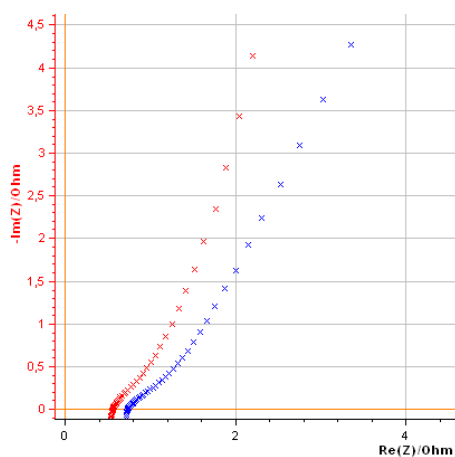


Figure 5.7: EIS for a 18mm diameter Flexible GDL performed by three-electrodes measurements.

Operating Voltage Window ranging between -0.5 V and $+0.2$ V, while a coulombic efficiency higher than 99% for an Operating Voltage Window ranging between -0.1 V and $+0.1$ V (Fig. 5.6) and an ESR ranging between 0.56Ω and 0.74Ω (Fig.5.7).

5.4 Electrolyte

The most used electrolytes in EDLC are aqueous, salts dissolved in organic solvents and Ionic Liquids (ILs). The characteristics of interest to evaluate an electrolyte are conductivity, viscosity and operating voltage. Mainly the latter affects a lot the specific energy of a supercapacitor. Aqueous electrolytes have high conductivity but a shrink operating voltage. Anyway, because of the huge dielectric constant of the aqueous systems also the capacitance is high but it has a lower impact on the specific energy than operating voltage [9]. Thus in order to develop high energy applications, the focus of the search has shifted to IL or mixture of it with compatible solvents. IL is made of pure salts, so cations and anions, featured by a negligible volatility, good electrochemical stability and conductivity at room temperature. But generally the conductivity of an IL is smaller than one of an

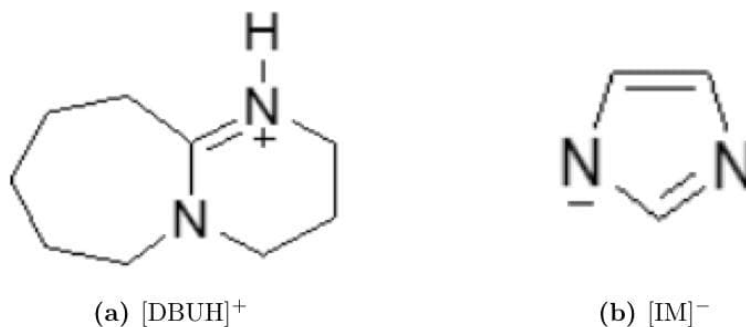


Figure 5.8: Cation (a) and anion (b) chemical structure composing DABCO-IM [25].

aqueous electrolyte, because of a greater viscosity, and therefore also the ESR of systems having IL as electrolyte is larger [9]. With the purpose of improving its performances higher temperatures can be exploited getting better viscosity and so an enhancement of ionic mobility but with temperature also leakage current of the cell increases thereby a trade-off is needed. When IL is used as electrolyte for a supercapacitor then the overall final capacitance of the system depends on the size of ions and the amount of used electrolyte. Indeed a relationship between the ions and pore size exists by which the maximum value of the capacitance is reached if the ions size is comparable with pore one of activated carbon electrodes ensuring a proper accessibility [26]. Another way to boost properties of ILs is to dilute it

realizing IL-mixture electrolytes. The main obtained improvements are a wider operating voltage and reduced viscosity, so better conductivity, compared to pure IL so that such electrolyte is even more ideal for supercap applications.

Specifically, the electrolyte used in this study is Diazabicycloundecanium Imidazolid (DABCO-IM) produced by Iolitec with a purity higher than 95%. The ions composing this IL are $[\text{DBUH}]^+$ as cation, and $[\text{IM}]^-$ as anion and their structures are depicted in Figure 5.8. Such IL is engineered to absorb CO_2 which is its main feature and making it fundamental for the interest application of the device under study. This ability is typical of IM-based IL and its mixtures. The CO_2 is activated by the anion forming a carbonate intermediate and then easily released by heating or inert gas bubbling like N_2 [27]. The formation of the carbonate is proved by means of ^{13}C spectrum, which shows a third peak in addition to those associated with cation and anion (See Figure 5.9) [25].

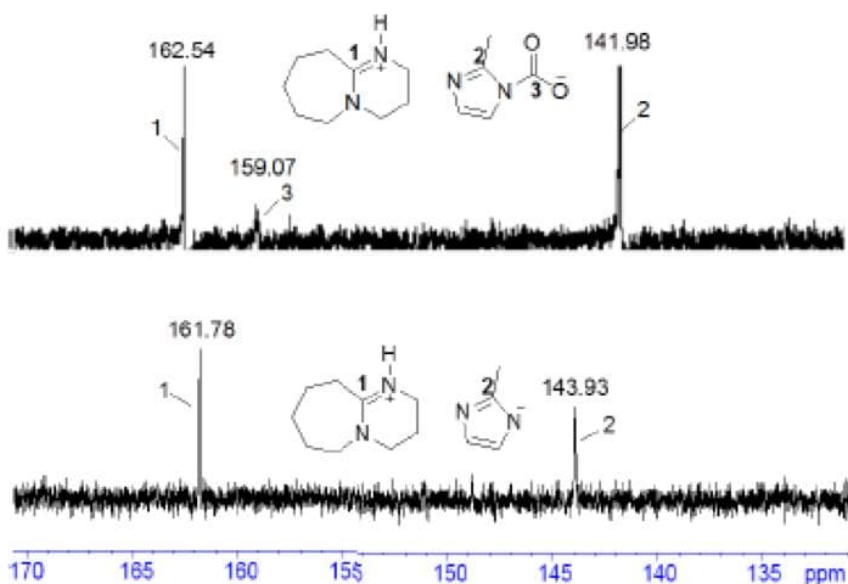


Figure 5.9: ^{13}C NMR spectra of $[\text{DBUH}]^+$ and $[\text{IM}]^-$ before (up) and after (down) the CO_2 exposure [25].

A deeper analysis on this IL was carried out by [19] highlighting a resistive contribution of 40Ω to the ESR of the cell and how the properties of the electrolyte vary depending on the bubbling of CO_2 and temperature variations. Indeed once CO_2 is absorbed, the viscosity of IL goes up as shown in Figure 5.10a and in [27] [25] but sweeping the temperature from 25°C to 80°C it is possible to observe how the viscosity of electrolyte is recovered decreasing and then coming back to pure electrolyte value. Moreover, CO_2 affects also the capacitance of the system as proved by measurement in figure 5.10b where, starting from a steady value related

to pure IL, the capacitance drops flushing CO_2 but a good regeneration is achieved through N_2 bubbling.

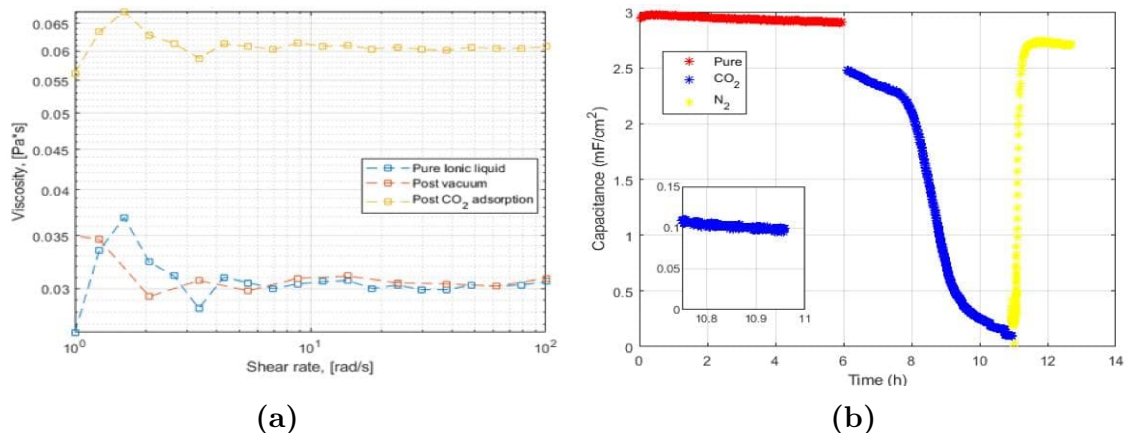


Figure 5.10: (a) Viscosity vs Shear Rate and (b) cell Specific Capacitance of pure and post absorption DABCO-IM [19].

5.5 Charge Balancing and associated Upgraded Assembling of the Cell

Before assembling the ECC-Air cell to test it under gases flux condition it is necessary to balance the charge stored on the two electrodes in order to ensure the maximum Operation Potential Window [12], mainly in the case of asymmetric cell, and approximately the same constant time during the charging and discharging of both positive and negative electrode. To chase this goal, electrodes optimization is based on Coulombic Efficiency (η) and Operating Voltage Window values extracted from three-electrodes measurement results shown in section 5.3. The ratio to be fulfilled is

$$\frac{D_+}{D_-} = \sqrt{\frac{C_- \Delta V_-}{C_+ \Delta V_+}}$$

where $D_{+/-}$ is the electrode diameter, $C_{+/-}$ is the specific capacitance in mF/cm² and $\Delta V_{+/-}$ is the selected Operating Voltage Window as function of η .

Starting with Hard GDL, a threshold of 98% for η means an Operating Voltage Window between -0.3 V and + 0.3 V since no potential window is able to achieve a coulombic efficiency greater than or equal to 99% for negative voltages and the probable identified cause is the poor purity of the used electrolyte [22]. With $C_+ = 10 \text{ mF/cm}^2$, $\Delta V_+ = +0.3 \text{ V}$ and $C_- = 19 \text{ mF/cm}^2$, $\Delta V_- = -0.5 \text{ V}$ and fixing $D_+ = 18 \text{ mm}$ it is possible to estimate $D_- \simeq 12 \text{ mm}$.

Then, regarding Flexible GDL a coulombic efficiency equal to or higher than 99% for an Operating Voltage Window ranging between -0.1 V and +0.1 V is selected. More precisely, $C_+ = 21 \text{ mF/cm}^2$, $\Delta V_+ = +0.1 \text{ V}$ and $C_- = 40 \text{ mF/cm}^2$, $\Delta V_- = -0.1 \text{ V}$ and fixing $D_+ = 18 \text{ mm}$ it is possible to estimate $D_- = 13$ but then rounded down to 12mm. Formerly specified, the used full-cell is designed to host 18mm diameter circular electrode. Thus, the location of the smaller electrode is manufactured applying a crown of KAPTON on the bottom of the cell as figured out in Fig.5.11.

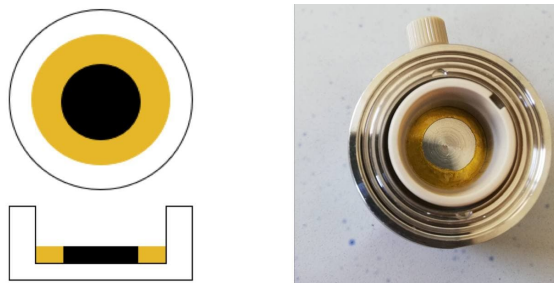


Figure 5.11: Fitting of the KAPTON crown on the ECC-Air full-cell bottom [19].

Besides keeping in place the electrode, this KAPTON layer is also fundamental to reduce unwelcome reactions taking place between electrolyte and steel of the cell itself observed in [22] through a CV (Fig.5.12).

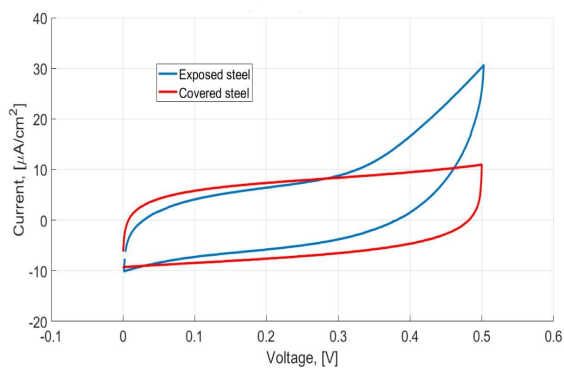


Figure 5.12: Cyclic Voltammetry with and without KAPTON layer [22].

Chapter 6

Experimental Results

6.1 New CapMix Procedure

In a previous work [19], a cell characterized by electrodes made of hard GDL and the ionic liquid DABCO-IM as electrolyte has been studied. In particular, the cell is such to force the positioning of the positive electrode at the top, while the negative electrode on the bottom. This choice is due to DABCO-IM which is an ionic liquid structured to absorb CO_2 , specifically the anion is the charged species reacting with CO_2 and its accumulation is at the positive electrode. Since the design of the cell allows the flowing of the gases only on the top electrode, then it is necessary to place the positive electrode on the top. The study was carried out by applying the following Capacitive Mixing procedure, also defined as CO_2Cap or CapMix , which is composed of four phases shown in figure 6.1:

1. Open Circuit Voltage (OCV) during which N_2 is flushed with Flow Rate of 150mL/min into the cell to facilitate desorption of CO_2 . The minimum time for effective desorption is 15 minutes;
2. Charging of the super-capacitive system by applying a constant voltage to a well-defined value which is kept constant for 10 minutes;
3. OCV during which CO_2 is flushed with Flow Rate of 80mL/min into the system to take advantage of the phenomenon called capacitive double layer expansion (CDLE) which induces the so-called Rise Voltage. It is important to note that CDLE is ideally the main phenomenon allowing Rise Voltage only by imposing the strong approximation that there are not any kind of charge losses as explained in the paragraph 2.1;
4. Constant current discharge which allows to draw out the gained energy from the previous phase as a result of the CO_2 absorption.

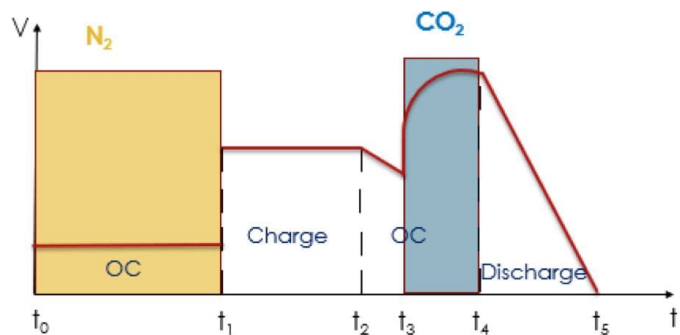


Figure 6.1: Previous procedure adopted for the CO₂Cap cycle [19].

In that particular work, both measurements at room temperature and at high temperatures were done and the most significant results were obtained at a temperature of 80°C which is also identified in the literature [27] as the ideal temperature for desorption of CO₂ by IMIDAZOLIDE-based Ionic Liquid combining it with the bubbling of an inert gas such as N₂.

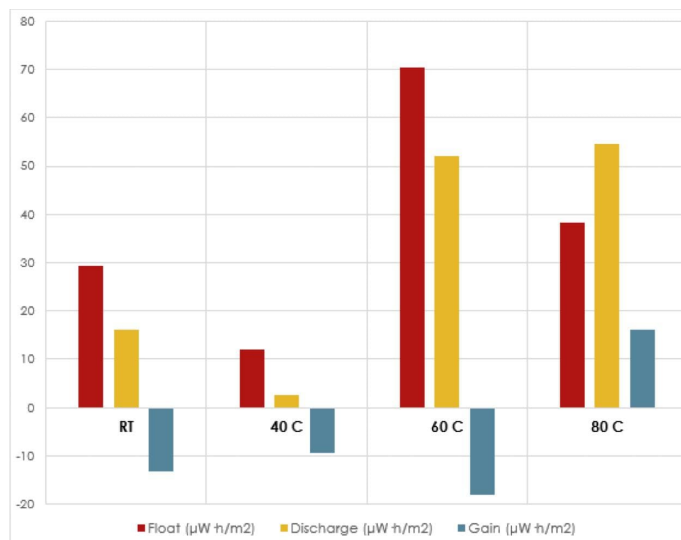


Figure 6.2: Energies obtained flushing CO₂ on hard GDL electrode exploiting the previous procedure (Fig. 6.1) [19].

Under these conditions, the energy gain is about 50%, while for lower temperatures the energy gain is strongly negative as shown in figure 6.2. It is necessary to remember that the reported energy gain is purely electrostatic and therefore the energy necessary to bring the system to the desired temperature has not been taken into account. In addition, the disadvantage of this CapMix procedure is

the introduction of inaccuracy in the assessment of the energy used to charge the system through the voltage step. In fact, the energy is calculated as indicated in paragraph 4.1.5, but the use of a voltage step implies an instantaneous current pulse with very high amplitude. So if the time constant $\tau=R_{ES}C_T$ is much smaller than the sampling time of the measuring instrument then the value of the current pulse amplitude is not correctly acquired but it will be much smaller. In order to evaluate more precisely the energy required for the super-capacitor charge, another procedure is adopted in this thesis work (Fig. 6.3).

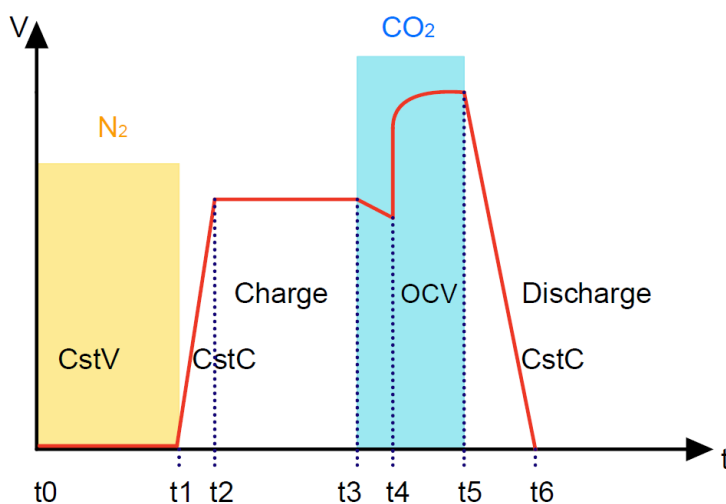


Figure 6.3: New procedure adopted for the CO₂Cap cycle.

The latter is characterized by two adjustments with respect to the previous procedure.

1. Constant Voltage or Open Circuit Voltage (OCV) during which N₂ is flushed with Flow Rate of 50mL/min into the cell to facilitate desorption of CO₂. The minimum time for effective desorption is 15 minutes;
2. Charging of the system up to a well-defined potential, called Float Potential, by means of a constant current whose density is 1 μ A/cm².
3. Float Phase: The system is kept to the Float Potential for 10 minutes;
4. OCV during which CO₂ is flushed with Flow Rate of 60mL/min into the system to exploit the CDLE which induces the Rise Voltage;
5. Constant current discharge which allows to extract the gained energy from the previous phase as a result of the CO₂ absorption.

Thus, from the point of view of a graph Voltage vs Time the Float phase is preceded by a voltage ramp, as depicted in figure 6.3, and the flow of N_2 is implemented while a constant voltage is set to 0 volts or in OCV condition. In this way, it is observed that the peak of current pulse has a much smaller amplitude than one recorded with the previous CapMix procedure and, moreover, the results are more repeatable. With this procedure the overall energy to charge the system is estimated more precisely. By assembling a cell theoretically identical to that used in the previous work and applying the new procedure, it is possible to observe that the energy used in the overall charging phase is comparable with one estimated through the use of Float only.

A comparison is given by the tables below.

Cycle	$E_{\text{Float}} (\mu\text{Wh}/\text{m}^2)$	$E_{\text{Discharge}} (\mu\text{Wh}/\text{m}^2)$	$E_{\text{Gain}} (\mu\text{Wh}/\text{m}^2)$
1	27.6982	14.1008	-13.5974
2	29.0916	17.2365	-11.8551
3	31.1637	17.2025	-13.9612

Table 6.1: Comparison of the energies per cycle for 60mV Float at Room Temperature exploiting the previous procedure (Fig. 6.1) [19].

Cycle	$E_{\text{Ch}} (\mu\text{Wh}/\text{m}^2)$	$E_{\text{Float}} (\mu\text{Wh}/\text{m}^2)$	$E_{\text{ChTOT}} (\mu\text{Wh}/\text{m}^2)$	$E_{\text{Discharge}} (\mu\text{Wh}/\text{m}^2)$	$E_{\text{Gain}} (\mu\text{Wh}/\text{m}^2)$
1	16.22	6.89	23.11	15.5	-7.61
2	14.79	4.68	19.47	10.04	-9.43

Table 6.2: Comparison of the energies per cycle for 60mV Float at Room Temperature exploiting the new procedure (Fig. 6.3).

6.2 CapMix Procedure exploited Flexible GDL Electrodes

The further purpose of this thesis work is to analyze and characterize new materials for the improvement of the performance of the system especially from the energy point of view. Therefore a new sample of GDL, identified as Flexible GDL, has been selected for the realization of the electrodes of the super-capacitor.

The main benefits sought by the use of this new material are a larger total cell capacitance which would allow an increase of the available energy during the discharge phase and an expansion of the operating potential window.

In order to evaluate these features both two electrode and three electrodes measurements are performed. In the case of two-electrode measurement, a Float

Conditioning Test is implemented. Through it, once the system has reached the stable state, it is possible to extract a coulombic efficiency greater than 99%, an energy efficiency of 21,2% and a capacitance of 4.47 mF/cm². With the exception of the capacitance, which is almost an order of magnitude greater than one observed in the case of the Hard GDL, the values of the two types of efficiency are similar for both gas diffusion layers. Therefore, analysing data extrapolated from such test, it is possible to assume a CapMix response similar to one observed in the case of Hard GDL but with a larger released energy.

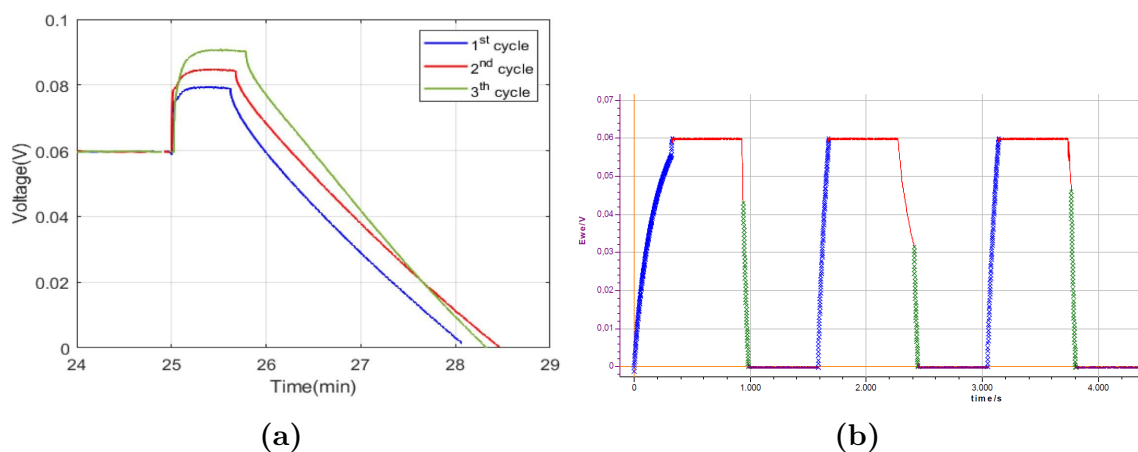


Figure 6.4: CapMix results obtained flushing CO₂ on hard GDL electrode [19] (a) and on flexible GDL electrode (b) at Room Temperature.

Regarding the results of the three-electrode measurements, these show that the operating potential windows related to the Flexible GDL are comparable with those obtained with Hard GDL, both for positive and negative voltages, but the coulombic efficiency is close to 99% while in the case of the Hard GDL at most a coulombic efficiency of 98% is obtained, as shown in paragraph 5.3.

Subsequently, the CapMix procedure is applied to a cell composed of electrodes made with Flexible GDL, sized according to the charge balancing explained in paragraph 5.5, and using the ionic liquid DABCO-IM as electrolyte. The results show absence of the Rise voltage. Indeed, only a dramatic drop of voltage occurs (Fig. 6.4b).

Moreover, because of a very high total cell capacitance, the charging and discharging time of the cell with a current density of 1 μ A/cm² is much longer than one observed in the case of a cell whose electrodes are made up of Hard GDL.

This is due to the time constant which is directly proportional to the capacitance, so if the latter is larger then, with the same applied current, both the charge and discharge of the super-capacitor with Flexible GDL are much more time demanding than a device with Hard GDL. All these observations shifted the focus on the

Float leakage current, which is positively related to the capacitance. Therefore, the Float leakage currents of both a cell with Hard GDL and with Flexible GDL have been analyzed and compared, since the final value of the leakage current is also the current with which the cell is discharging when it is in open circuit condition. From the data analysis, a relationship between leakage current and Rise voltage is observable. More precisely, it is possible to notice how the Rise voltage occurs for currents less than or near to 250nA as shown in the figure 6.5a, where the Float leakage current value per cycle is labeled and if the Rise Voltage occurs is specified with the word "GAIN".

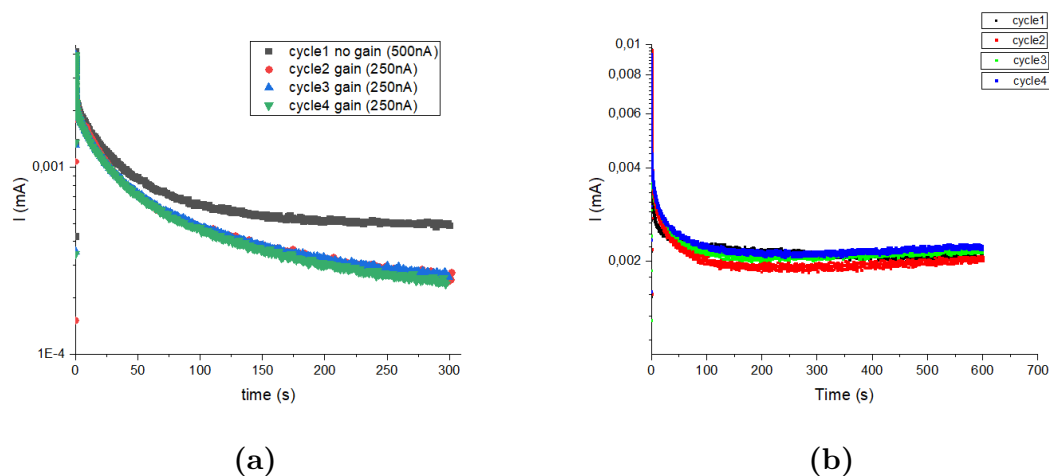


Figure 6.5: Float leakage currents related to a cell with hard GDL electrodes (a) and flexible GDL electrodes at room temperature (b).

Furthermore, it is also observable as after each cycle the leakage current assumes lower values. This last observation is in agreement with the results of the Float Conditioning Test, where it is observed as increasing of the lasting of the Float or increasing the number of cycles keeping constant the duration of the Float allows to reduce the leakage current. All these led to the conclusion that when the Float leakage current exceeds a certain upper threshold, which is near to 250nA (Fig. 6.5a), then it prevents the phenomenon of Rise Voltage because the parasitic discharge is stronger.

In addition, since in a capacitive system the current and the time constant are proportional to the capacitance then it is possible to assert that the high capacitance due to Flexible GDL makes the system ineffective for the applications of interest because the dropping of the current takes place with longer times than a system characterized by Hard GDL and therefore the final value of the leakage current is almost an order of magnitude higher, ranging between 1 - 2mA as shown in the figure 6.5b. On the basis of the results obtained and shown, it has been decided to

use only Hard GDL.

6.3 CapMix Procedure with Float Reduction

A further strategy to enhance energy gain at room temperature is the reduction of Float time. The energy used in the Float corresponds up to 30% of the total energy exploited to charge the device (See table 6.2).

However, the main purpose of the Float Phase is not the charge of the system but the stabilization and polarization of electrode-electrolyte interfaces in order to reduce the Charge Redistribution Effect and therefore the leakage current. In this way, it is possible to ensure an appropriate accumulation and diffusion of the desired chemical species in the respective interfaces with the aim of obtaining the maximum interaction between CO₂ and Imidazolid and, therefore, the best possible gain. By identifying the minimum Float time which allows to meet the

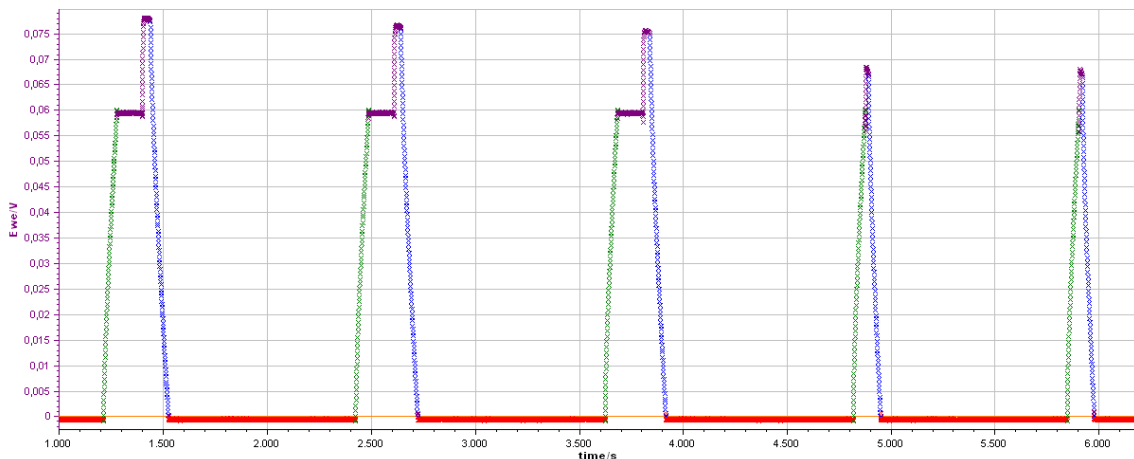


Figure 6.6: Example of CapMix with progressive reduction of the Float time.

purposes of the Float, especially the achievement of the minimum leakage current, then it is possible to reduce the duration of the Float Phase to the identified minimum time. This significantly reduces the overall energy used to charge and for the conditioning of the system before flushing CO₂, increasing the extractable energy gain. To assess the effectiveness of this strategy, the CapMix procedure has been modified by introducing, cycle by cycle, a gradual reduction of the Float. Precisely, the Float times taken into account are 10 minutes, 5 minutes, 2 minutes and 0 minutes exactly in this order as shown in the figure 6.6.

By means of a first visual analysis of the curves, it is possible to understand that using the DABCO-IM as electrolyte a reduction of the maximum amplitude of the Rise Voltage occurs as well as the Float time is shortened.

This can be explained by the fact that reducing the duration of the Float a consequent increase of the Float leakage current happens. Thus, this current strongly opposes to the Rise Voltage.

Nevertheless, an analysis of energy gains shows that the optimal case is the one with zero Float time indeed by reducing the Float an improvement in energy gain is obtained even if it is always negative (Fig. 6.7).

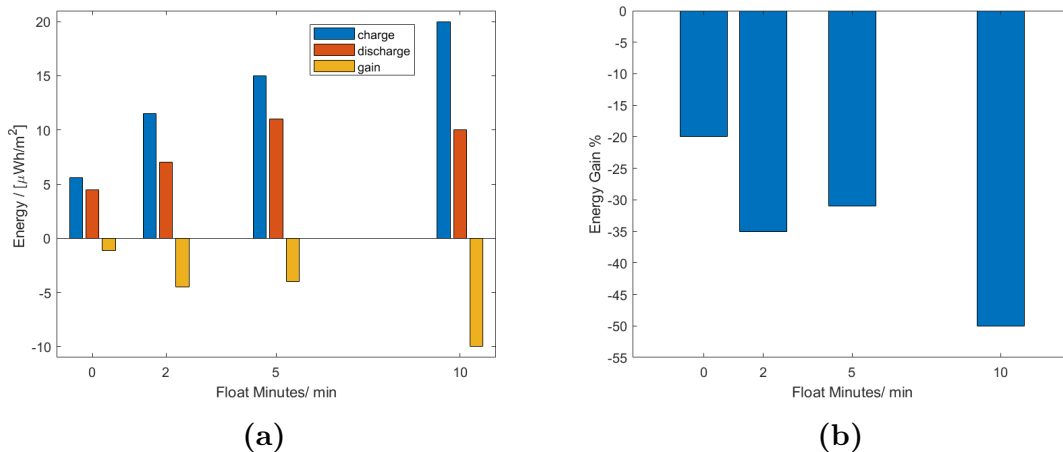


Figure 6.7: (a) Comparison of energies and (b) Percentage Energy Gains obtained for several Float lasting adopting the CapMix procedure shown in figure 6.3.

Thus, the Float reduction strategy shows promising results but in order to be useful it is necessary to reduce the leakage current at the end of the Float phase. In addition, the minimum leakage current must be reached in a very short time, in such way it is possible to obtain simultaneously a very large and repeatable Rise Voltage proceeding in the cycles and an important overall energy gain thanks to the reduction of the Float time.

6.4 CapMix Procedure with Discharge until Float Potential

Besides the Float reduction, another possible approach, which could reduce the overall energy in order to charge the device, is to reduce the charging component related to the constant current charge. In this case, the procedure (labeled for simplicity as 2nd Procedure) involves charging the device only once using a constant current, similar to the previous procedure at section 6.3 (labeled for simplicity as 1st Procedure). Subsequently, the cell is not discharged up to 0 volt but until the Float potential and then passed into an OCV condition as shown in the Figure

6.8. Therefore, the flow of N_2 with Flow Rate of 50mL/min, which has the aim to

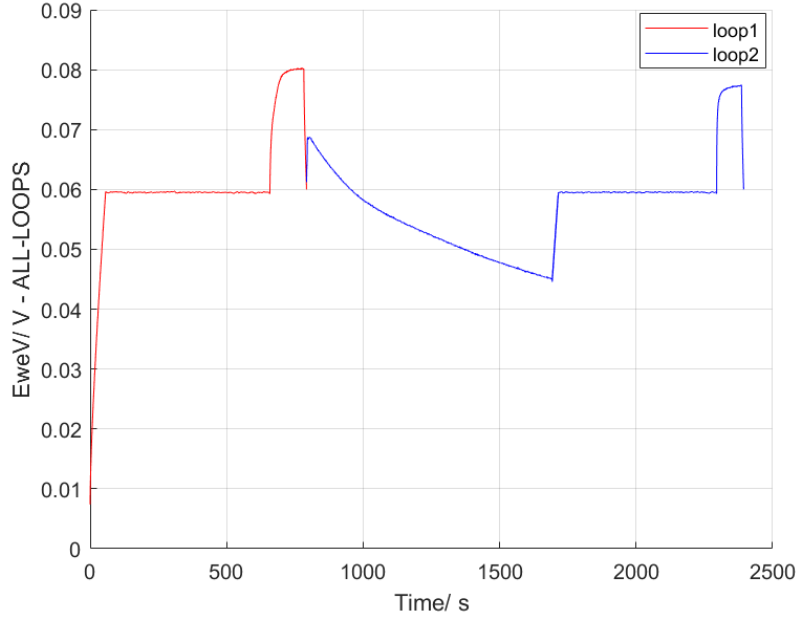


Figure 6.8: Example of CapMix procedure with constant current discharge until Float Potential.

desorb the CO_2 captured by the ionic liquid, occurs during a OCV state which, however, does not start from a potential of 0 volts but from a potential equal to Float one. In this way, it is possible to reduce the energy spent for the charge of the cell with constant current after each cycle. Moreover, it can be expected the Charge Redistribution effect and Float leakage current decrease significantly as the device keeps a potential that is very close to Float one during the desorption phase. Thus, the only energy contribution to charge and for conditioning of the device is one linked to Float. The latter then, as shown in the previous paragraph, can be reduced to the minimum time needed to reach the minimum Float leakage current. From the energy and Float leakage current analysis associated to this CapMix procedures with progressively decreasing of the Float time, it is observed that the energy used for a much smaller charge and to keep the cell to the Float potential, during the Float phase, is reduced of a quantity between 66% and 50% (Fig. 6.9a) compared to the overall energy consumption observed when exploiting the former procedure which is reported in the table 6.2.

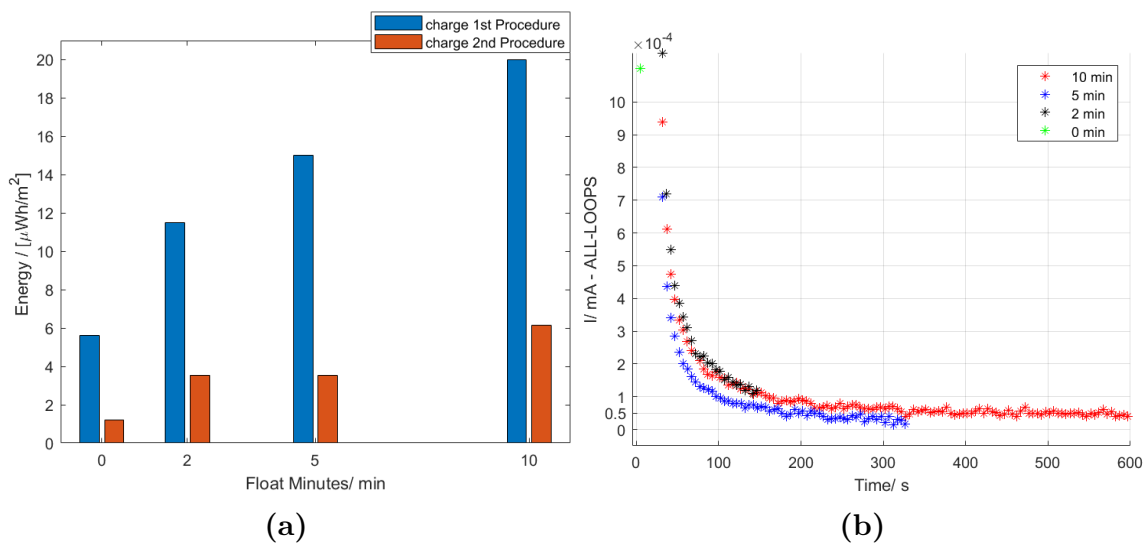


Figure 6.9: (a) Comparison of charging energies between the procedure in Fig. 6.3 (1st Procedure) and one in Fig. 6.8 (2nd Procedure) obtained for several Float times; (b) Comparison of Float leakage currents related to the procedure in Figure 6.8 for several Float times.

But, above all the leakage currents in the case of 10 minutes, 5 minutes and 2 minutes Float show a value between 30nA and 100nA, while in the case of 0 minute Float the magnitude of the leakage current is of the order of 1 μA (Fig 6.9b).

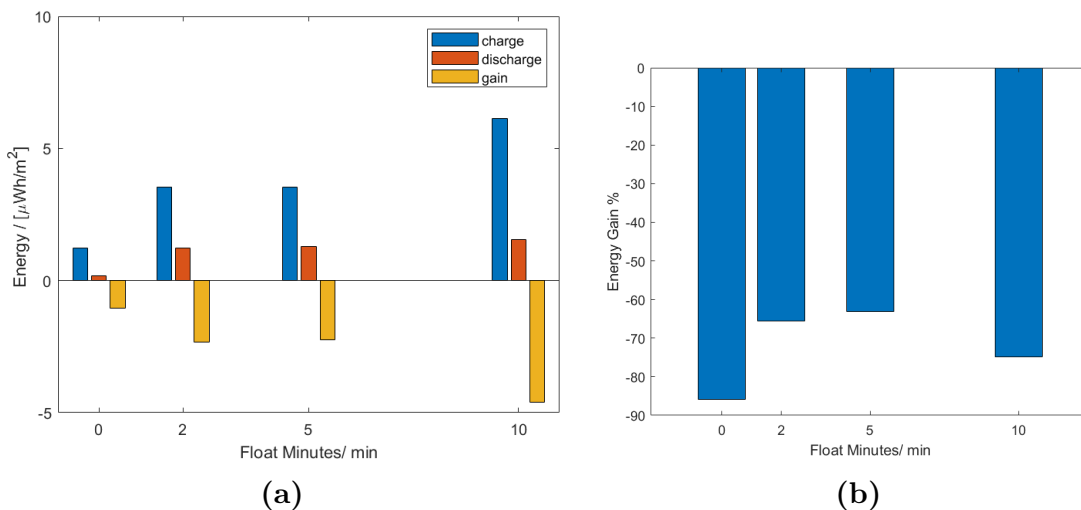


Figure 6.10: (a) Comparison of energies and (b) Percentage Energy Gains obtained for several Float lasting adopting the CapMix procedure shown in figure 6.8.

This difference between the case at 0 minutes of Float and the others can also be

observed in terms of percentage energy gain since it improves as the Float shrinks but the worst case is recorded at just 0 minutes of Float, as shown in the Figure 6.10b. Indeed, despite the reduction of energy consumption related to the charge and conditioning phase and the lowering of the leakage currents with respect to those observed in the case of the previous paragraph, the energy gain at room temperature is still negative and especially the obtained results are much worse than previous analyzed in paragraph 6.3. These results are due to the fact that since the constant current discharge does not end at 0 volts but is blocked at the Float potential then the amount of energy extrapolated in this procedure is much smaller than one extracted with the previous one (See "Discharge" values in Fig. 6.7a and Fig. 6.10a).

Chapter 7

Dabco-IM diluted in Propylene Carbonate 1M

Taking into account the results obtained and shown in the previous chapters, it is clear that in order to get a positive energy gain at room temperature through the CapMix procedure it is necessary to maximize the mobility of the electrolyte to improve its conductivity and viscosity allowing CO₂ to diffuse more easily through the electrode - electrolyte interface. Therefore, the goal of this chapter is to show the dilution of the ionic liquid DABCO-IM in Propylene Carbonate as adopted solution after the analysis of the structure and the microscopic electrochemical properties of the IL molecules, which are at the origin of energy issues.

7.1 Theoretical Elements of Diluted Electrolyte in Supercapacitors

With the purpose to identify the most effective strategy to achieve the desired improvements, the analysis of the ionic liquid molecules features is carried out. In particular, imidazole is characterized by two important charge centers, associated with the two nitrogen atoms (Fig. 7.1a), giving rise to strong inter-molecular interactions through coulombian forces. While, the other points of the molecule interact through weak interactions such as Van der Waals forces.

When this molecule reacts with CO₂, the formation of imidazole carbamate originates. So, one nitrogen remains active while the other loses its charge by bonding with the oxygen of carbon dioxide (Fig. 7.1b).

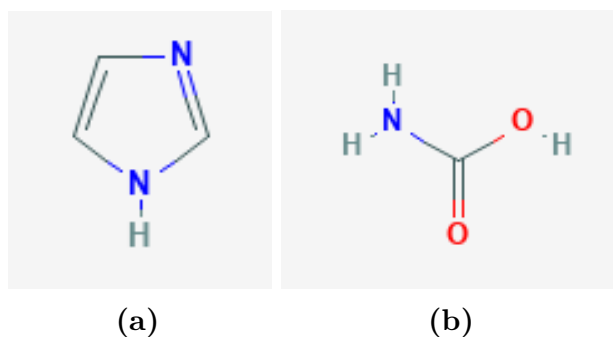


Figure 7.1: (a) 2D chemical structure depiction of Imidazole; (b) 2D chemical structure depiction of Imidazole Carbamate [28].

Thus, it is observed that during the CO_2 absorption the dominant charge center no longer corresponds to the nitrogen atom, but rather it is in correspondence with the two oxygen atoms which are much more charged than the nitrogen, resulting in stronger bonds. As direct consequence, this leads to the increase of the viscosity of the ionic liquid, phenomenon that has been observed experimentally (Fig. 7.2) and also confirmed through simulations. The latter confirm both an increase in the density and viscosity of the electrolyte when imidazole carbamate is formed. Therefore, the distance between the ions is reduced leading to the Ion-Pairing situation and reducing the mobility of ions, the conductivity of the electrolyte and the diffusion of CO_2 . The worsening of the CO_2 diffusion is one of the main issues

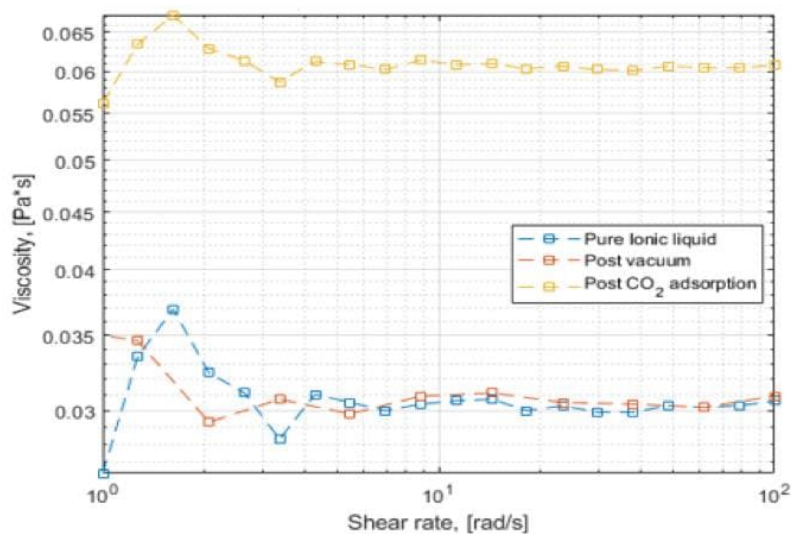


Figure 7.2: Comparison of viscosity between pure ionic liquid and post CO_2 absorption ionic liquid [19]

of the system under examination, which prevents the maximum exploitation of the cell capabilities. Since the CO₂ flowing occurs through a single electrode, then the growing density, and therefore the viscosity too, of the electrolyte happens only at the concerned electrode interface preventing the migration of CO₂ up to the second electrical double layer at the interface between the second electrode and the electrolyte. Therefore, the phenomenon driving the CO₂cap process is concentrated on a single double layer limiting the effectiveness of the device.

In literature [29] viscosity and conductive troubles are often mitigated through the use of solvents. The solvent molecules, placed between the electrolyte ions, make them less interactive and consequently their mobility is enhanced. This improvement of the electrochemical properties is due to a dielectric effect of the solvent which is attributable to the chains and the geometry of the solvent molecule. In addition, when it is also polar then it is able to screen the charge of ions.

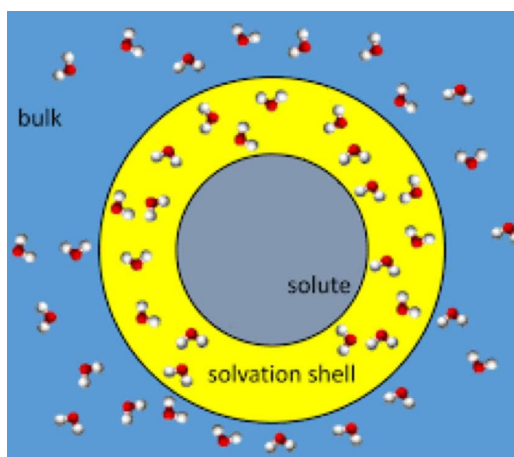


Figure 7.3: Solvation shell made up of solvent molecules surrounding solute in a solution [30]

Thus, in an electrochemical super-capacitor based on an electrical double layer (EDL), the solvent plays an important role as it determines the dielectric of the electrolyte and provides the solvation shell of the ions (Fig. 7.3). As well, the microscopic properties of the solvent establish the specific capacitance associated with the double layer and the performance in terms of energy and power density. Focusing in particular on ions in close proximity of EDL, both positive and negative charge carriers will be present in this region interacting through Coulombian Force (F) shown by the next equation, which describes the repulsion or attraction between two charges, Q_1 and Q_2 .

$$F = \frac{Q_1 Q_2}{\epsilon R^2}$$

Where ϵ is the dielectric constant corresponding to the product between the vacuum

dielectric constant ϵ_0 and the relative dielectric constant of the medium ϵ_r . While R is the distance between the two charged species. Therefore, increasing ϵ the repulsive or attractive force is attenuated.

Then, the solvent molecules in a double layer capacitor are polarized by the electric field related to the potential difference dropping at the electrode - electrolyte interface. The origin of the dielectric polarization in an electrochemical capacitor is due to the presence of inter-molecular dipole-dipole electrostatic interactions between the molecules of the dielectric medium, as in the case of Propylene Carbonate (PC). In this solvent the orientational polarization process is cooperative [29], so the polarization of a dipole induces the polarization of neighboring dipoles in the same direction, giving rise to a much larger and stronger polarization per unit of volume for a given applied electric field. Moreover, this type of medium is characterized by a dielectric constant with a high value [29].

From the the theory of dielectric polarization it is possible to derive the following relationship [29]

$$P = (\epsilon - 1) \frac{E}{4\pi}$$

where P is the medium polarization induced by the electric field E . P influences the redistribution and distortion of the charged species in the solvent which assume a preferential average direction [29]. Therefore, a high value of the dielectric constant means a greater polarization of the solvent dipoles allowing a reduction of the Charge Redistribution Effect and therefore a reduction of the self-discharge.

Moreover, the use of a solvent has the further purpose of expanding the operating potential window (OPW) and in this case the use of aprotic nonaqueous solvents is recommended in the literature [29] as these are characterised by the absence of electrically active centres. An example of this class of solvents is the PC.

In particular, the dielectric properties of the solvent affect the absorption of the charged species from the electrolyte to the carbon electrode, the specific capacitance of the system and mainly the ion pairing which influences the conductance and which can be of three types [29] (Fig. 7.4). All these cases can be identified as undissociated ions, so ions are not free to move.

Finally, the properties of the electrolytic solution, made up of solvent and solute, determine the conductance of the electrolyte, then ESR too which is strongly influenced by the accessibility of the electrolyte in the pores, the mobility of ions and their concentration. Accessibility and mobility are highly dependent on the ion pairing [29]. Ion pairing is affected by the dielectric capability of the solvent medium, but also by its viscosity and long-range electrostatic interaction between dissociated ions. Even such interactions are function of the dielectric constant of the medium [29].

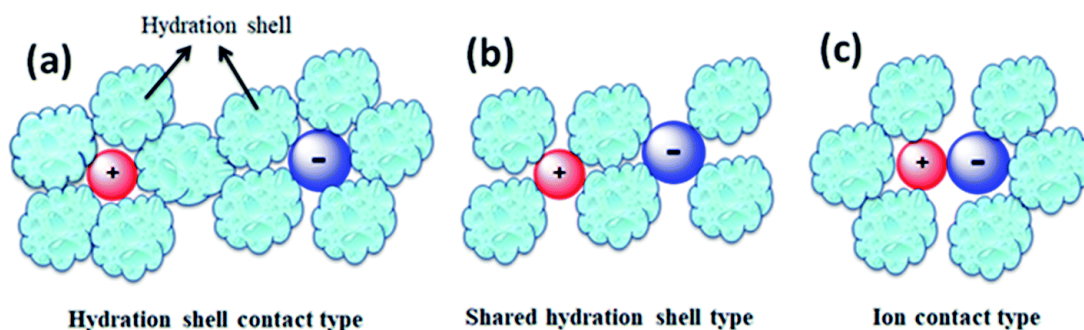


Figure 7.4: Types of ion pairs in an electrolyte solution: (a) Hydration shell contact type, (b) Shared hydration shell type and (c) Ion contact type [29]

Hence, a high ϵ value decreases the ion pairing and improves the equivalent conductivity of the electrolyte and, thus, of the system for a given ion concentration, enhancing the energy and power output [29]. This is due to the action of solvent molecules which attenuate coulombian interactions between ions. Indeed, charged species having opposite sign can interact and an attractive force is established, causing the reduction of the distance between the ions. When this distance is comparable with the radius of the ions then the situation of ion pairing occurs decreasing the ions mobility, and so also the conductivity of the electrolyte falls with the energy and power delivery capability [29].

Therefore, the chosen solvent for the dilution of the ionic liquid is the Propylene Carbonate which is a nonaqueous polar solvent characterized by a strong electrostatic dipole-dipole interaction but without a specific directionality. It has high dielectric constant ($\epsilon_r = 64$) and high solution decomposition voltages allowing an enhancement of the OPW of electrochemical stability [29]. In addition, its high polarity endows dissociation ability for dissolved electrolytes allowing the creation of the solvation shell around the ions so that the attenuation the ion pairing is possible maximizing the mobility and concentration of the dissociated ions and making the electrolyte more conductive [29]. Thereby, through this dilution higher energy and power density is achievable.

7.2 Preliminary analysis of Dabco-IM diluted in Propylene Carbonate 1M

In this section, the characterisation of DABCO-IM dilution in PC with 1M concentration is analysed. Specifically, a half-cell was assembled using Hard GDL as porous carbon electrode and the dilution as electrolyte.

The results obtained from the three-electrode analysis show a behaviour of the electrochemical properties which is in line with that described in the literature [29]. In fact, it can be observed that the ESR has decreased to 3,6 Ohm (Fig. 7.5b) which is smaller than one obtained by using pure DABCO-IM which is 25 Ohm.

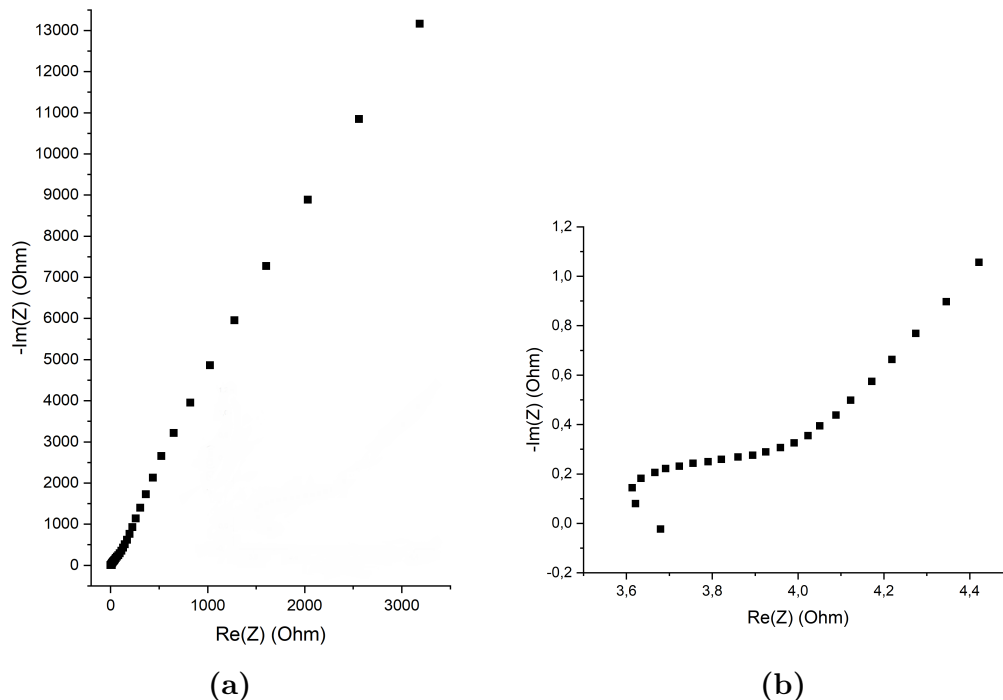


Figure 7.5: (a) Electrochemical Impedance Spectroscopy (EIS) of the Supercapacitive system characterized by DABCO-IM diluted in Propylene Carbonate 1M as electrolyte; (b) Magnification of the highest frequencies results related to the EIS.

As regards the specific capacitance, the dilution has reduced the value of this figure of merit. Indeed, in the case of pure IL the specific capacitance associated with a potential window of 100mV is 33mF/cm² while using the diluted electrolyte in the same conditions is observed a value near to 1mF/cm² (Fig. 7.6a). This could be attributed to an enlargement of EDL because in the case of dilution, the dielectric consists of PC molecules which could make the double layer thicker by reducing the related capacitance. Instead, as stated in the literature [29], the OPW is reinforced by the presence of the solvent. As explained in section 5.5, the system consisting of Hard GDL as porous electrode and pure DABCO-IM as electrolyte does not allow a coulombic efficiency (η_C) greater than 99%. Thus, the improvement of dielectric properties enables to identify an OPW which ensures a

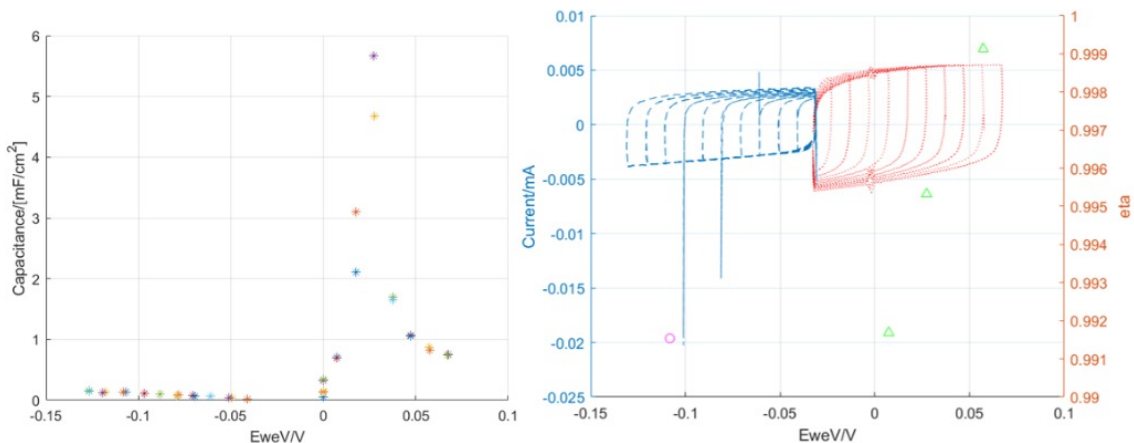


Figure 7.6: (a) On the left: Specific Capacitance values related to several potential windows, both in cathodic and anodic sides, of the Super-capacitive system characterized by DABCO-IM diluted in Propylene Carbonate 1M as electrolyte; (b) On the Right: Cyclic Voltammetry overlapped with Coulombic Efficiency for several potential windows whose width differ by a gap voltage equal to 10mV, both in cathodic and anodic sides.

η_C greater than 99%, as shown in the Figure 7.6b, having a $\Delta V^- \simeq -100\text{mV}$ and a $\Delta V^+ \simeq +100\text{mV}$, which is an ideal potential window for ongoing applications of interest.

In addition, the pure DABCO-IM not wetting properly the surface of the GDL causes a reduction in the energy efficiency of the system, roughly equal to 20%, since the accumulation of the charged species within the pores of the electrode occurs with greater difficulty and therefore the system tends to self-discharge more easily. An energy efficiency around 80% is recorded for DABCO-IM diluted in Propylene Carbonate 1M (see next), perfectly in line with the organic solvents used in commercial super-capacitors devices.

Therefore, the obtained ESR and coulombic and energy efficiencies confirm a strong enhancement in conductivity and electrolyte mobility as well as an improvement in electrode wettability, so the charge carriers are able to access more effectively in the pores of the electrode.

7.3 CO₂Cap Procedure to select the Best Float Potential

An appropriate Float potential has to be chosen, the one allowing to achieve the highest possible voltage gain and the lowest spent energy for charging. Therefore, several measurements have been performed sweeping the Float potential and the time of the Float phase with the aim of reducing as much as possible the charging and conditioning energy. The evaluated Float potentials are 0 V, 10mV, 20mV, 30mV, 40mV, 50mV, 60mV while the duration of the Float taken into account are 5 minutes, 2 minutes, 1 minute and 0 minutes. The CapMix adopted procedure is one in Figure 6.3, but in this case the duration of 10 minutes has been discarded from the beginning as it is observed that the leakage current reaches the minimum value, which varies between 30nA and 100nA, in less than 30 seconds, so in a very short time, thanks to the dielectric effect of the solvent on ions. Indeed, it would be acceptable to exclude also the Float time equal to 5 minutes but it is decided to show it for the sake of completeness and clarity, allowing to exalt more evidently the improvements obtained with the diluted electrolyte. All measurements shown in this paragraph are performed using a full-cell assembled with both electrodes in Hard GDL and as electrolyte the DABCO-IM diluted with PC in 1M concentration. Two setups have been studied, namely a symmetrical cell whose electrodes have a diameter of 18mm and an asymmetrical cell in which the positive electrode has a diameter of 7mm and the negative one of 18mm. The sizing of the latter is a direct consequence of the charge balancing procedure shown in section 5.5. In addition, the gases (CO₂ and N₂) flow only through the positive electrode, placed on the top of the cell, for reasons explained in the section 6.1. In particular, the CO₂ Flow Rate is 60mL/min and N₂ Flow Rate is 50mL/min. Both the charge and discharge of the cell is driven by a constant current density of 1 μ A/cm². The energy is calculated as indicated in paragraph 4.1.5.

7.3.1 Symmetric Cell

Before the symmetric cell is subjected to the CapMix procedure, it is conditioned through the "Potentiostatic Floating Test or Float Conditioning Test" procedure described in section 4.2.4. The obtained data show that the electrochemical system once it has reached the stable state assumes a specific capacitance of 264 μ F/cm² with a coulombic efficiency of 96% and an energetic efficiency of 82%. In particular, the energy efficiency is four times greater than one linked to a system made with Hard GDL used as electrodes material and pure DABCO-IM as electrolyte, allowing to have a voltage gain, and therefore energy, much more important.

Float of Zero Volt

The first applied Float Potential is 0 Volt. The voltage gain obtained flushing CO₂ is increasing as the duration of the Float phase is reduced. The highest recorded voltage gain is 53mV when the Float time is 0 minutes, so the Float phase is absent. But in general the voltage gain is between 48mV and 53mV as shown in the Figure 7.7. So it can be stated that the Rise Voltage amplitudes are about constant in

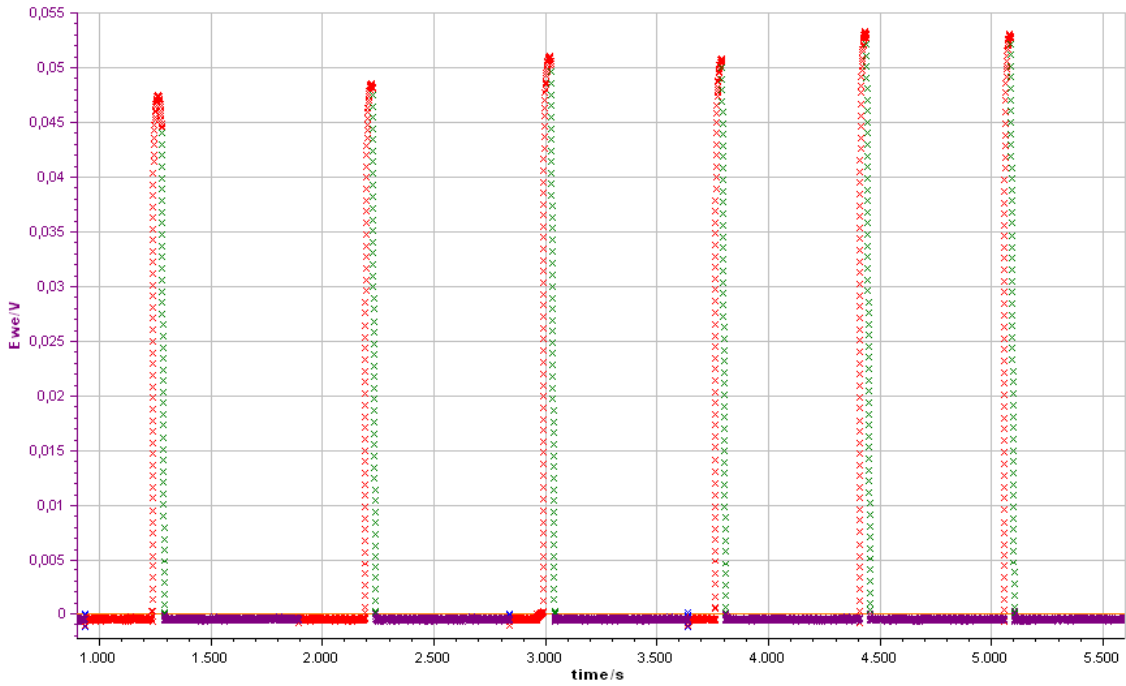


Figure 7.7: Voltage vs Time of the CO₂Cap with a null Float Potential using a symmetrical cell.

all loops. This is indicative for the effectiveness of interface regeneration flushing N₂ and of the appropriate choice of the flow time. The energy gains obtained for each loop are shown in graph 7.8a, while graph 7.8b displays the energy obtained as a percentage of the charge energy and/or the energy spent on the Float for the conditioning of the EDLs of the cell. The energy spent on Float is reduced shortening its duration. This can be observed through graph 7.8a, since being the recovered energy almost constant for each cycle, then the increasing gain can be justified solely by a reduction of the energy spent during the Float phase. This behavior is consistent with what is expected as the longer Float time the greater is the energy spent.

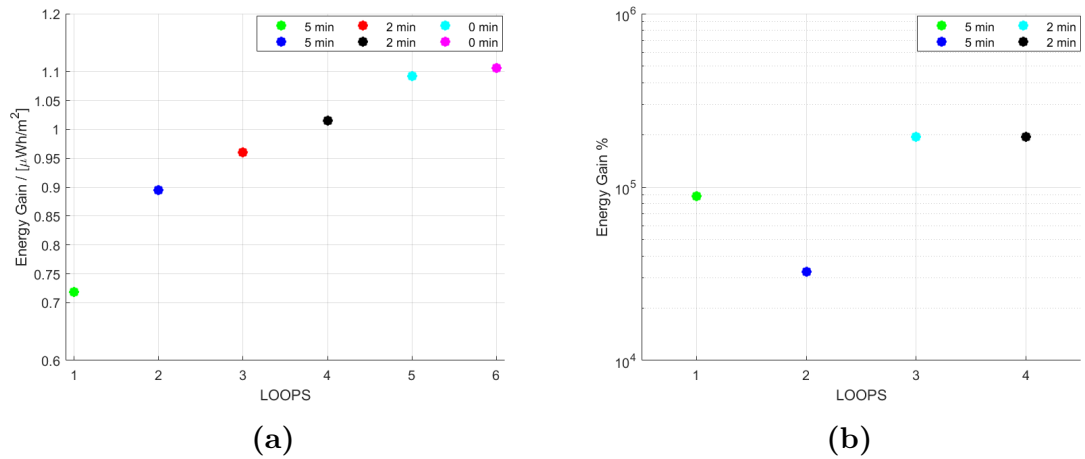


Figure 7.8: (a) Energy gain obtained for different duration of the 0 volt Float; (b) Percentage of achieved Energy gain with respect to spent energy for different duration of the Float phase.

In addition, in Figure 7.8b it can be observed as the percentage of gained energy increases reducing the Float time. But, it is generally possible to assert that in this specific case, being the spent energy almost zero then the released one is totally gained. For this reason the percentage energy gains are in the order of 10^5 %.

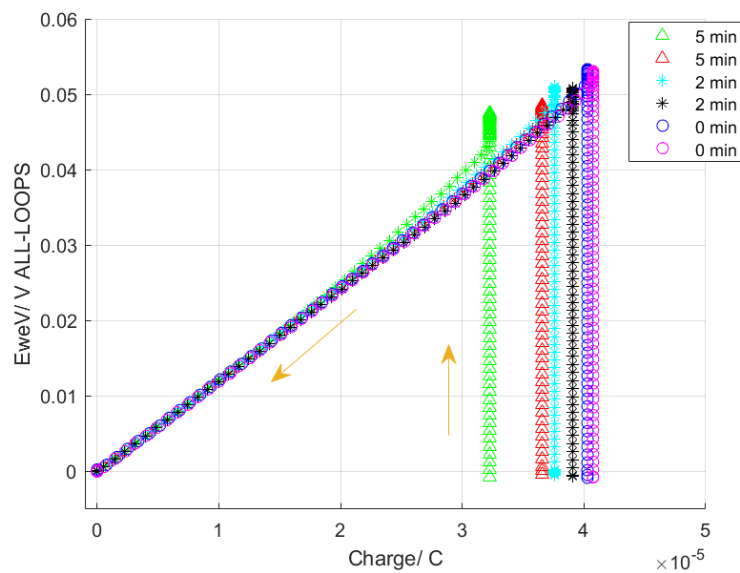


Figure 7.9: Voltage vs Charge graph of the CO₂Cap procedure marked out by a value of Float Potential equal to 0 volt and a progressive reduction of the Float time.

Thus, in the case of Float Potential equal to zero volt, the gain can only be strictly positive and also, looking at the graph in the Figure 7.9, since the charge curve does not exist then the discharge can only be associated with useful contributions from which drawing energy. Moreover, the shifting more and more towards positive charge values reducing the Float time is revelatory of the fact that the energy increases by shrinking the duration of the Float.

Float of 10mV

The next applied Float Potential is 10mV. The voltage gain obtained flushing CO₂ exhibits still the same behaviour of the previous case, but now two main differences are noted. The first is a greater consistency for each loop of Rise Voltage, which remains almost constant at 50mV (see Fig. 7.10) regardless of the reduction of the Float time. Later, it is noted that in this case the maximum amplitude of Rise

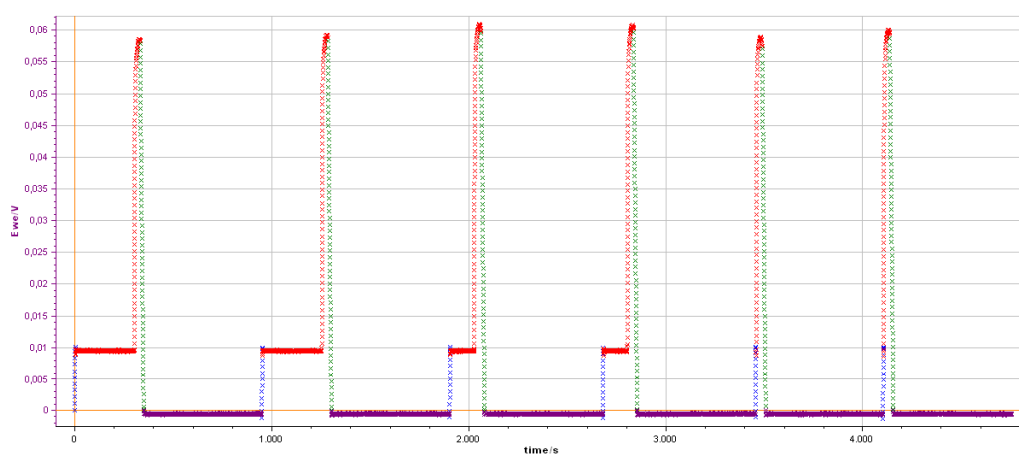


Figure 7.10: Voltage vs Time of the CO₂Cap with a 10mV Float Potential using a symmetrical cell.

Voltage is no longer associated to the zero Float time situation. Indeed, the highest recorded voltage gain, which is 51mV, and the best energy gain (Fig. 7.11a) are related to the scenario of 2 minutes of Float, which wins over the remaining one even if from the percentage energy gain point of view (Fig. 7.11b), the zero minutes Float case is again the most promising. Maybe this is due to the slightly higher leakage current in the case of zero minutes Float which has not been reduced by an adequate conditioning because of absence of the Float. Again, the quite constant Rise Voltage amplitudes are indicative for the effectiveness of interface regeneration flushing N₂.

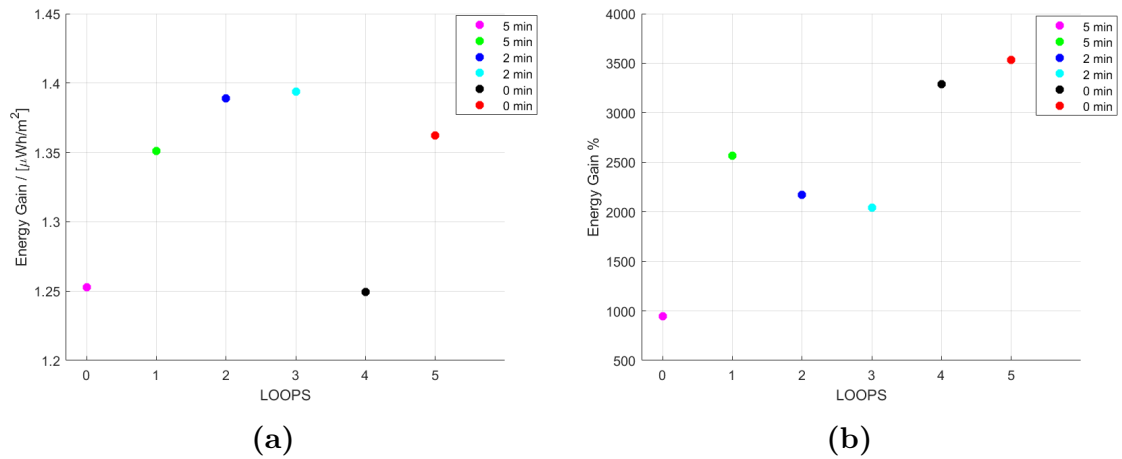


Figure 7.11: (a) Energy gain module for different duration of the 10mV Float; (b) Energy gain in percentage referred to spent energy.

The energy spent to charge and bias the interface is diminished with the duration of the Float, but the energy gain is kept more or less constant after each loop as depicted in graphs 7.11. In the event of Float Potential equal to 10mV,

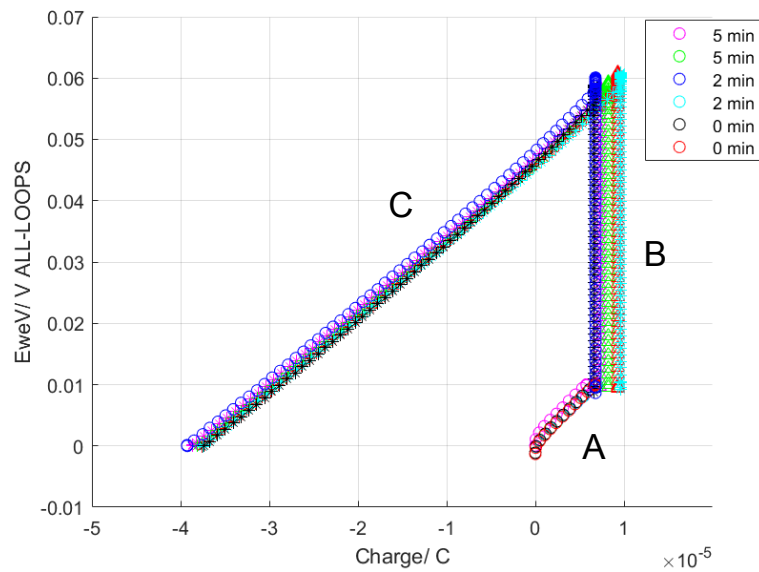


Figure 7.12: Voltage vs Charge graph of the CO₂Cap procedure with a Float Potential equal to 10mV and a progressive reduction of the Float time.

the gain is still lonely positive and checking the graph in the Figure 7.12, it is possible to observe that the discharge curve (C) is continuously greater than the

charge curve (A) without intersecting it at any point. Now, the charge curve (A) is due to the addition of the constant current charge step and it is noticed that at fixed charge (B), related to Rise Voltage in OCV condition, the voltage becomes higher when the EDL capacitance is lowered. This effect should only be associated with the electrostatic phenomenon of Capacitive Double Layer Expansion (CDLE), explained in section 2.1, and therefore the Rise Voltage should depend only on the initial charge accumulated in the double layers and then demise when the discharge is completed [13].

Instead, being the system under examination an electrochemical system, characterized by the combination of electrostatic and chemical phenomena, then it is more plausible the contribution of both to Rise voltage.

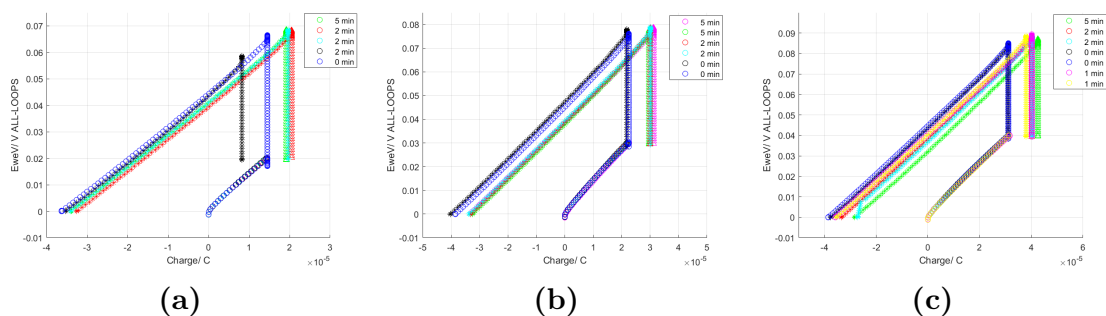


Figure 7.13: (a) Voltage vs Charge curve related to 20mV Float; (b) Voltage vs Charge curve related to 30mV Float; (C) Voltage vs Charge curve related to 40mV Float.

A completely similar behaviour has been observed in the cases of Float potential equal to 20mV, 30mV and 40mV. Meaning that, the Rise Voltage retains a constant amplitude of 50mV regardless of the applied Float potential, and the graphs V vs Q (Fig. 7.13) have exactly the same shape in all cases indicated. The only difference noticeable in these graphs (7.13) is how the curves move to positive charge values increasing the Float potential. This is due to the fact that growing the Float potential then even the initial accumulated charge is greater, thus the V vs Q curve belongs more and more to positive charge values and resulting in a small increase in energy gain module for the same reasons, although maintaining the same trend show in Fig. 7.11a reducing the duration of the Float.

Considering that the amplitude of the Rise Voltage is about constant as the duration of the Float changes and especially by varying the applied Float potential, then this allows to hypothesize that this variation of potential is not only attributable to an electrostatic phenomenon. This hypothesis is based on the fact that specifically the working principle of the system taken in consideration is built on the reaction

between imidazole and CO₂ giving rise, therefore, to a change of chemical species. Then, it is also possible to assume that the chemical potential component is the dominant one compared to the electrostatic component, which was initially the only one hypothesized. Therefore, this variation of potential may not only be due to an electrostatic phenomenon but also to a chemical component, which is not linked to oxidation and/or reduction of imidazole but it is a chemical potential due to chemical species change.

This could be further confirmed by the fact that the shape of the V vs Q curve differs from the canonical one of EDLC (see Figure 3.1). In fact, the curve shown in Fig. 7.12 instead of ending at zero charge, it continues towards negative charge values which can be attributed to a chemical component. Finally, as seen formerly, the shifting of V vs Q curves towards positive charge values lowering the Float time is related to an enhanced energy by shrinking the duration of the Float.

Float of 50mV and 60mV

Using 50mV and 60mV Float Potential a small modification is added to the CapMix procedure, because in the cases of 10mV, 20mV, 30mV and 40mV the steps associated to 2 and 0 minutes of Float are always the most encouraging both

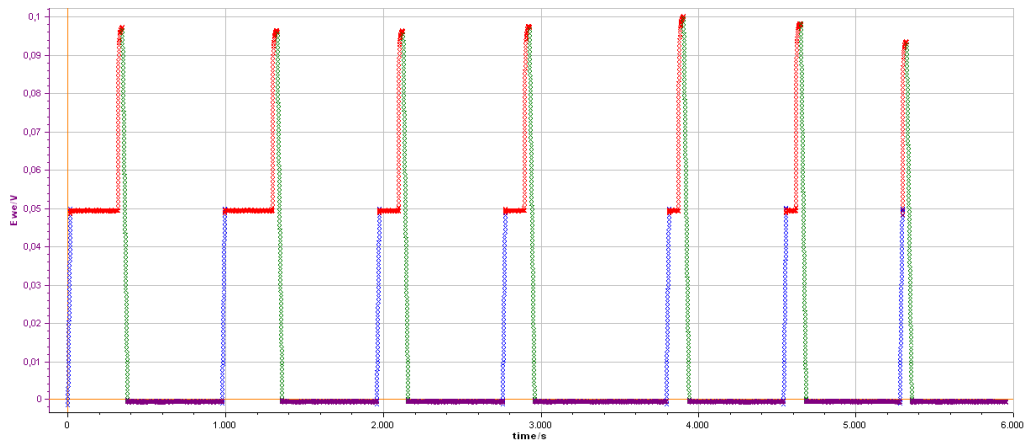


Figure 7.14: Voltage vs Time of the CO₂Cap with a 50mV Float Potential using a symmetrical cell.

from the point of view of the energy gain in module and percentage. Therefore, the step with one minute of Float is added to the measurements of the CapMix procedure (Fig. 7.14) with the aim of obtaining a Rise Voltage greater than or equal to one achieved in the case of 2 minutes Float, which, so far, is always the best Rise voltage, and at the same time the lower energy required for charging and conditioning of the device. The Rise voltage still is around 50mV in every loop showing the same behaviour of the former cases with reference to dependence on

reduction of the Float time. Now, the highest recorded Rise Voltage is 50mV mated

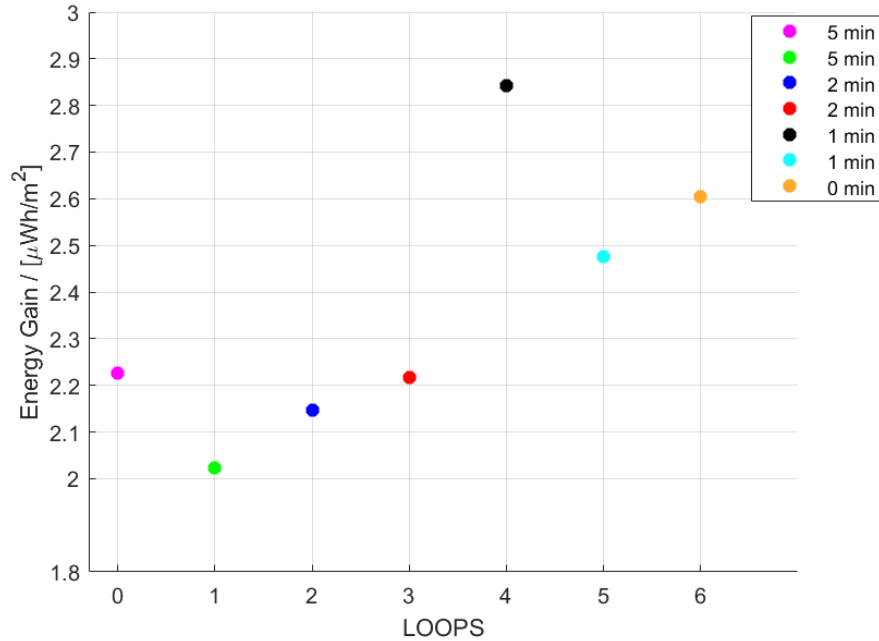


Figure 7.15: Energy gain module for different duration of the 50mV Float.

to 1 minute Float as displayed in Figure 7.14. This is due to a good conditioning of the double layer, indeed the leakage current reaches its minimum value in almost 30 seconds. The values of the energy gains are approximately equal between the case at 50mV Float and one at 60mV Float, which are shown in Figure 7.15.

The increase of the Float potential concurrently with an amplitude of Rise Voltage roughly constant arise, as consequence, an increase of the module of the energy gain. In particular, the module of the energy gain with 50mV and 60mV of Float is $2,9 \mu\text{Wh}/\text{m}^2$, which is greater than one obtained with 10mV, 20mV, 30mV, 40mV, which is between $1,4 - 2 \mu\text{Wh}/\text{m}^2$.

In turn, these last four cases have and energy gain that is greater than one extracted with zero volt Float potential, which is $1,1 \mu\text{Wh}/\text{m}^2$.

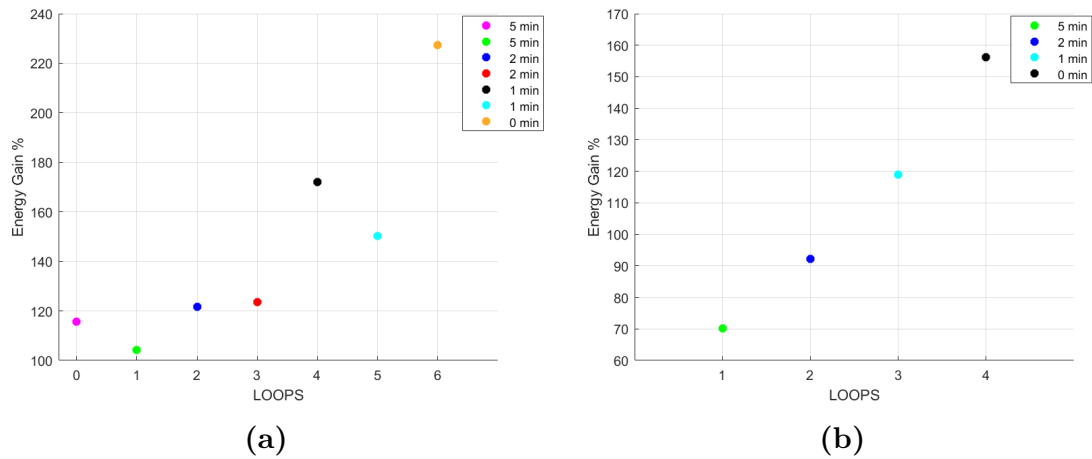


Figure 7.16: (a) Energy gain in percentage referred to spent energy for 50mV Float; (b) Energy gain in percentage referred to spent energy for 60mV Float.

However, it is observed that by increasing the applied Float potential, a progressive reduction of the maximum percentage energy gain occurs. In fact, the absolute maximum percentage energy gain is 10^5 % recorded in the case of zero volt Float, which is greater than one of 10mV Float, which is 3500%, and so on up to 50mV Float, equal to 230% (Fig. 7.16a), and 60mV Float, tantamount to 160% (Fig. 7.16b). The reached results are in agreement with what is hypothesized. Actually, the energy gain obtained with 1 minute of Float is between 12 - 32% greater than one measured with 2 and 0 minutes of Float (Fig. 7.15).

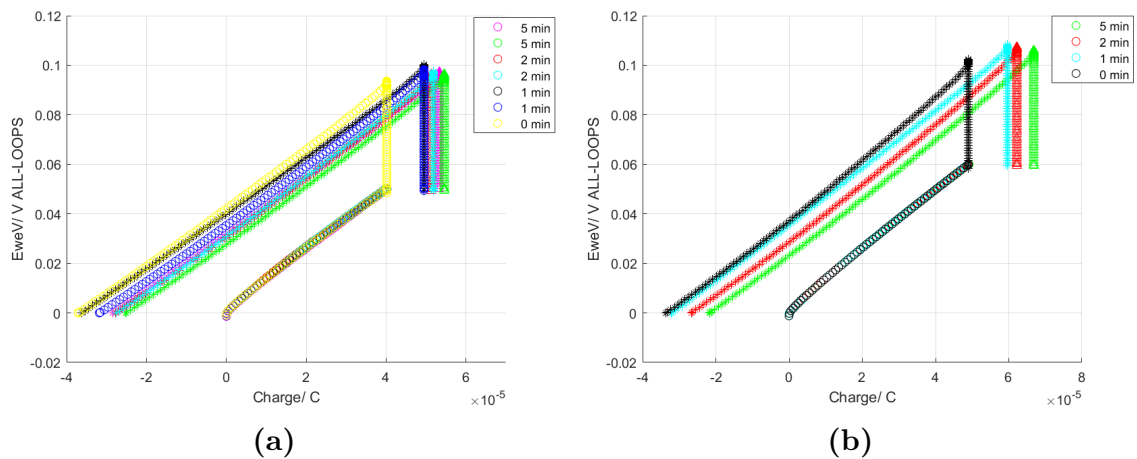


Figure 7.17: (a) Voltage vs Charge curves related to 50mV Float; (b) Voltage vs Charge curve related to 60mV Float.

Though, from the point of view of the percentage energy gain the case with null Float is always the strongly dominant one (Fig. 7.16). After analyzing the CapMix procedure at different Float potentials (0 V, 10mV, 20mV, 30mV, 40mV, 50mV, 60mV) and experiencing the quality of interface regeneration flushing N₂ in all analyzed loops, then it is possible to confirm that the reduction of the duration of the N₂ flushing from 15 minutes, in the case of pure DABCO-IM, to 10 minutes, when using DABCO-IM diluted with PC, it is suitable. This is indicative of a definite improvement in electrolyte solubility and CO₂ diffusion. Also for 50mV and 60mV Float, V vs Q curves show a different shape from the theoretical one (see Figure 3.1) as observed in all examples having a Float potential other than zero volt.

7.3.2 Asymmetric Cell

Before the asymmetric cell is subjected to the CapMix procedure, it is conditioned through the "Potentiostatic Floating Test or Float Conditioning Test" procedure described in section 4.2.4. Once it has reached the stable state, the cell assumes a specific capacitance of 105 μ F/cm² with a coulombic efficiency around 99,9% and an energetic efficiency of 74%. The energy efficiency is greater than one linked to a system made with Hard GDL as electrodes material and pure DABCO-IM as electrolyte but lower than one obtained with a symmetrical system using DABCO-IM diluted in PC. In any case, also this setup allows to have a voltage gain and an appreciable amount of energy.

Float of 0 V

Starting with the application of zero volts as Float Potential, the voltage gains obtained flushing CO₂ are lower with respect to the symmetrical analogous, but fairly constant in all loops.

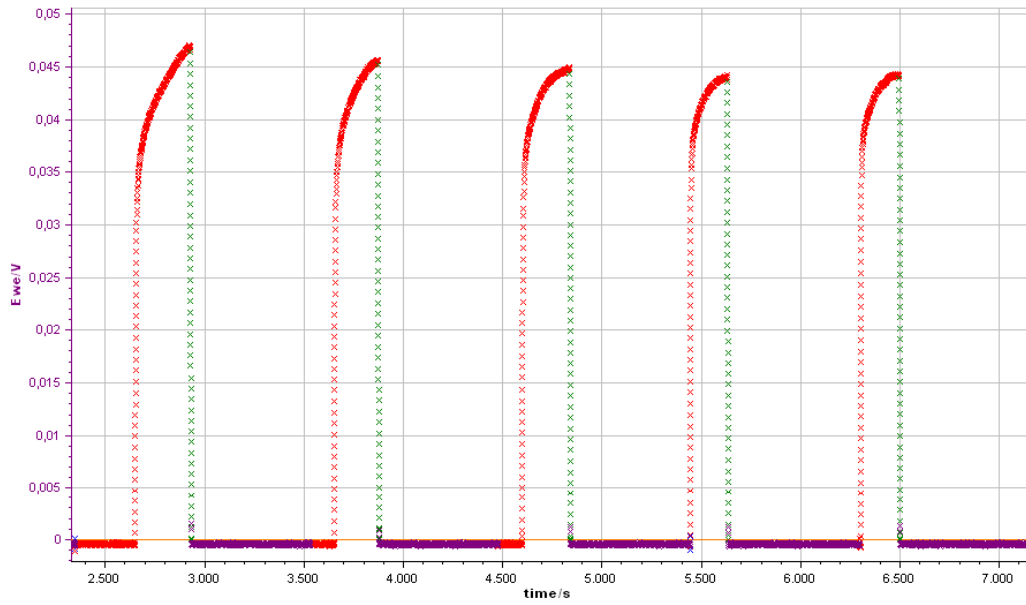


Figure 7.18: Voltage vs Time of the CO₂Cap with null Float Potential using an asymmetrical cell.

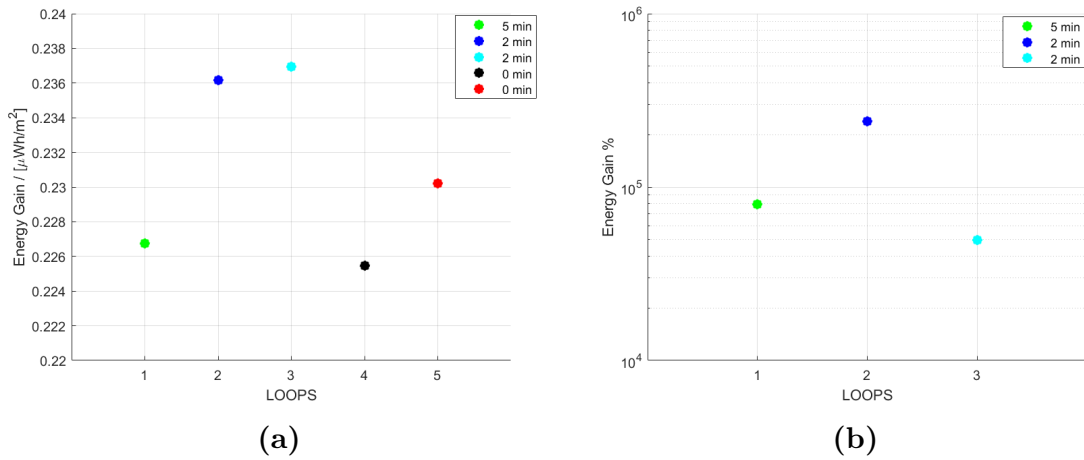


Figure 7.19: (a) Energy gain obtained for different Float time at zero potential; (b) Percentage of achieved energy gain with respect to spent one.

Indeed, all acquired voltage gains are around 45mV as shown in the Figure 7.18. Again, this is the proof of an effectiveness of interface regeneration flushing N₂. The energy gains obtained for each loop are shown in graph 7.19a. It can be possible to see that the energy gain ranges between 0.23-0.24 μWh/cm² in cases of 2 minutes and 0 minutes of Float. This is a further demonstration of the retention of the

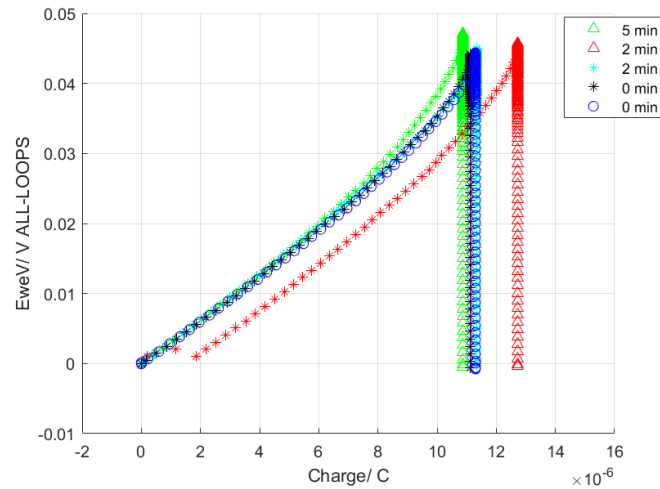


Figure 7.20: Voltage vs Charge graph of the CO₂Cap procedure related to zero Float Potential using the asymmetrical cell.

Rise Voltage amplitude in each loop. While, graph 7.19b displays how shortening the Float time makes the process more advantageous as the energy spent on Float is smaller. Exactly as in the analogous case but using the symmetric cell, being the spent energy almost zero then the released one is totally gained. For this reason the percentage energy gains are in the order of 10^5 %. As for graph V vs Q (Figure 7.20), the behavior is almost the same of the symmetric cell at zero Float potential, but it is noted that the accumulated charge in this specific case is lower of one order of magnitude than one obtained with the symmetrical system. Then again, the gain is strictly positive since a charge step does not exist. The shifting towards positive charge values is also present in this case as consequence of the shrinking of the Float duration.

Float of 10mV

In the case of Float Potential equal to 10mV, instead, it is clear that the amplitude of the Rise voltage is not perfectly uniform by varying the duration of the Float, as displayed in Figure 7.21. In fact, in the case of 5 minutes, 2 minutes and 1 minute Float the voltage gain is about 40mV, which is less than one obtained in the case of Zero Float Potential and then with the zero minutes Float step, a further 5mV reduction in the amplitude of Rise Voltage is observable. The energy gains obtained for each loop, shown in graph 7.22a, confirm the trend of voltage gains.

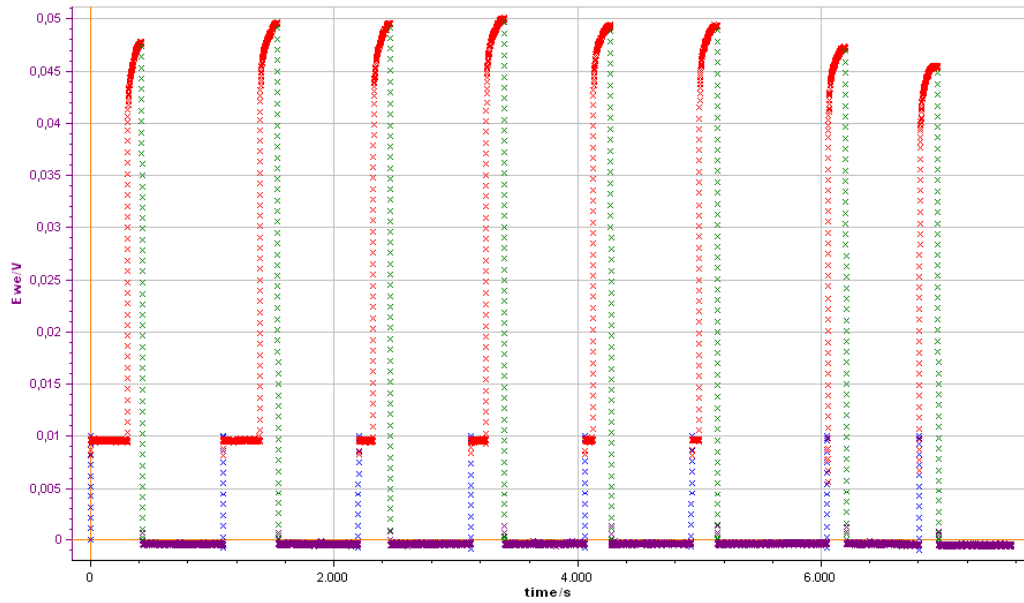


Figure 7.21: Voltage vs Time of the CO₂Cap with 10mV Float Potential, using an asymmetrical cell.

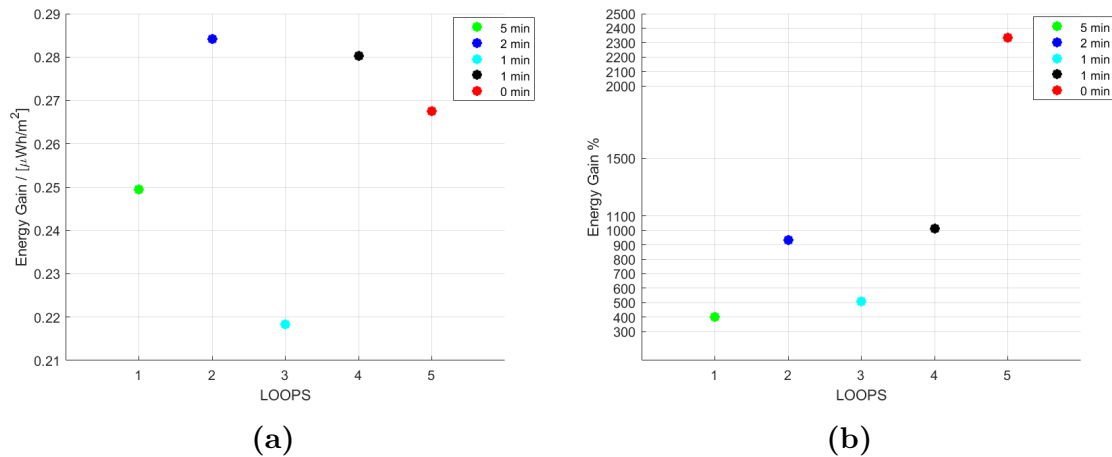


Figure 7.22: (a) Energy gain for different duration of the 10mV Float; (b) Energy gain in percentage referred to spent energy for 10mV Float.

Despite this, the energy gain ranges between 0.27-0.29 μ Wh/cm² in cases of 2 minutes, 1 minute and zero minutes of Float. While, by means of the graph 7.22b it is possible to observe how the step characterized by the absence of the Float is the most advantageous as the energy spent on Float is reduced shortening its duration. Checking the graph V vs Q in the Figure 7.23, the gain is still lonely positive being

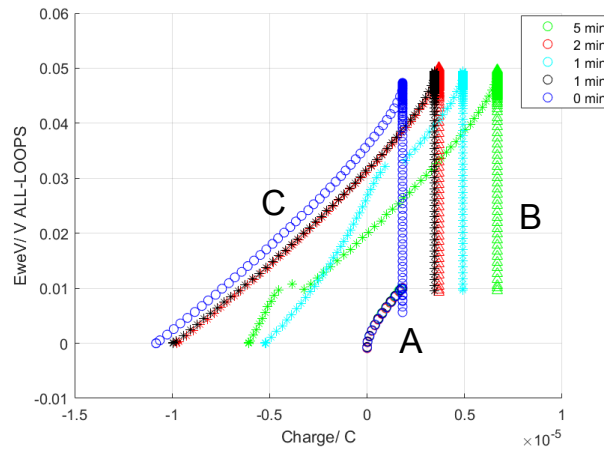


Figure 7.23: Voltage vs Charge curves related to 10mV Float potential, using an asymmetrical cell.

the discharge curve (C) greater than the charge one (A) and not crossing it in any point. A completely similar behaviour in the responses of the 20mV, 30mV and 40mV Float potential has been observed. Indeed, in these four cases the Rise Voltage amplitude ranges between 35mV and 40mV while energy gains between 0,1 - 0,4 $\mu\text{Wh}/\text{m}^2$ regardless of the applied Float potential. The graphs V vs Q (Fig. 7.24) have exactly the same shape in all cases indicated. Once again, there is a shifting towards positive charge values as a response to an increasing the Float potential, because of the growing of the initial accumulated charge, and lowering the Float time causing a tiny increase in energy gain.

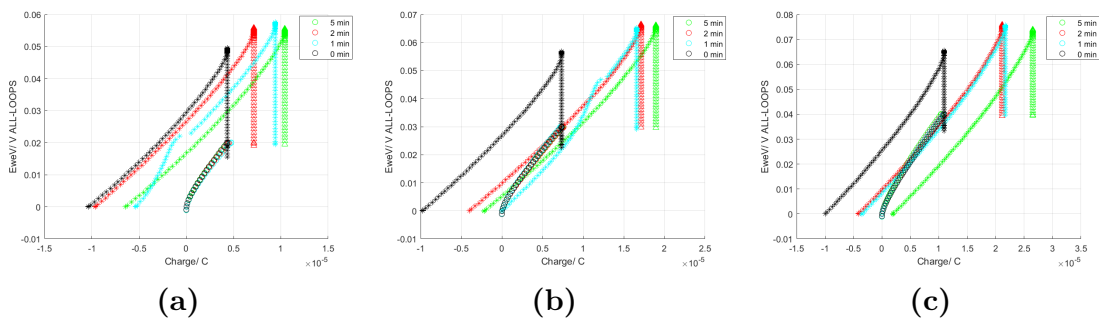


Figure 7.24: (a) Voltage vs Charge curve related to 20mV Float; (b) Voltage vs Charge curve related to 30mV Float; (c) Voltage vs Charge curve related to 40mV Float, using an asymmetrical cell.

The shape of the V vs Q curve also in this sample differs from the theoretical one of EDLC (see Figure 3.1). It is important to highlight the 5 minutes Float step

in case of 40mV Float potential in figure 7.24c (green curve). In fact, that curve is the only one having the discharge part totally below the charge one so in that specific case the energy gain is negative. More details will be provided in the next paragraph.

Float of 50mV and 60mV

When a Float potential at 50mV and 60mV is applied, the Rise voltage is about 35mV in every loop having the Float phase. Now, the highest recorded Rise Voltage is 37mV related to 5 minute Float as displayed in Figure 7.25. Thus, rising the Float potential the degradation of the Rise Voltage amplitude is noticed both for 50mV and 60mV Float and focusing the attention on the step with 0 minutes of Float, a dramatic voltage drop is obtained being the Rise voltage equal to 25mV. This is due to the need for a longer duration of the Float in order to effectively reduce the leakage current, which has not been lowered because of the absence of conditioning which can only be obtainable through the Float phase. Moreover, the leakage Float current is directly affected by the potential of Float. That is, by increasing the Float potential then also the leakage float current increases therefore reducing the maximum obtainable amplitude of the Rise Voltage. The values of the energy gains are approximately the same between the case at 50mV and 60mV Float, which

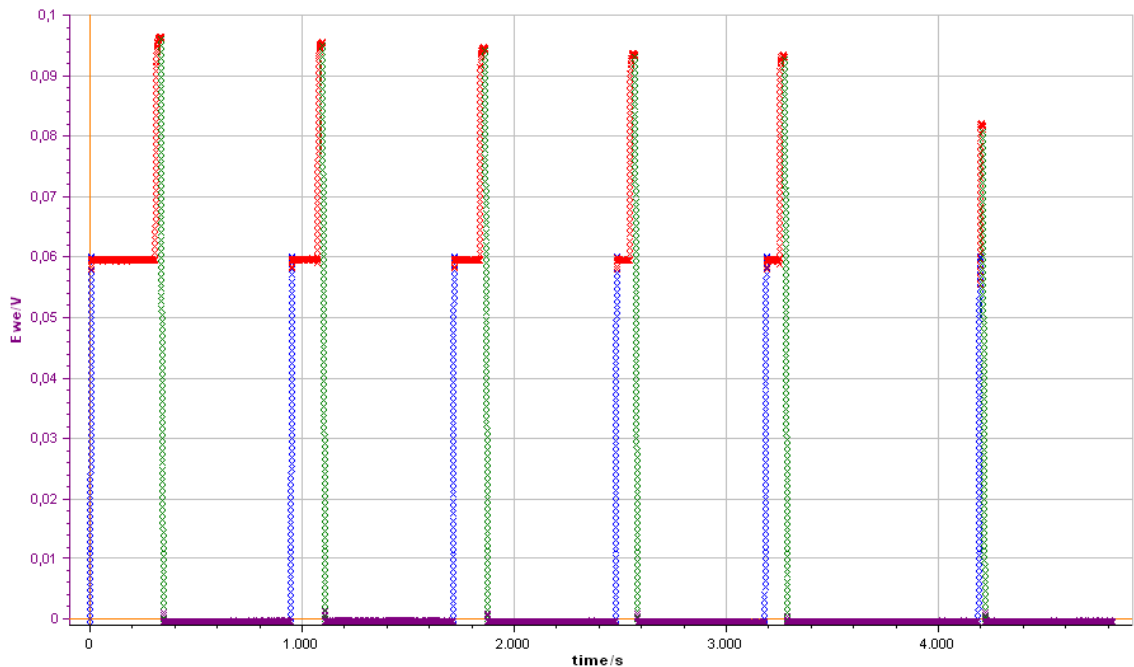


Figure 7.25: Voltage vs Time of the CO₂Cap with 60mV Float Potential, using an asymmetrical cell.

are shown in Figure 7.26. The maximum energy gain is $0,4\mu\text{Wh}/\text{m}^2$ both with 50mV and 60mV of Float which is comparable with one obtained with 10mV, 20mV, 30mV, 40mV and this is further confirmation of the efficiency degradation of the system increasing the Float potential.

In the case of the energy gain, there is a substantial difference compared to earlier seen. Which is the presence of a negative energy gain with reference to 5-minute step for the 50mV Float, while there are negative energy gains related to 5-minute, 2-minute and 1-minute steps for the 60mV Float. So, only on the occasion of null Float a positive energy gain is achieved. This issue can be looked at and then confirmed by observing the graphs of percentage energy gain in figure 7.27, which show negative percentages relative to the same cases. The only case with positive value is one associated to null Float. Clear sign that the energy extracted with the constant current discharge is not able to compensate the one used to charge and for conditioning of the electrochemical cell in those specific situations.

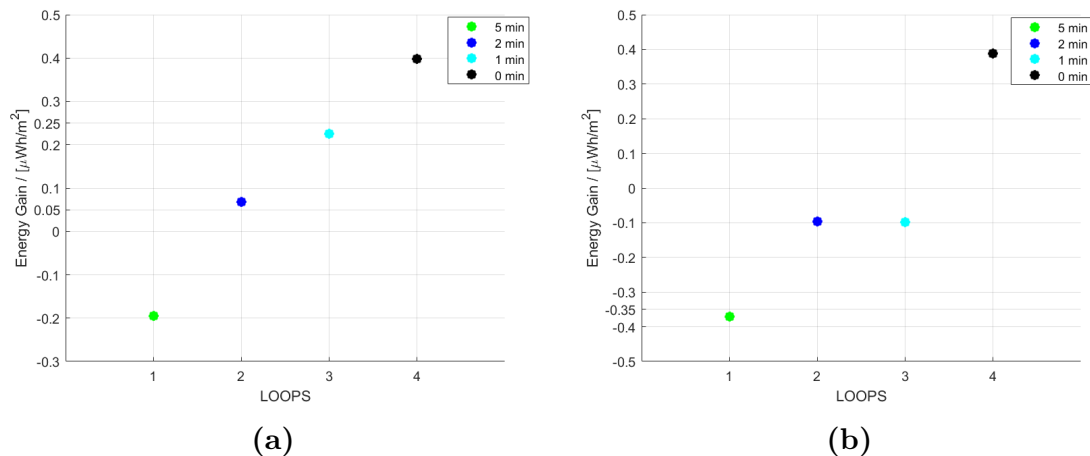


Figure 7.26: (a) Energy gain for different duration of the 50mV Float; (b) Energy gain for different duration of the 60mV Float

As for the symmetric cell, also in the case of the asymmetric cell is observable a progressive reduction of the maximum percentage energy gain, occurring increasing the Float potential. Without doubt, the absolute maximum percentage energy gain is still related to zero volt Float and it is $10^5\%$, then for 10mV Float is 2300%, and so on up to 50mV Float with 90% (Fig. 7.27a), and 60mV Float with 60% (Fig. 7.27b).

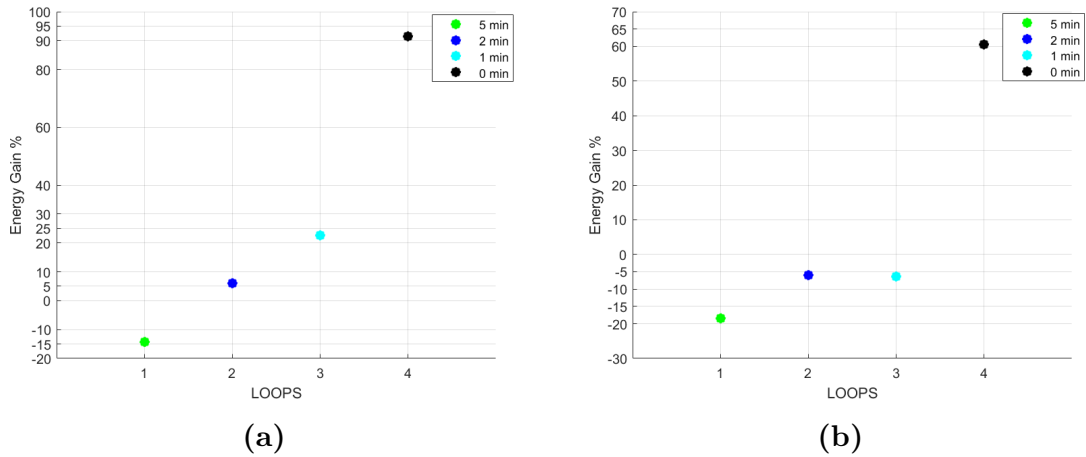


Figure 7.27: (a) Percentage Energy gain referred to spent energy for 50mV Float; (b) Percentage Energy gain referred to spent energy for 60mV Float.

What is observed with energy gain and percentage energy gain can be validated through the analysis of the V vs Q graphs (Fig. 7.28). In fact, for 50mV and 60mV Float, V vs Q curves besides being different from the theoretical one (see Figure 3.1), those show that curves related to cases with negative energy gains are characterized by the fact that the values of the discharge curves are lower than charge one.

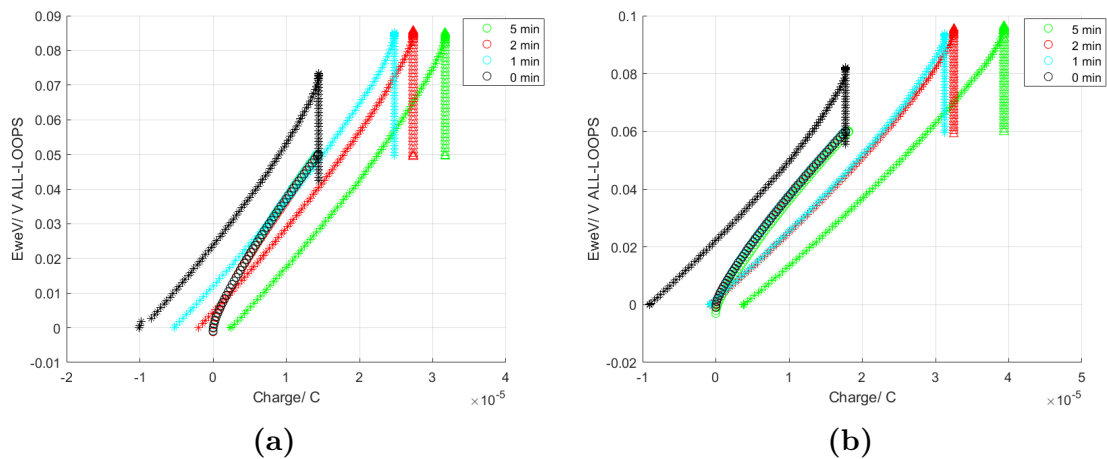


Figure 7.28: (a) Voltage vs Charge curve related to 50mV Float; (b) Voltage vs Charge curve related to 60mV Float.

7.4 Comparison of symmetrical and asymmetrical system

Comparing the symmetrical and asymmetrical setups features, it is possible to conclude that the energy efficiency is greater in the symmetrical cell than in the asymmetric one. This also affects the energy gain, both in modulus and percentage, and the accumulated charge. These parameters in an asymmetric cell are from 2 to 10 times smaller. The difference in energy efficiency between symmetric and asymmetric cell can be associated with the difference in the size of the electrode subjected to the flow. In fact, in the case of an asymmetric cell the electrode flushed by the gas has a diameter of 7 mm, while in the case of symmetric cell the electrode has a diameter of 18 mm.

In addition, since the cell is designed in order to accommodate a symmetrical system then it can be asserted that the gas flow is more effective in the case of a symmetrical cell than in asymmetrical. Moreover, the asymmetric cell is also characterized by an handcrafted Kapton shielding in order to mitigate the presence of reactions, not yet well defined, with the steel of the ECC-Air cell, as explained in section 5.5, which can reduce the cell performance despite the adopted artifice.

Moreover, a larger electrode surface also implies a greater amount of electrolyte at the interface affected by the flushing as well as better wettability of the electrode itself. Finally, a smaller electrode surface also implies a lower specific capacitance value. Indeed, the symmetric system has a specific capacitance of $264\mu\text{F}/\text{cm}^2$ while the asymmetrical system specific capacitance is $105\mu\text{F}/\text{cm}^2$.

While regarding coulombic efficiency, it is higher in the asymmetric cell than in the symmetric one. This can be easily explained considering that the sizing of the asymmetric cell is due to the purpose of charge balancing on the two electrodes in order to improve the coulombic efficiency of the final system.

In fact, comparing the Rise Voltage of the asymmetric cell with the symmetric one (see Fig. 7.7 and Fig. 7.18), in the latter when the Rise Voltage reaches the peak, it does not remain constant for long time giving rise to a rapid self-discharge after almost 10 seconds. While in the case of the asymmetric cell, the peak value of Rise Voltage is kept spontaneously constant even for several minutes.

From the energy analysis, it is observable that the energy extracted by means of the constant current discharge by the system characterized by DABCO-IM diluted as electrolyte is lower than one obtained with a system using pure DABCO-IM as electrolyte. This can be explained by observing the charge and discharge time of the two systems. That is, using diluted DABCO-IM the charge and discharge times are reduced a lot compared to the case with pure DABCO-IM. This is due to the reduction of both the ESR and the total capacity of the system, affecting

the time constant of the device. Consequently, the variation of the voltage during the discharge occurs in a much smaller time giving rise to a higher power.

In order to obtain more energy, a charge and discharge with a constant current which is much smaller than previous one should be performed. In particular, instead of adopting a current density of $1\mu\text{A}/\text{cm}^2$, a density of $200\text{nA}/\text{cm}^2$ can be exploited, so that the charge and discharge time are approximately equal to one observed in the case of a cell with pure DABCO-IM.

Chapter 8

Conclusions and Future Developments

8.1 Conclusions

8.1.1 Improved CapMix procedure

A more precise evaluation of the energy required to charge and condition the super-capacitive system is carried out through a four-step procedure called CO₂Cap (Fig. 8.1) which are: constant voltage flushing N₂ for the desorption of the CO₂; charging of the system up to Float potential; Float phase for conditioning of the EDLs; OCV flushing CO₂ to get the Rise Voltage; discharging to extract the gained energy.

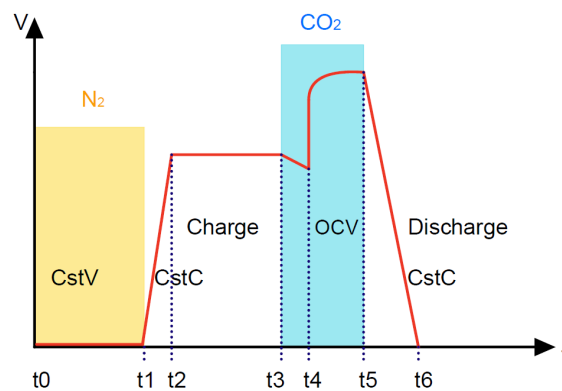


Figure 8.1: New procedure adopted for the CO₂Cap cycle.

8.1.2 New electrode material

The new tested electrode material, defined Flexible GDL, does not improve the performances of the cell as expected. Indeed, a larger capacitance is observed with an important improvement of the coulombic efficiency of the system achieving 99%. Nevertheless, by applying the CO₂Cap procedure on a cell assembled with electrodes made of Flex GDL and DABCO-IM as electrolyte, the obtained results show a dramatic drop of the voltage instead of a Rise Voltage. This effect is due to the high capacitance of the Flex GDL and therefore of the system since the leakage float current and time constant are directly proportional to the capacitance. Thus, the dropping of the leakage current happens with longer time and so its final value is too high exceeding the limit value of 250nA and preventing the Rise Voltage.

8.1.3 Effect of the Float reduction

An enhancement of the gained energy is made possible by reducing the Float time, whose energy cost corresponds up to 30% of the total energy used for charging and conditioning of the device. Through a CO₂Cap characterized by the progressive reduction of the Float, performed on a cell made with Hard GDL as electrode material and DABCO-IM as electrolyte, it has been identified that the situation with 0 minutes of Float, that is absence of Float, is the one allowing an improved energy gain even if it is still negative as shown in figure 8.2.

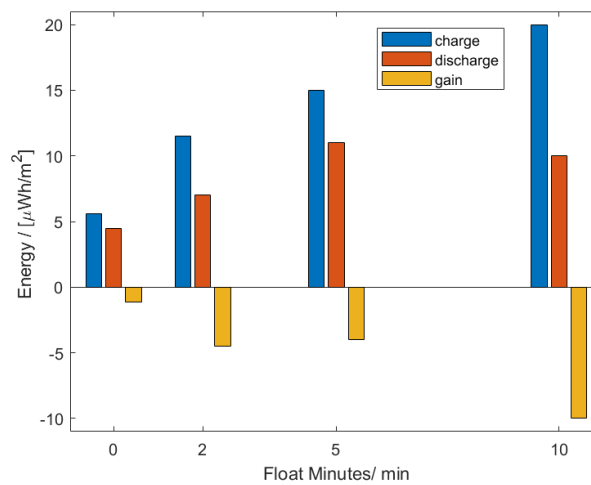


Figure 8.2: Comparison of energy gains obtained for several Float times adopting the CapMix procedure shown in figure 8.1.

8.1.4 Effect of the Ionic Liquid dilution exploiting Propylene Carbonate

DABCO-IM dilution with Propylene Carbonate (PC) led to significant improvements in the performances of the device at room temperature. The solvent molecules, placed between the electrolyte ions, attenuate coulombic forces maximizing the mobility of the charge carriers and lowering the viscosity of the electrolyte which allows CO₂ to diffuse more easily through the electrode-electrolyte interface. Moreover, the solvent improves the dielectric of the electrolyte and provides the solvation shell of the ions determining better accessibility of the electrolyte in the electrodes pores. All these upgrades boost the conductance of the electrolytic solution achieving a higher energy output. CapMix measurements, performed at different Float potentials (0, 10mV, 20mV, 30mV, 40mV, 50mV, 60mV) and Float time (5 min, 2 min, 1 min and 0 min) using diluted DABCO-IM as electrolyte and electrodes made of Hard GDL, show that in the case of symmetric cell it is possible to obtain a very huge and constant Rise voltage amplitude equal to 50mV irrespective of the Float potential and time (Fig. 8.3). In addition, the energy obtained at room temperature is always positive. The maximum recorded value is 53mV for null Float

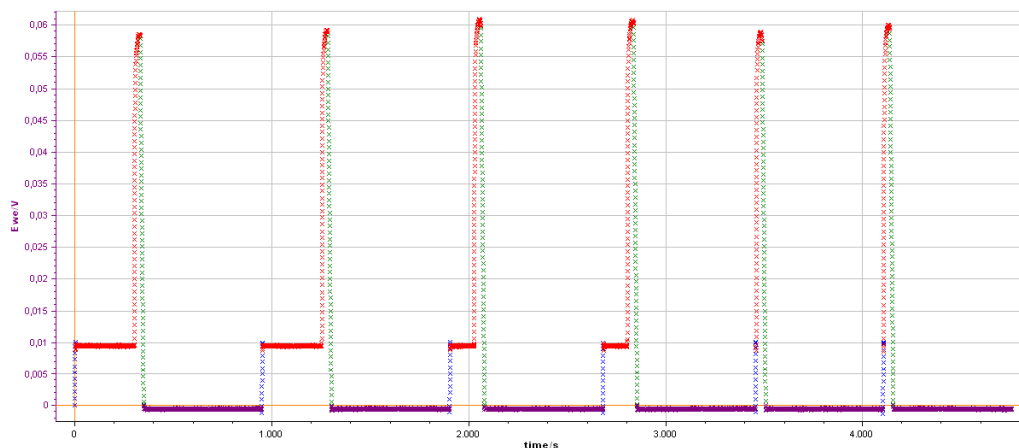


Figure 8.3: Voltage vs Time of the CO₂Cap using a symmetrical cell.

potential and absent Float phase. Once fixed the Float potential, the recovered energy is almost constant for each loop but the spent energy decreases as reducing the duration of the Float. Thus, the energy gain increases (Fig. 8.4a). Analysing the energy gain module as varying the Float potential, a slight increase of energy is observed because of the corresponding increasing of the initial accumulated charge.

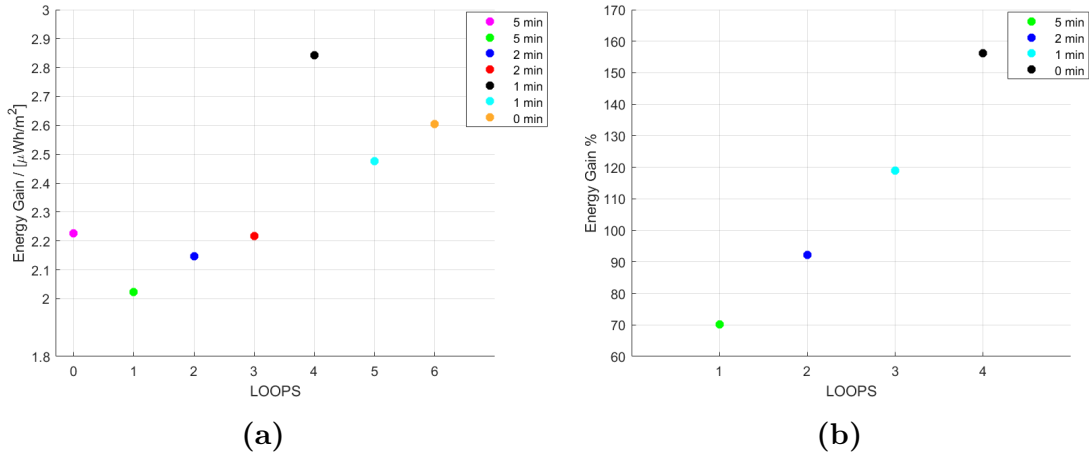


Figure 8.4: (a) Energy gain module for different duration of the Float; (b) Energy gain in percentage referred to spent energy for several Float time.

Instead studying graphs of percentage energy gain an opposite trend occurs. A higher percentage of gained energy is obtained by reducing the Float potential and however the best case is Zero min Float step (Fig. 8.4b) which is the most promising in order to gain more by consuming less. The V vs Q plot helps to confirm the results. The discharge curve (C) assumes values greater than charge one (A) and without meeting it never (Fig. 8.5), testifying that the extracted energy is greater than one required for the charge and conditioning of the device. Moreover,

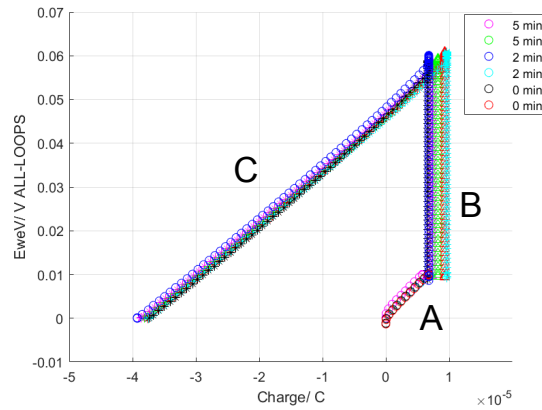


Figure 8.5: Voltage vs Charge.

considering that the shape of the V vs Q curves is different from theoretical one of an EDLC as it does not end at zero charge but for negative charge values (Fig. 8.5) and accounting that the amplitude of the Rise Voltage is enough constant as the duration of the Float changes (Fig. 8.3) and mainly by adjusting the applied Float

potential, then it can be hypothesized that the voltage variation is not only linked to an electrostatic phenomenon but also to a chemical one. This can be considered reasonable being the system electrochemical like. Anyway, it is important to stress that this component of chemical potential is not due to redox phenomena but solely to a change of chemical species due to the reaction between electrolyte and CO_2 . Finally, the V vs Q curves move towards positive values of charge both increasing the Float potential and reducing the Float time confirming an increase in energy gain in both situations. Although, in terms of percentage energy gain, results improve by reducing the Float potential and Float duration. In any case the best step of Float time is 1 minute as the energy extracted in this condition is between 12% and 32% higher than one collected with 2 min and 0 min of Float (Fig. 8.4a).

In the case of an asymmetric cell, the obtained results show that the voltage gains are between 35mV and 40mV (Fig. 8.6) so lower than symmetrical one and rising the Float potential a significant degradation of the Rise Voltage occurs obtaining only 25mV in the case of 0 min Float both in 50mV and 60mV Float

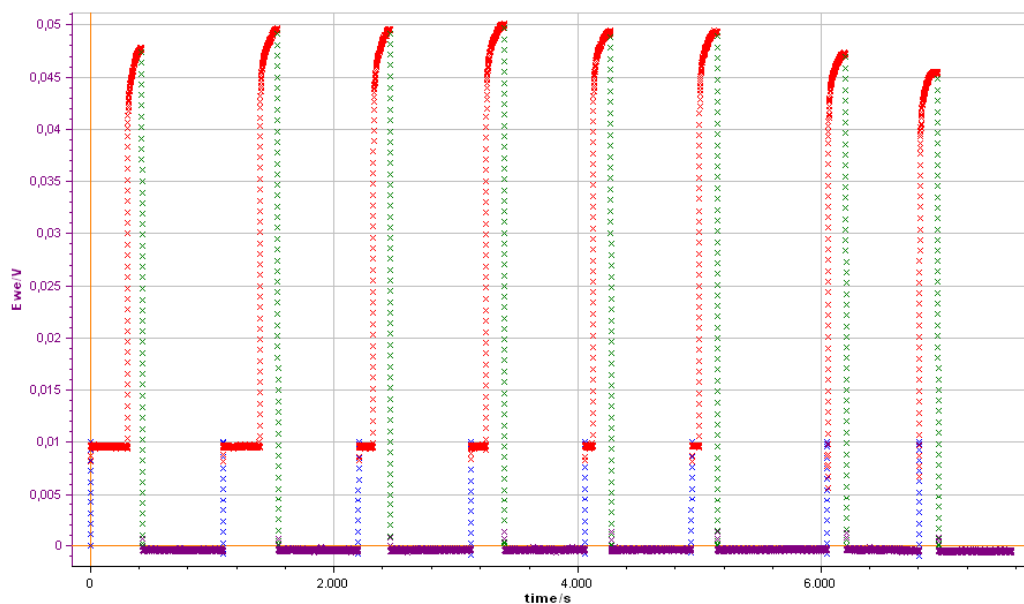


Figure 8.6: Voltage vs Time of the CO_2 Cap using an asymmetrical cell.

potential due to an increasing of the leakage current as growing the Float potential. In fact, when Float potential is 50mV and 60mV some energy gains are negative, more precisely in 5-min, 2-min and 1-min steps despite the use of dilution. While the 0-min Float step is the only one positive (Fig. 8.7a).

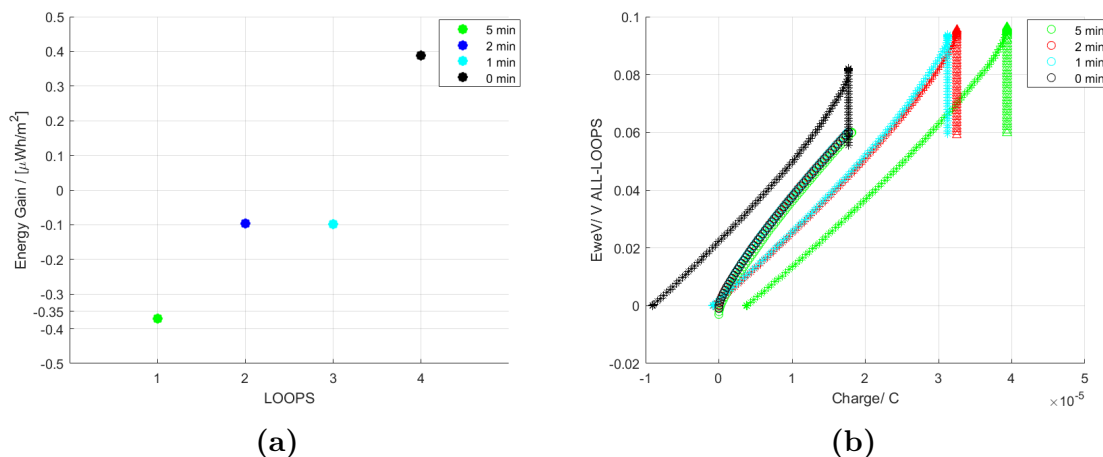


Figure 8.7: (a) Energy gain for different 60mV Float times; (b) Voltage vs Charge.

Indeed, the V vs Q curves related to the cases with negative energy gains show that the discharge curves are lower than charge one (Fig. 8.7b). This great difference between symmetrical and asymmetric cells is due to the energy efficiency which is 82% in symmetric device and 74% in asymmetric one. This affects the energy gain, both in module and percentage, and the accumulated charge. These parameters are from 2 to 10 times lower in asymmetric cell because of its smaller positive electrode. Indeed a larger electrode means a greater amount of available electrolyte for the reaction at the interface and a better flushing quality of the gases. Moreover, a larger electrode implies a greater specific capacitance and so higher energy output.

8.2 Future Developments

- Focusing on cases with 0 V, 10mV and 30mV Float potential which are those offering the best trade off between energy gain in module and percentage. These three cases will be studied using only the 1-minute Float step and exploiting a new CapMix procedure aiming to take advantage not only from positive voltages, flowing CO_2 , but also from negative one, during the flushing of N_2 . In fact, in a completely similar but opposite way with respect to the flushing of CO_2 , the flow of this inert gas causes a more than exponential fall of the voltage when the device is in OCV conditions. The purpose of this stratagem is to exploit both OCV phases to which the cell is subjected in every loop in order to double the energy gain;
- Make the cell slightly asymmetrical in order to meet a coulombic efficiency very close to 99% and at the same time try to keep the high energy efficiency

attributed to a symmetrical device;

- Design a new cell in order to accommodate a system characterized by interdigitated electrodes. The purpose of this system is to solve the problem related to the flow of gases on a single electrode preventing the migration of CO_2 up to the second electrical double layer and so limiting the capability of the device.
- New design of the cell, as the used one is a commercial cell which has inlet and outlet gas on top. Therefore, it is not optimal to get a symmetrical work of the cell. In fact, the cell can be symmetrical, but from the point of view of the gas flow, the latter is forced to follow a path which is asymmetrical, then it exits and enters from the same portion of the cell. This could worsen the electrolyte regeneration phase.
- New materials for the electrodes could be tried and Ion Exchange Membrane could be used to enhance the performances of the cell. The best situation would be using a membrane able to separate the charges and at the same time absorb CO_2 .

Bibliography

- [1] Myoung Jun Park Jihye Kim Kwanho Jeong. «Recent Advances in Osmotic Energy Generation via Pressure-retarded osmosis (PRO): A Review». In: doi:10.3390/en81011821 (Oct. 2015) (cit. on pp. 2, 3).
- [2] Joon Ha Kim Jihye Kim Jijung Lee. «Overview of pressure-retarded osmosis (PRO) process and hybrid application to sea water reverse osmosis process». In: doi:10.1080/19443994.2012.672170 (Feb. 2012) (cit. on p. 2).
- [3] <https://wetlab.net.technion.ac.il/research/sg/>. In: () (cit. on p. 3).
- [4] Yongsheng Chen Jin Gi Hong. «Nanocomposite reverse electrodialysis (RED) ion-exchange membranes for salinity gradient power generation». In: *Journal of Membrane Science* 460 (Feb. 2014), pp. 139–147 (cit. on pp. 3–5).
- [5] Enver Guler David A. Vermaas. «Theoretical power density from salinity gradients using reverse electrodialysis». In: *Energy Procedia* 20 (2012), pp. 170–184 (cit. on p. 4).
- [6] Bruce E. Logan Taeyoung Kim. «A pH-Gradient Flow Cell for Converting Waste CO₂ into Electricity». In: *Environmental Science Technology LETTERS* (2017), pp. 49–53 (cit. on pp. 5, 6).
- [7] Raül A. Rica Dorian Brogioli. «Capacitive Mixing for Harvesting the Free Energy of Solutions at Different Concentrations». In: doi:10.3390/e15041388 (Apr. 2013) (cit. on pp. 6, 15, 18, 19).
- [8] J.M.Paz-García H.V.M.Hamelers O.Schaetzle. «Harvesting Energy from CO₂ Emissions». In: *Environmental Science Technology LETTERS* (2014), pp. 31–35 (cit. on pp. 6, 7).
- [9] Seepalakottai Sivakkumar Tony Pandolfo Vanessa Ruiz. «General Properties of Electrochemical Capacitors». In: John Wiley Sons, Incorporated (2013), pp. 69–109 (cit. on pp. 8–11, 13, 24, 37).
- [10] unspecified. «Electrical Double Layer in Ionic Liquids». In: unspecified (unspecified), unspecified (cit. on pp. 9, 17, 18).

- [11] Ning Pan Sanliang Zhang. «Supercapacitors Performance Evaluation». In: *ADVANCED ENERGY MATERIALS* (2015), pp. 1–19 (cit. on pp. 11, 14, 21–25, 27, 28, 30).
- [12] Yury Gogotsi Tyler S.Mathis Patrice Simon. «Energy Storage Data Reporting in Perspective-Guidelines for Interpreting the Performance of Electrochemical Energy Storage System». In: *ADVANCED ENERGY MATERIALS* (2019), pp. 1–13 (cit. on pp. 12, 13, 22, 24, 28–31, 39).
- [13] D.Salerno D.Brogioli R.Ziano. «Exploiting the spontaneous potential of the electrodes used in the capacitive mixing techniques for the extraction of energy from salinity difference». In: *Energy Environmental Science* (2012), pp. 9870–9880 (cit. on pp. 16–18, 64).
- [14] B.B.Sales H.V.M.Hamelers P.M.Biesheuvel. «Direct Power Production from a Water Salinity Difference in a Membrane-Modified Supercapacitor Flow Cell». In: *ENVIRONMENTAL SCIENCE TECHNOLOGY* (2010), VOL.44, 5661–5665 (cit. on pp. 19, 20).
- [15] Marcin Biegun Andrzej Lewandowski Pawel Jakobczyk. «Self-discharge of electrochemical double layer capacitors». In: *Phys.Chem.Chem.Phys.* (2013), pp. 15, 8692–8699 (cit. on pp. 22, 26, 27, 31).
- [16] Marina Mastragostino Francesca Soavi Catia Arbizzani. «Leakage currents and self-discharge of ionic liquid-based supercapacitors». In: *J Appl Electrochem* (2014), pp. 44, 491–496 (cit. on pp. 22, 27, 30, 31).
- [17] Heather A. Andreas. «Self-Discharge in Electrochemical Capacitors: A Perspective Article». In: *Journal of The Electrochemical Society* (2015), 162(5), A5047–A5053 (cit. on pp. 27, 31).
- [18] François Béguin Ann Laheäär Ana Arenillas. «Change of self-discharge mechanism as a fast tool for estimating long-term stability of ionic liquid based supercapacitors». In: *Journal of Power Sources* (2018), pp. 396, 220–229 (cit. on pp. 27, 31).
- [19] Maite Landaluce Abad. «Energy Harvest from CO2 emissions through Capacitive Mixing». In: (2021) (cit. on pp. 32, 35, 38–42, 44, 45, 53).
- [20] EL-cell. «Electrochemical test equipment». In: URL: <https://el-cell.com/> (visited on 23/06/2021) (cit. on pp. 33, 34).
- [21] EL-cell. «Electrochemical test equipment». In: <https://el-cell.com/new-separator-for-pat-insulation-sleeves/> (visited on 01/07/2021) (cit. on p. 34).
- [22] Davide Molino. «Study and development of new materials for harvest energy from CO2 emissions». In: (2020) (cit. on pp. 34, 35, 39, 40).
- [23] fuelcellstore. «<https://www.fuelcellstore.com/spec-sheets/SGL-GDL24-25.pdf>». In: () (cit. on p. 35).

- [24] MIT KOREA. «[http://mtikorea.co.kr/product/detail/5139.html?product no=5139| cate no=1305](http://mtikorea.co.kr/product/detail/5139.html?product%20no=5139&cate%20no=1305)». In: () (cit. on p. 36).
- [25] Zhiyong Li Jikuan Qiu Yuling Zhao. «Efficient Ionic-Liquid-Promoted Chemical Fixation of CO₂ into α -Alkylidene Cyclic Carbonates». In: 9 (2016), ChemSusChem., 1–9 (cit. on pp. 37, 38).
- [26] Linpo Yu and George Z. Chen. «Ionic Liquid-Based Electrolytes for Supercapacitor and Supercapattery». In: 7 (2019), Frontiers in Chemistry, Article 272 (cit. on p. 37).
- [27] Sheng Dai Congmin Wang Huimin Luo. «Equimolar CO₂ capture by imidazolium-based ionic liquids and superbase systems». In: 12 (2010), Green Chem., 2019–2023 (cit. on pp. 38, 42).
- [28] pubchem. «<https://pubchem.ncbi.nlm.nih.gov/compound/Imidazole-Carbamate>». In: () (cit. on p. 53).
- [29] B. E. Conway. «Electrochemical Supercapacitors: Scientific Fundamentals and Technological Applications». In: Kluwer Academic/Plenum Publishing (New York, 1999), Chap.: 5-7-8–13 (cit. on pp. 54–57).
- [30] Marianne Grognot and Guilhem Gallot. «Relative Contributions of Core Protein and Solvation Shell in the Terahertz Dielectric Properties of Protein Solutions». In: J. Phys. Chem. B 2017, 121, 41, 9508–9512 (2017) (cit. on p. 54).

Acknowledgments

Alla fine di questa esperienza è doveroso un grande ringraziamento a tutte le persone che mi hanno supportato e guidato. In particolare, il Prof. Andrea Lamberti, Pietro, Davide e Alessando per tutto quello che mi hanno insegnato con grande pazienza e disponibilità permettendomi di affrontare al meglio e con serenità la mia tesi. Grazie a tutto "Lo Zoccolo Duro della Ricerca" che è stata per me come una grande famiglia a Torino. Persone eccezionali dentro ma soprattutto fuori al laboratorio che mi hanno accolto rendendo unici questi mesi insieme. Per la prima volta ho conosciuto nuovi luoghi e sapori di torino come le pizzette di Aldos, gli scogliattoli al Valentino e quella "pozza" d'acqua che è il Po.

Non può mancare un immenso ringraziamento alla mia famiglia. Questa laurea è anche loro in quanto mi hanno sempre sostenuto e incoraggiato dandomi forza durante i momenti di difficoltà.